

UNCLASSIFIED

AD 257 171

*Reproduced
by the*

ARMED SERVICES TECHNICAL INFORMATION AGENCY
ARLINGTON HALL STATION
ARLINGTON 12, VIRGINIA



UNCLASSIFIED

NOTICE: When government or other drawings, specifications or other data are used for any purpose other than in connection with a definitely related government procurement operation, the U. S. Government thereby incurs no responsibility, nor any obligation whatsoever; and the fact that the Government may have formulated, furnished, or in any way supplied the said drawings, specifications, or other data is not to be regarded by implication or otherwise as in any manner licensing the holder or any other person or corporation, or conveying any rights or permission to manufacture, use or sell any patented invention that may in any way be related thereto.

4 MAY 1960

(1)

DOPPLER SYSTEM

RESEARCH LABORATORY

PROVING GROUND

BERDEEN, MARYLAND

AD No. _____

ASTIA FILE COPY

257171

ASTIA
 RECEIVED
 JUN 6 1961
 TIPDR

334

ARPA Cont. No. _____

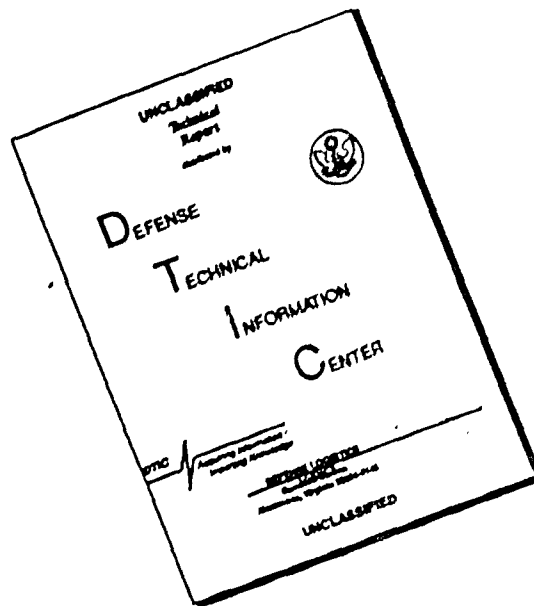
PHILCO

CORPORATION WESTERN DEVELOPMENT LABORATORIES

647 700

XEROX

DISCLAIMER NOTICE



THIS DOCUMENT IS BEST QUALITY AVAILABLE. THE COPY FURNISHED TO DTIC CONTAINED A SIGNIFICANT NUMBER OF PAGES WHICH DO NOT REPRODUCE LEGIBLY.

ORAL PROGRAM ARPA Order 8-58,
ORAL PROGRAM Satellite Index Series
Index No. 31 to 34 series

ARPA Program Order Contract No.
68-04-200-703-ORD-1002 for the
Ballistic Research Laboratories,
Aberdeen Proving Ground, Maryland.

Department of the Army Project No.
5B03-C5-011

Ordinance Management Structure Code
to 5210 11, 115

Ordinance Research and Development
Project No. 5B3-C538

POLYSTATION DOPPLER SYSTEM

for

BALLISTIC RESEARCH LABORATORY

ABERDEEN PROVING GROUND

Aberdeen, Maryland

Contract DA-04-200-21X4992-509-ORD-1002

by

PHILCO CORPORATION

WESTERN DEVELOPMENT LABORATORIES

Palo Alto, California

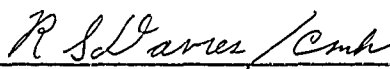
Submitted by


P. L. Besag
Project Engineer

Approved by


C. M. Hammack
Doppler Group Supervisor

Approved by


R. S. Davies
Advanced Programs Section Manager

PHILCO

GOVERNMENT & INDUSTRIAL GROUP
WESTERN DEVELOPMENT LABORATORIES

TABLE OF CONTENTS

<u>Section</u>		<u>Page</u>
1	INTRODUCTION	1-1
	1.1 Reason for the Study and Statement of Problem Conditions	1-1
	1.2 Scope	1-1
2	RESULTS AND CONCLUSIONS	2-1
3	RECOMMENDATIONS FOR FUTURE WORK	2-1
4	SYSTEM DESCRIPTION	4-1
	4.1 General	4-1
	4.2 Configuration	4-1
	4.3 Operation	4-1
	4.4 System Synthesis Assumptions and Definitions . .	4-2
	4.5 System Synthesis	4-3
	4.6 Selection of Optimum Beamwidth	4-4
	4.7 Error Propagation for Fixed Beamwidth	4-4
	4.8 Statistical Evaluation of the System	4-5
5	DATA REDUCTION	5-1
	5.1 Wavelength	5-1
	5.2 Time Duration of Cycle Count	5-1
	5.3 Cycle Count	5-1
	5.4 Station Location	5-2
	5.5 Range-Sum Differences from Cycles Counted	5-2
	5.6 Position Determination	5-2
	5.7 Velocity Determination	5-7
6	TEST CASE FOR DATA REDUCTION MODEL	6-1
	6.1 Feasibility Study	6-1
7	ERROR PROPAGATION STUDY	7-1
	7.1 General Discussion	7-1
	7.2 Position Derivations	7-4
	7.3 Velocity Derivations	7-5
<u>Appendixes</u>		
A.	NOTATION	A-1
B	GENERATION OF SYNTHETIC ORBIT DATA	B-1
C	ILLUSTRATIONS	C-1

SECTION 1

INTRODUCTION

1.1 Reason for the Study and Statement of Problem Conditions

The Ballistics Research Laboratory (BRL) has developed an iterative method to determine orbital parameters. A need exists to have an initial approximation correct to approximately 10 per cent. This study has been undertaken by the Philco Western Development Laboratories to determine a method for finding initial values. Errors of less than 50 to 75 miles in position, and 1/2 to 1 mile/sec in velocity are specified.

The following conditions were specified for the system:

- a. Method: Polystation Doppler
- b. Ability: Acquire and track a body to 1000 miles altitude.
- c. Limitations:
 - (1) No knowledge of vehicle position prior to acquisition
 - (2) No assumption about the nature of the path
 - (3) No cooperative equipment aboard the vehicle.

1.2 Scope

An error study was performed to determine the dependence of rms error in position and velocity on rms error in the observed quantities. The latter were assumed equal and independent. The error matrix was calculated for a number of circular orbits passing through points in a pre-assigned grid.

A mathematical model was constructed for data reduction.

Position-finding consists of a system of fourteen linear equations solved for approximate values of the position coordinates. These are then adjusted by the standard least square method to their maximum-likelihood values. For technique, see flow chart (Fig. 2a)

For velocity, the interval immediately following the vehicle's passage through the grid plane is considered. For this interval, readings to two stations are used, in conjunction with the adjusted position coordinates, to find approximate values of the horizontal and vertical velocity components. These are then adjusted to their maximum-likelihood values by the use of least squares technique on all four of the readings available for this interval.

Test cases were designed for the mathematical model using circular orbits passing through points in a grid in the fan beam's central plane. The orbit plane inclination was varied through several different values (see Section 4.8 and Fig. 4). For sequence of steps see flow chart, Fig. 3.

SECTION 2

RESULTS AND CONCLUSIONS

The error study made indicates that the BRL conditions can be met by the proposed system. Errors of the order of ten wavelengths can be tolerated at 300 mc. The error study which was performed for circular orbits, resulted in data which is presented in the form of graphs, some as curves and some as straight-line graphs.

To permit selection of optimum beamwidth, errors were studied for values from 8° to 30° . For evaluation of the selected case, charts are presented for constant beamwidths. In order to aid in evaluating a system after beamwidth has been decided upon, graphs of error propagation factors were plotted holding beamwidth constant.

SECTION 3

RECOMMENDATIONS FOR FUTURE WORK

First in priority for further work would be continuation of the test case computation for the data reduction model. (See Section 6)

Second, as a less major task, a more realistic error calculation for the special case of minimum-time-in-beam orbits should be done

Third, it would be desirable to vary the number of time increments. This might decrease the accuracy of the approximate values determined, but would improve the least squares adjustments. There is reason to believe a net improvement would result.

Fourth, a review of the conditions imposed on the system reveals that the most stringent are embodied in the following two assumptions:

- a Passage through the beam's mid plane is assumed to occur at mid-time
- b Time of entry into and exit from the inner beam are assumed known

In the present system it is the coordinates of this 'piercing point' for which the system is solved. Unless the vehicle is so cooperative as to maintain a velocity configuration and reflection characteristics so that it actually does pierce the mid-plane at the mid-time between first and last discernible signals, there is no reason to suppose that this assumption will hold in an operational system. Of course, this point is always discernible if a split beam is employed. However, in the process of writing the final report, it was determined that both of these conditions could be removed for a fan beam as well and thus permit the solution of the system for any point on the path of the vehicle as it travels through the beam. Further, it is possible to commence and cease taking readings at will, rather than having to assume that reading commence simultaneously with entry into the beam and cease simultaneously with exit from the beam. Uncertain boundary knowledge of the beam renders this technique questionable. For the above reasons, it is strongly suggested that the scope of the present task be extended to include a thorough investigation of the above system.

SECTION 4

SYSTEM DESCRIPTION

4.1 General

The Polystation Doppler System has the ability to acquire and track a moving vehicle. A system is said to acquire if it can determine the position of a body without prior knowledge of its position or velocity. A system is said to track if it can find successive points on a vehicle's path using prior position information. A Doppler Polystation System as used herein refers to an acquisition and tracking system of more than one station which gathers only information regarding diminution or augmentation of received cycles due to motion of the vehicle relative to the station complex.

This particular system must be able to acquire and track any vehicle up to 1000 miles in altitude. The region of coverage is 800 miles long and 1000 miles high, and is limited laterally by the sides of a wedge-shaped beam.

4.2 Configuration

The system is composed of four receivers and one transmitter, located along an arc of a great circle, with the transmitter at one end of the array. All RF signals are transmitted from the ground, reflected from the vehicle and received at four ground stations. No equipment is required aboard the vehicle. A computer to reduce data from the tracking system is the only other equipment required.

4.3 Operation

A continuous signal of constant frequency is transmitted from a ground station. This signal is reflected from the vehicle and received by the several receivers. The time during which signals are received by all four receivers is the period of observation for collecting data to be reduced for position and velocity information. The distance from the transmitter to the vehicle plus the return to the receiver is defined as the range-sum.

During this interval a certain number of cycles are received. This is compared with the number of cycles transmitted in the same

time interval. Alternatively, having determined the total time of observation, divide it into a number of sub-intervals and determine the cycle count difference for these time increments. We shall do this in the following way. Take the total time of signal reception. Divide this into fourteen parts. Let the end of the seventh reading be the reference point. Calculate the cycle count differences received in intervals of time ending (for the first half) or beginning (for the second half) at this reference time. These will be denoted by Δ_{1j} . They will represent the range-sum differences between the i^{th} time and the reference time measured in wavelengths; that is, Δ_{1j} is the increase or decrease in the range-sums. The difference between the transmitted cycle count and received cycle count of the i^{th} time and the reference time ($t = 0$) is determined by using a common time reference. The data is presented to a computer which solves for vehicle position and velocity. The time at the center of the total time of observation is determined and position and velocity for that time are determined. Knowing this point, position coordinates are easily determined for the other times.

4.4 System Synthesis Assumptions and Definitions

The operational requirements of this system do not demand any assumptions about the shape of the earth or its rotation. The only requirement is that the five stations be co-planar. In synthesizing a system for discussion in this report, a spherical earth was assumed for computational convenience in placing the ground stations along a great circle. In the study of error as a function of grid position (g-dop), circular orbits were chosen because they were sufficiently general to permit reliable conclusions to be drawn, yet not so complex as to hamper the study or draw attention from the true purpose. The term "cycle count" is defined as the number of doppler cycles counted in some definite time selected for measurement, as opposed to "frequency" which usually indicates the number of cycles in one second.

Position is referenced to a right-handed Cartesian coordinate system, rotating with the earth, centered at the transmitter, and oriented as follows. (1) The x-axis passes through the transmitter and the last receiver, positive in the direction of the receiver; (2) the z-axis lies in the plane of the stations and passes through the transmitter, positive

"upward" relative to the earth; (3) the y-axis is chosen to complete a right-handed Cartesian system.

Approximate position and velocity data are determined by the solution of certain condition equations. It is assumed that these values sufficiently coincide with the true values to warrant a first order approximation. These unadjusted solutions are used as input to the least squares adjustment technique. This does not mean that this is an iterative technique. One, and only one, adjustment in values is made.

The effects of both special and general relativity were studied. In both cases, the effects were found to be non-existent. Special relativistic effects are cancelled since the transmitter and receivers do not move relative to each other. The possible introduction of an effect due to accelerations of the vehicle relative to the station complex are nullified by assuming that the energy is reflected from the vehicle in zero time.

General relativistic effects are also non-existent. In the proposed system the stations are all located on the surface of a spherical earth. Therefore, all stations are at the same gravitational potential. While this will not be absolutely true for any operational system, nevertheless the anticipated variation in gravity potential at different station locations would be beyond the precision of measurement in the foreseeable future.

4.5 System Synthesis

Having defined the coordinate system, the coordinates of the ground stations may be defined as follows. (1) Successive ground stations are located so that the differences of their x coordinates are equal. (2) Since the ground stations lie along a great circle and the x-axis is defined as a chord intersecting the circle at the transmitter and the most remote receiver, the z-coordinates are determined by knowing the radius of the earth, see Appendix B.4.1. (3) The y-coordinates are, of course, zero. Thus, viewed as points in the x-z plane, the transmitter is located at (0,0) and the four receivers at $R_1(a,b)$, $R_2(2a,c)$, $R_3(3a,b)$, $R_4(4a,0)$. (See Appendix B.4.1 for derivation of expressions for b,c.) (See Figure 5.) The only condition required by this system is that the five stations be co-planar For computational convenience we assume they are located along a great circle on the surface of a spherical earth.

In our case, the x-coordinate difference referred to in (1) was taken at 200 miles. The resulting values of z were, respectively, for the four receiving stations, approximately 15, 20, 15, 0 miles. Exact figures are derived in Appendix B 4 1. The more accurate figures were used in all computations in order to preserve consistency with an assumed spherical earth of 4000 mile radius.

The direction and beamwidth of transmission and reception create a region of observation which is wedge shaped, with the center plane of symmetry being the az plane. The edge of the outermost wedge is the x-axis, the inner beam edge being tangent to the sphere at receiver three. (See Fig 4, The generating angle of the wedge is the beamwidth.

4 6 Selection of Optimum Beamwidth

To permit the selection of an optimum beamwidth, sigma matrices for position and velocity were calculated for beamwidths of 8° , 10° , 15° , 20° , 25° , and 30° . Charts of $\frac{\sigma_x}{\sigma_M}$, $\frac{\sigma_z}{\sigma_M}$, $\frac{\sigma_{\dot{x}}}{\sigma_M}$, and $\frac{\sigma_{\dot{z}}}{\sigma_M}$ are presented for

contours of constant altitudes for various combinations of horizontal displacement x_0 and orbital-plane angle. (See Fig 4 and Figs 6 to 14.) σ is the standard deviation and M is the range-sum difference.

4 7 Error Propagation for Fixed Beamwidth

Having selected a beamwidth, Figs 15 to 20, showing the behavior of

$\frac{\sigma_x}{\sigma_M}$, $\frac{\sigma_z}{\sigma_M}$, are presented as functions of altitude, holding constant x_0

(horizontal displacement) and \emptyset . Figures 21 to 28 are also presented

showing the behavior of $\frac{\sigma_x}{\sigma_M}$, $\frac{\sigma_z}{\sigma_M}$, as functions of horizontal displacement

for constant altitude and \emptyset . These charts are for constant beamwidths and are presented for values of 8° and 15° . By super-imposing on a light table, many of these 8° to 15° pairs of charts may be compared and interpolations performed to find σ values for intermediate values of beamwidth

4.8 Statistical Evaluation of the System

In order to demonstrate the statistical practicability of solving for position and velocity within the error bounds stipulated, a number of representative paths were synthetically generated. These paths pass through the beam at 35 places, intersecting the grid plane (the xz plane) at angles of 0, 15, 30, 45, 60, 75, 90 degrees at each grid point.* In order to synthesize a situation representative of operational conditions, circular orbits were selected which intersected the grid plane at points defined by distances of 50, 200, 350, 500, and 650 statute miles along the x-axis and distances of 150, 300, 450, 600, 750, 900, and 1050 statute miles along the z-axis. (See Fig. 4) The data resulting from this study are presented throughout the text. The equations of the model are included in Appendix B.

* Those for 90° , of course, lie in the grid plane.

SECTION 5

DATA REDUCTION

Approximate position and velocity data are determined by the solution of certain condition equations. It is assumed that these values coincide sufficiently with the true values to warrant a first order approximation. This is equivalent to saying that the value of the variance-covariance matrix does not change appreciably in the region containing both the adjusted and true values.

This does not mean that the mathematical model requires an initial point or prior knowledge of the vehicle's movement. It means that the model only requires that the (as yet unadjusted) solutions to the model's equations be sufficiently free from arithmetic error propagation to warrant the first order approximations, for it is these unadjusted solutions that are used as input to the least squares adjustment technique.

It has not been implied that this is an iterative technique. One, and only one, adjustment in values is made. If the unadjusted value is close enough to the correct values to warrant the first order assumptions made, the adjusted value may be shown to be the maximum-likelihood value in a least-squares sense.

5.1 Wavelength

In this system wavelength, λ , is assumed to be known, since the transmitter is on the ground.

5.2 Time Duration of Cycle Count

The time of entry is defined as the first point in the beam at which the vehicle is simultaneously observed by all four receivers. We shall assign as the time of exit from the beam, a point which is symmetric to the entry point on the opposite side of the grid plane. Zero time will be the time of passage through the grid plane, the centermost plane of the beam.

5.3 Cycle Count

Information is received in the form of a plot of doppler frequency in cycles/sec vs time in seconds at each of the four receiver locations for the full period of time (t_{in} to t_{out}) that the vehicle is in the beam.

of antenna 2 This may then be integrated to yield total cycles counted in any given interval

Alternatively, cycles may be counted directly, thus eliminating several steps. It may be possible to utilize the computer itself as a counter This would be especially attractive since many modern computers could serve as a self-contained time reference while accepting and processing data in real time

5.4 Station Location

It is assumed that the position of the receiver stations (X_j, Z_j) relative to one another and to the transmitter are known to the necessary accuracy. As described earlier (see Section 4, System Description) all results are relative to a coordinate system moving with the stations

5.5 Range-Sum Differences from Cycles Counted

The observed values of range-sum differences will be referred to as M_{ij} or M_k and will be determined as follows:

$$M_{ij} \begin{cases} = \left[c (i-8)\Delta t - Q_{ij} \right] / \lambda & i = 1, \dots, 7 \\ = \left[c (i-7)\Delta t - Q_{ij} \right] / \lambda & i = 8, \dots, 14 \end{cases} \quad j = 1, \dots, 4$$

where c is the velocity of propagation in miles per second and λ is the wavelength of the transmitted frequency in miles

When written with a single subscript $M_k = M_{ij}$

for $k = j + 4 (i-1) \quad j = 1, \dots, 4$

and $k = 1, \dots, 56 \quad i = 1, \dots, 14$

5.6 Position Determination

5.6.1 Range-Sums (Approximate) From Range-Sum Differences

Let r_{ij} denote the distance from the transmitter to the i^{th} vehicle position to the j^{th} station; r_{ic} , the distance from the transmitter to the vehicle position; r_{ij} , the distance from the i^{th} vehicle position to the j^{th} receiver; (X_j, Z_j) the coordinates of the j^{th} ground station (note that the transmitter is at the origin); and (x_o, z_o) the coordinates of any point in the grid plane.

$$\rho_{ij} = r_{io} + r_{ij}$$

$$\rho_{ij} - r_{io} = r_{ij}$$

Therefore

$$r_{io}^2 = x_i^2 + y_i^2 + z_i^2$$

$$r_{ij}^2 = (x_i - x_j)^2 + (y_i - y_j)^2 + (z_i - z_j)^2$$

Let

$$d_j^2 = x_j^2 + z_j^2$$

Then

$$(\rho_{ij} - r_{io})^2 = (r_{ij})^2$$

and therefore

$$\rho_{ij}^2 - 2 r_{io} \rho_{ij} + r_{io}^2 = r_{ij}^2 = 2 x_j x_i - 2 z_j z_i + d_j^2$$

and so

$$2 x_j x_i + 2 z_j z_i - 2 \rho_{ij} r_{io} = \rho_{ij}^2 - d_j^2$$

Four equations of this form may be written in determinant form as follows (ρ_{oj} is written as ρ_j for convenience)

$$f_o = f = \begin{vmatrix} \rho_1^2 & d_1^2 & \rho_1 & x_1 & z_1 \\ \rho_2^2 & d_2^2 & \rho_2 & x_2 & z_2 \\ \rho_3^2 & d_3^2 & \rho_3 & x_3 & z_3 \\ \rho_4^2 & d_4^2 & \rho_4 & x_4 & z_4 \end{vmatrix} = 0$$

The determinant is zero since $2z_i$ column (4) + $2x_i$ column (3) - $2r_{io}$ column (2) = column (1)

Now this equation is valid for any point (x_i, y_i, z_i) in space

When this is written for the i^{th} vehicle position,

$$f_i = \begin{vmatrix} (\rho_1 + M_{i1})^2 - d_1^2 & \rho_1 + M_{i1} & x_1 & z_1 \\ (\rho_2 + M_{i2})^2 - d_2^2 & \rho_2 + M_{i2} & x_2 & z_2 \\ (\rho_3 + M_{i3})^2 - d_3^2 & \rho_3 + M_{i3} & x_3 & z_3 \\ (\rho_4 + M_{i4})^2 - d_4^2 & \rho_4 + M_{i4} & x_4 & z_4 \end{vmatrix} = 0$$

By subtraction, $g_i = f_i - f = 0$ which may be written in the form

$$g_i = \sum_{p=1}^{14} \alpha_{ip} U_p - \beta_i = 0$$

(These will be used as condition equations for the least squares adjustment.)

Where

$$\begin{array}{lll} U_1 = \rho_1 & U_5 = \rho_1^2 & U_9 = \rho_1 \rho_2 & U_{13} = \rho_2 \rho_4 \\ U_2 = \rho_2 & U_6 = \rho_2^2 & U_{10} = \rho_1 \rho_3 & U_{14} = \rho_3 \rho_4 \\ U_3 = \rho_3 & U_7 = \rho_3^2 & U_{11} = \rho_1 \rho_4 & \\ U_4 = \rho_4 & U_8 = \rho_4^2 & U_{12} = \rho_2 \rho_3 & \end{array}$$

The solution U_1, \dots, U_{14} of these fourteen "pseudo" linear equations will be treated as approximations $\rho_1^0, \rho_2^0, \rho_3^0, \rho_4^0$ to the true ρ_j .

5.6.2 Range-Sums to Rectilinear Grid Coordinates

Using three (say ρ_k, ρ_1, ρ_m) out of four of the $\rho_1^0, \dots, \rho_4^0$, the values x_o^0, z_o^0 and incidentally r_o^0 , may be found by solving

$$2X_k x_o^0 + 2Z_k z_o^0 - 2\rho_k^0 r_o^0 = (d_k)^2 - (\rho_k^0)^2$$

$$2X_1 x_o^0 + 2Z_1 z_o^0 - 2\rho_1^0 r_o^0 = (d_1)^2 - (\rho_1^0)^2$$

$$2X_m x_o^0 + 2Z_m z_o^0 - 2\rho_m^0 r_o^0 = (d_m)^2 - (\rho_m^0)^2$$

For example

$$x_o^0 = \frac{\begin{vmatrix} d_k^2 - (\rho_k^0)^2 & Z_k & \rho_k^0 \\ d_1^2 - (\rho_1^0)^2 & Z_1 & \rho_1^0 \\ d_m^2 - (\rho_m^0)^2 & Z_m & \rho_m^0 \end{vmatrix}}{\begin{vmatrix} X_k & Z_k & \rho_k^0 \\ X_1 & Z_1 & \rho_1^0 \\ X_m & Z_m & \rho_m^0 \end{vmatrix}} = \frac{N}{D}$$

(It is not suggested Cramer's rule be applied in actual cases. Modern matrix inversion techniques almost invariably yield more reliable results.)

The "best" set c_k, c_1, c_m may be determined by evaluating the Jacobian, J , of the transformation for the $C_3^4 = 4$ possible combinations of $c_1^0, c_2^0, c_3^0, c_4^0$

$$J = \begin{vmatrix} \frac{\partial x_o^0}{\partial c_k} & \frac{\partial z_o^0}{\partial c_k} & \frac{\partial r_o^0}{\partial c_k} \\ \frac{\partial x_o^0}{\partial c_1} & \frac{\partial z_o^0}{\partial c_1} & \frac{\partial r_o^0}{\partial c_1} \\ \frac{\partial x_o^0}{\partial c_m} & \frac{\partial z_o^0}{\partial c_m} & \frac{\partial r_o^0}{\partial c_m} \end{vmatrix}$$

For example

$$\frac{\partial x_o^0}{\partial c_k} = \frac{N \begin{vmatrix} X_k & Z_k & 1 \\ X_1 & Z_1 & 0 \\ X_m & Z_m & 0 \end{vmatrix} + D \begin{vmatrix} 2c_k^0 & 0 & .1 \\ d_1^2 \cdot c_1^0 & Z_1 & c_1^0 \\ d_m^2 \cdot c_m^0 & Z_m & c_m^0 \end{vmatrix}}{D^2}$$

5.6 3 Residuals

Using approximations x_o^0, z_o^0 rather than true values will cause the condition equations to yield non-zero values. Therefore, we shall define ϵ_i as the residual of the i^{th} condition function

$$g_i(x_o^0, z_o^0) = \sum_{j=1}^{14} \alpha_{ij} U_j^0 - \beta_i = \epsilon_i \quad i=1, \dots, 14$$

Where

U_j is evaluated at $x = x_o^0, z = z_o^0$

5 6.4 Least Squares Adjustment

The observed values M_k ($k = 1, \dots, 56$) and the 2 approximate parameters x_o, z_o will be adjusted to satisfy the condition equations while simultaneously minimizing the sum of the squares of the M_k adjustments δ_k ; each observation is given equal weight since the errors in the M_k were assumed of equal variance (see Sec. 7.2)

Consider the 14 condition equations, r_i , $i=1, \dots, 14$ (see Section 5.6.1)

Let the column vector of the residuals ϵ_i be E

$$E = \begin{bmatrix} \epsilon_1 \\ \vdots \\ \epsilon_{14} \end{bmatrix} \quad A = \left\| \frac{\partial g_i}{\partial M_k} \right\|; \quad B = \left\| \frac{\partial g_i}{\partial x_0} \quad \frac{\partial g_i}{\partial z_0} \right\|; \quad \delta = \begin{bmatrix} \delta_1 \\ \vdots \\ \delta_{14} \end{bmatrix}$$

Let

$$\begin{bmatrix} x_0 \\ v \\ z_0 \end{bmatrix} = V \quad \text{be the correction vector of} \quad \begin{bmatrix} x_0 \\ x_z \end{bmatrix}$$

The condition equations can be expanded as Taylor series and retaining only the first powers and constant terms, they become

$$h_i = \sum_{k=1}^{56} a_{ik} \delta_k + \sum_{q=1}^2 b_{iq} v_q + \epsilon_i = 0$$

or in matrix form

$$A \delta + B V + E = 0$$

Define the sum of squares to be minimized as s and subtracting 14 zero terms as follows

$$s = \frac{1}{2} \sum_{k=1}^{56} \delta_k^2 - 2 \sum_{i=1}^{14} \lambda_i h_i$$

where the λ_i are a set of 14 Lagrange multipliers whose column matrix is λ .

To obtain a minimum, differentiate s with respect to δ_k and v_q and equate the resulting expressions to zero.

$$\frac{1}{2} \frac{\partial s}{\partial \delta_k} = \frac{1}{2} \frac{\partial}{\partial \delta_k} \sum_{k=1}^{56} \delta_k^2 - \sum_{i=1}^{14} \lambda_i a_{ik}$$

$$\frac{1}{2} \frac{\partial s}{\partial v_q} = \sum_{i=1}^{14} \lambda_i b_{iq}$$

Let τ^0 be a diagonal matrix each element of which has the value σ_M^2

These expressions may be written in matrix form as

$$\begin{aligned} (\sigma^0)^{-1} \delta + A^T \lambda &= 0 \\ B^T \lambda &= 0 \end{aligned}$$

then

$$\delta = -(\sigma^0)^{-1} A^T \lambda \text{ and}$$

$$A \delta - B^T \lambda + E = 0 \text{ becomes}$$

$$A (\sigma^0)^{-1} A^T \lambda + B^T \lambda + E = 0 \text{ or}$$

$$\lambda = (A \sigma^0 A^T)^{-1} (B^T \lambda + E) \text{ and}$$

$$B^T (A \sigma^0 A^T)^{-1} (B^T \lambda + E) = 0$$

therefore

$$V = (B^T (A \sigma^0 A^T)^{-1} B^T)^{-1} (B^T (A \sigma^0 A^T)^{-1} E)$$

Let

$$H = B^T (A \sigma^0 A^T)^{-1} B^T$$

$$N = H^{-1}$$

(N^{-1} may be a desired output,

then

$V = N^{-1} H E$ is determined as the column matrix of the adjustments and the adjusted values of x , z are obtained from

$$\begin{bmatrix} x \\ z \end{bmatrix} = x^0 + V$$

5.7 Velocity Determination

5.7.1 Definitions and Assumptions

Velocity, as used here, is defined as the average velocity in the interval Δt immediately following passage through the beam's central plane

In the determination of velocity, it is assumed that the adjusted values of the position coordinates are available

5.7.2 Condition Equations

Refer to Section 5.6.1 on position finding condition equations for definitions

The four condition equations for velocity are:

$$\frac{\dot{M}_{ij}}{\Delta t} = x_o \frac{\partial \rho_j}{\partial x_o} + z_o \frac{\partial \rho_j}{\partial z_o} \quad j = 1, 4$$

where

$$\frac{\partial \rho_j}{\partial x_o} = \frac{x_o}{r_o} + \frac{x_o \cdot X_j}{r_j}$$

$$\frac{\partial \rho_j}{\partial z_o} = \frac{z_o}{r_o} + \frac{z_o \cdot Z_j}{r_j}$$

As may be seen $\frac{\partial \rho_j}{\partial x_o}$ and $\frac{\partial \rho_j}{\partial z_o}$ are evaluated for the

adjusted values x_o , z_o of position

Of these four equations, one particular pairing may yield better results than all others. To determine which set of two will yield best results, the Jacobian of the transformation $M_p, M_q \rightarrow x_o^o, z_o^o$ may be evaluated for each of the $C_2^4 = 6$ cases

$$J = (\Delta t)^2 \begin{vmatrix} \frac{\partial \rho_p}{\partial x_o} & \frac{\partial \rho_p}{\partial z_o} \\ \frac{\partial \rho_q}{\partial x_o} & \frac{\partial \rho_q}{\partial z_o} \end{vmatrix}$$

Where the elements of J are evaluated for $x = x_o$, $z = z_o$

The solution of this system will yield values of velocity components which we view as approximations. These will be denoted by \dot{x}_o^o and \dot{z}_o^o .

5.7.3 Residuals

Define $\epsilon_j + 14$ $j = 1, 2, 3, 4$ as follows.

$$\frac{\partial g_j}{\partial t} - x_0 \frac{\partial \rho_j}{\partial x_0} - z_0 \frac{\partial \rho_j}{\partial z_0} = \epsilon_p$$

where $p = j + 14$

Using approximate values x_0^0 and z_0^0 instead of true values will cause the $\epsilon_j + 14$ to be non-zero.

5.7.4 Least Square Adjustment

Let v_x , v_z denote the adjustments to \dot{x}_0^0 , \dot{z}_0^0 , and \dot{x}_0 , \dot{z}_0 the adjusted values. It is assumed that the adjusted values x_0 and z_0 used are error-less.

To find the corrections to \dot{x}_0^0 and \dot{z}_0^0 we evaluate

$$S^{-1} = \begin{pmatrix} \sigma_{xx} & \sigma_{xz} \\ \sigma_{zx} & \sigma_{zz} \end{pmatrix}$$

as in section 7.3 and the matrix

$$\begin{pmatrix} \frac{\partial \rho_1}{\partial x_0} & \dots & \frac{\partial \rho_4}{\partial x_0} \\ \frac{\partial \rho_1}{\partial z_0} & \dots & \frac{\partial \rho_4}{\partial z_0} \end{pmatrix} \quad \text{Then}$$

$$\begin{bmatrix} v_x \\ v_z \end{bmatrix} = (\Delta t)^2 \begin{pmatrix} \sigma_{xx} & \sigma_{xz} \\ \sigma_{zx} & \sigma_{zz} \end{pmatrix} \begin{pmatrix} \frac{\partial \rho_1}{\partial x_0} & \dots & \frac{\partial \rho_4}{\partial x_0} \\ \frac{\partial \rho_1}{\partial z_0} & \dots & \frac{\partial \rho_4}{\partial z_0} \end{pmatrix} \begin{pmatrix} \epsilon_{15} \\ \epsilon_{16} \\ \epsilon_{17} \\ \epsilon_{18} \end{pmatrix}$$

$$\text{and so } \begin{bmatrix} x_0 \\ z_0 \end{bmatrix} = \begin{bmatrix} \dot{x}_0^0 \\ \dot{x}_0^0 \\ \dot{z}_0^0 \\ \dot{z}_0^0 \end{bmatrix} + \begin{bmatrix} v_x \\ v_x \\ v_z \\ v_z \end{bmatrix}$$

SECTION 6

TEST CASE FOR DATA REDUCTION MODEL

6.1 Feasibility Study

In order to show the feasibility of the data reduction method described in section 5 a typical case was selected for simulation on a computer. This work was in progress at the termination of the contract. The following is a description of the proposed test case, (see flow chart, Figure 3). At the time of cessation of work, the matrix involved in position finding had not been inverted. It presently developed that this was due to calculation of erroneous coefficients. A delay caused by the unavailability of the computer and subsequent funds shortages did not permit the simulation of the typical case to be resumed. As mentioned in Section 3, it is hoped that an extension in scope of the present work may permit us to pursue this investigation.

Synthetic data was generated for the minimum beam width of 8° and $x_c = 400$, $z_c = 450$, $\theta = 75^\circ$, and a circular orbit using the methods of Appendix B. As in an actual case, an approximate position was to have been found, then adjusted. See section 5 for technique.

In the calculation of the position variance-covariance matrix for the least squares adjustment of position in the test case, the approximate values of x_c and z_c are used rather than the true grid point coordinates. This is done to simulate most closely operational conditions. For velocity, we proceed as follows. Using the corrected values of x_c and z_c , x_o^0 and z_o^0 are found, and these are then corrected using least squares as before. (See section 5).

SECTION 7

ERROR PROPAGATION STUDY

7.1 General Discussion

This section describes the method used in the preparation of the σ/σ curves. (There is, therefore, some duplication between this section and the discussion of least squares in Section 5, Data Reduction.) To permit the selection of an optimum beamwidth, the position error matrix, M^{-1} , and the velocity error matrix, S^{-1} , were calculated for beamwidths of 8° and $10.5:30^\circ$.

7.1.1 Results

Charts of $\frac{\sigma_x}{\sigma_M}$, $\frac{\sigma_z}{\sigma_M}$, $\frac{\sigma_x}{\sigma_M}$, $\frac{\sigma_z}{\sigma_M}$ vs beamwidth as abscissa are

presented for contours of constant altitude, z_0 , for various combinations of horizontal displacement x_0 and circular orbit inclination (Figures 6 to 14).

Having selected a beamwidth, line charts showing the behavior of $\frac{\sigma_x}{\sigma_M}$, $\frac{\sigma_z}{\sigma_M}$ are presented as functions of altitude (z_0), holding x_0 and θ constant (see Figures 15 to 20). Charts are also presented showing the behavior of $\frac{\sigma_x}{\sigma_M}$, $\frac{\sigma_z}{\sigma_M}$, $\frac{\sigma_x}{\sigma_M}$, $\frac{\sigma_z}{\sigma_M}$ as a function of horizontal displacement (x_0), for constant altitude (z_0), and for orbit plane angle (θ) (see Appendix C for complete list of Figures).

7.1.2 Derivation

The variance-covariance matrix among the set of variables M_1, \dots, M_{56} is a symmetrical square array whose elements are the expected values of the cross products of the errors in the M 's

$$\sigma_{M_i M_j} = E(\Delta M_i \Delta M_j)$$

$$\sigma_{MM}^T = \begin{vmatrix} \sigma_{M_1 M_1} & \sigma_{M_1 M_{56}} \\ \sigma_{M_{56} M_1} & \sigma_{M_{56} M_{56}} \end{vmatrix}$$

$\sigma_{M_i M_i} = E [(\Delta M_i)^2] = \sigma_{M_i}^2$ is the variance. The notation σ_{MM}^T arises from considering the column matrix of the M_i ; thus

$$M M^T = \begin{bmatrix} M_1 \\ \vdots \\ M_{56} \end{bmatrix} \begin{bmatrix} M_1 & \dots & M_{56} \end{bmatrix} = \begin{bmatrix} M_1 M_1 & \dots & M_1 M_{56} \\ \vdots & & \vdots \\ M_{56} M_1 & \dots & M_{56} M_{56} \end{bmatrix}$$

Suppose that y_j ($j = 1, 2$) are a set of variables which are functions of M_k

$$y_1 = x_0 (M_1, \dots, M_{56})$$

$$y_2 = z_0 (M_1, \dots, M_{56})$$

then

$$\Delta y_j = \sum_{i=1}^{56} \frac{\partial y_j}{\partial M_i} \Delta M_i$$

And

$$\begin{aligned} \Delta y_j \Delta y_k &= \left(\sum_{i=1}^M \frac{\partial y_j}{\partial M_i} \Delta M_i \right) \left(\sum_{q=1}^M \frac{\partial y_k}{\partial M_q} \Delta M_q \right) \\ &= \sum_{i=1}^M \sum_{q=1}^M \frac{\partial y_j}{\partial M_i} \frac{\partial y_k}{\partial M_q} \Delta M_i \Delta M_q \text{ and taking} \end{aligned}$$

expected values

$$\sigma_{y_j y_k} = \sum_{i=1}^M \sum_{q=1}^M \frac{\partial y_j}{\partial M_i} \frac{\partial y_k}{\partial M_q} \sigma_{M_i M_q};$$

then

$$\sigma_{YY}^T = \begin{bmatrix} \frac{\partial y_j}{\partial M_i} \end{bmatrix} \sigma_{MM}^T = \begin{bmatrix} \frac{\partial y_j}{\partial M_i} \end{bmatrix}^T.$$

Let the x and z coordinates of the grid point be denoted by x_0 and z_0 , respectively. ALL FUNCTIONS OF x AND z IN THIS SECTION WILL BE TREATED AS THOUGH EVALUATED AT $x = x_0$, $z = z_0$, $\dot{x} = \dot{x}_0$, $\dot{z} = \dot{z}_0$. Note for actual solution (including the test case): to adjust the approximate values, x_0^0 , z_0^0 and \dot{x}_0^0 , \dot{z}_0^0 , by the use of least squares methods, the variance-covariance matrix is calculated for these approximate values.

The values of the parameters for which σ/σ matrices are calculated as

$$x_0 = 50(150)650 \text{ statute miles}$$

$$z_0 = 150(150)1050 \text{ statute miles}$$

$$\phi = 0(15)90^\circ$$

$$\text{beamwidth} = b w = 8^\circ, 10(5)30^\circ$$

(For $\phi = 0^\circ$, the first run showed values of σ/σ which are probably the square of the true values ⁽¹⁾ This is due to the symmetry of this case which causes readings on the two sides of the central plane to be equal. This effectively reduces the amount of information by one-half and also diminishes the number of condition equations by one-half. It was intended that this case be re-run with a more irregular scale, but it was not possible to do so in the time remaining.)

Assumptions

- 1 Covariances $\sigma_{M_q M_p}$ of the observed quantities M_1, \dots, M_{56} are zero for $p \neq q$
- 2 Variances $\sigma_{M_p}^2$ of the observed quantities are equal for all p and will be denoted by σ_M^2 .
- 3 One observation is made for each of the quantities M_1, \dots, M_{56} .
- 4 Fourteen condition equations are used for position.
- 5 Four condition equations are used for velocity.
- 6 Second order terms in the Taylor expansion of the condition equations (written as residuals) may be ignored.
- 7 The variance-covariance matrix remains approximately constant in regions containing both the approximate and adjusted values.

(1) This hypothesis is made on the basis of a study of the trend in behavior of σ/σ as ϕ varies from 75° to 15° . Extrapolation seems to indicate a good fit for $\phi = 0$ for the square root of the values for the symmetric case

7.2 Position Derivations

The condition equations are

$$A^{(i)} - A^{(o)} = g_i (M_{ij}, x_o, z_o) = \epsilon_i \quad i = 1, \dots, 14$$

$$\text{Let } E = \begin{bmatrix} \epsilon_1 \\ \vdots \\ \epsilon_{14} \end{bmatrix}$$

$$A = \left\| a_{ik} \right\| = \left\| \frac{\partial \epsilon_i}{\partial M_k} \right\| \quad i = 1, \dots, 14 \quad k = 1, \dots, 56$$

Note: $a_{ik} \neq 0$ only for $k = j + 4 (i-1)$

$$j = 1, \dots, 14 \quad i = 1, \dots, 14$$

$$a_{ik} = 2 (\rho_j + M_{ij}) A_{j1}^{(i)} + A_{j2}^{(i)}$$

where

$j = k - 4 (i-1)$ and $A_{jq}^{(i)}$ is the jq^{th} cofactor (signed minor) of the determinant

$$A^{(i)} = \begin{vmatrix} (\rho_1 + M_{i1})^2 - d_1^2 & \rho_1 + M_{i1} & X_1 & Z_1 \\ (\rho_2 + M_{i2})^2 - d_2^2 & \rho_2 + M_{i2} & X_2 & Z_2 \\ (\rho_3 + M_{i3})^2 - d_3^2 & \rho_3 + M_{i3} & X_3 & Z_3 \\ (\rho_4 + M_{i4})^2 - d_4^2 & \rho_4 + M_{i4} & X_4 & Z_4 \end{vmatrix}$$

Let

$$B = \left\| b_{iq} \right\| = \left\| \frac{\partial \epsilon_i}{\partial x} \quad \frac{\partial \epsilon_i}{\partial z} \right\|$$

$$= \left\| \sum_{j=1}^4 \frac{\partial \epsilon_i}{\partial \rho_j} \quad \frac{\partial \rho_j}{\partial x} \quad \sum_{j=1}^4 \frac{\partial \epsilon_i}{\partial \rho_j} \quad \frac{\partial \rho_j}{\partial z} \right\|$$

Let

$$C = \left\| c_{ij} \right\| = \left\| \frac{\partial \epsilon_i}{\partial \rho_j} \right\| \quad \begin{matrix} i = 1, \dots, 14 \\ j = 1, \dots, 4 \end{matrix}$$

$$D = \left\| \frac{\partial \rho_1}{\partial x} \quad \frac{\partial \rho_1}{\partial z} \right\|$$

Then

$$c_{ij} = 2 (\rho_j + M_{ij}) A_{j1}^{(i)} + A_{j2}^{(i)} \\ - 2 \rho_j A_{j1}^{(0)} - A_{j2}^{(0)},$$

and

$$D = \left\| d_{jq} \right\| = \left\| d_{j1} \quad d_{j2} \right\| \\ = \left\| \frac{x}{r_o} + \frac{x - X_j}{r_j} \quad \frac{z}{r_o} + \frac{z - Z_j}{r_j} \right\| \\ j = 1, \dots, 4$$

$$\text{Note that } (r_o)^2 = (x)^2 + (z)^2$$

$$(r_j)^2 = (x - X_j)^2 + (z - Z_j)^2$$

Then $B = CD$

Let σ^0 be a diagonal matrix each element of which has the value σ_{MM} . In our case we assume the $\sigma_{MM} = \sigma_M^2$ are all equal and set $= 1$.

$$\text{Then let } H = B^T (A \sigma^0 A^T)^{-1} \\ = B^T (A A^T)^{-1}$$

and let $N = H B$

$$\text{then } N^{-1} = \begin{vmatrix} \sigma_{xx} & \sigma_{xz} \\ \sigma_{zx} & \sigma_{zz} \end{vmatrix}$$

7.3 Velocity Derivations

The condition equations are

$$\frac{M_{ij}}{\Delta t} - \dot{x}_o \frac{\partial \rho_j}{\partial x} - \dot{z}_o \frac{\partial \rho_j}{\partial z} = \epsilon_p$$

$$j = 1, \dots, 4 \quad p = j + 14$$

where

$$M_{8j} = M_k \text{ with } k = 28 + j$$

and where

$$\frac{\partial \rho_i}{\partial x} \text{ and } \frac{\partial \rho_i}{\partial z} \text{ - are evaluated for the adjusted } x_0 \text{ and } z_0.$$

$$\text{Let } A_v \equiv A_{\text{velocity}} = \left\| a_{rj} \right\| = \left\| \frac{\partial \epsilon_p}{\partial M_{8j}} \right\| \quad \begin{array}{l} r = 1, \dots, 4 \\ j = 1, \dots, 4 \\ p = r + 14 \end{array}$$

$$\begin{aligned} \text{Then } a_{rj} &= \frac{1}{\Delta t} \quad \text{for } r = j \\ &= 0 \quad \text{for } r \neq j \end{aligned}$$

$$\text{Let } B_v \equiv B_{\text{velocity}} \left\| b_{rq} \right\| = \left\| \frac{\partial \rho_p}{\partial x} \quad \frac{\partial \rho_p}{\partial z} \right\|$$

$$\begin{aligned} \text{Then } b_{p1} &= - \frac{\partial \rho_p}{\partial x} & r = 1, \dots, 4 \\ & & q = 1, 2 \\ b_{p2} &= - \frac{\partial \rho_p}{\partial z} & p = j + 14 \end{aligned}$$

$$\begin{aligned} S^{-1} &= \left[\begin{array}{cc} B_v^T & (A_v A_v^T)^{-1} B_v \end{array} \right]^{-1} \\ &= \left\| \begin{array}{cc} \sigma_{\dot{x}\dot{x}} & \sigma_{\dot{x}\dot{z}} \\ \sigma_{\dot{z}\dot{x}} & \sigma_{\dot{z}\dot{z}} \end{array} \right\| \end{aligned}$$

The curves for $\frac{\sigma_{\dot{x}}}{\sigma_M}$ and $\frac{\sigma_{\dot{z}}}{\sigma_M}$ are straight lines on log log paper,

(see Figures 6abcd to 14abcd), when plotted vs beamwidth, and so

$$\frac{\sigma_{\dot{x}}}{\sigma_M}, \quad \frac{\sigma_{\dot{z}}}{\sigma_M} = k (b.w.)^n. \quad \text{It turns out that in all cases } n = -1 \text{ and the}$$

value of k is 10 times the sigma ratio evaluated for $b.w. = 10^0$.

APPENDIX A

NOTATION

APPENDIX A NOTATION

x	horizontal dimension coordinate
y	transverse horizontal dimension coordinate
z	vertical dimension coordinate
x_0	x coordinate of grid point
z_0	z coordinate of grid point
t	time parameter
Δt	duration of single time increment Δt
i	vehicle path point index (reading index)
j	station index
g_i	condition equation functions
A	least squares matrix
$E()$	expected value of ()
E_i	residuals
H_{ij}, M_k, Δ_{ij} or Δ_k	range sum differences corresponding to the j^{th} reading at the i^{th} station. $k=4(i-1)+j$
R_1, \dots, R_4	receivers
T	transmitter
\emptyset	orbital plane inclination angle
ψ	beamwidth
ρ_{ij}	range-sum, i e distance transmitter-vehicle-ground.
$\sigma_{xx}, \sigma_{yy}^2$	variance
σ_{xz}	covariance
ρ_j	range sums to grid point
x_i	x coordinate of the i^{th} path-point
y_i	y coordinate of the i^{th} path-point
z_i	z coordinate of the i^{th} path-point
$x_0, z_0, \hat{x}_0, \hat{z}_0$	adjusted values of unknowns

$x_o^o, z_o^o, \dot{x}_o^o, \dot{z}_o^o$
approximate values of $x_o, z_o, \dot{x}_o, \dot{z}_o$
 $v_x, v_z, v_{\dot{x}}, v_{\dot{z}}$
adjustments for $x_o^o, z_o^o, \dot{x}_o^o, \dot{z}_o^o$ to obtain $x_o, z_o, \dot{x}_o, \dot{z}_o$
 Q_{ij}

observed total cycle counts.

Units lengths: miles (statute)
 time: seconds
 angles: degrees

APPENDIX B

GENERATION OF SYNTHETIC ORBIT DATA

B 3 Selection of Period of Cycle Count

Time of entry is artificially determined by incrementing time until an orbit point is found which lies inside the inner beam. (A point at which the vehicle is acquired by all receivers.) This will not, except in most unusual cases, be the actual time of entry.

B 3 1 Calculations of Δt for $\theta = 0$ (15) 75°

Calculate

$$(R + h) = \left[(x_0 - 2a)^2 + (z_0 - b')^2 \right]^{1/2}$$

$$\omega = \frac{1}{R} \frac{24 \times 10^{-3}}{(R + h)^{3/2}}$$

$$t^0 = \frac{1}{\omega} \sin^{-1} \frac{(z_0 - b') \tan \psi}{(R + h) \cos \theta}$$

$$t^1 = t^{i-1} + \Delta \quad (\text{in this case } \Delta = .2 \text{ sec})$$

Determine the smallest s such that

$$y(t^s) \leq \left[z(t^s) - c \right] \tan \psi$$

where

$$y(t) = (R + h) \cos \theta \sin \omega t$$

$$z(t) = b' + (x_0 - 2a) \sin \theta \sin \omega t + (-b' + z_0) \cos \omega t$$

Let

$$\Delta t = t^s //$$

Let

$$t_i = (i-8) \Delta t \quad 1 \leq i \leq 7$$

$$= (i-7) \Delta t \quad 8 \leq i \leq 14$$

$$= 0 \quad i = 0$$

B 3 2 Calculation of Δt for $\theta = 90^\circ$

For each of the 7 sets

$$x_0 = 400 \text{ miles } \theta = 90^\circ$$

$$z_0 = 150/150/1050 \text{ miles}$$

$$\text{Calculate } (R + h) = \left[(x_0 - 2a)^2 + (z_0 - b')^2 \right]^{1/2}$$

$$\omega = \frac{1.74 \times 10^{-3}}{\frac{R-h}{R} \cdot 3/2}$$

$$\Delta t = \frac{1}{\omega} \tan^{-1} \frac{2a}{z_0 b'}$$

B 4 Orbit Generation Equations

B 4 1 Position

Given "a" and assuming a constant earth radius R to each of the five stations

$$b = \left(R^2 - a^2 \right)^{1/2} - \left(R^2 - 2a^2 \right)^{1/2}$$

$$b = - \left(R^2 - (2a)^2 \right)^{1/2}$$

$$c = \left(R^2 - a^2 \right)^{1/2} - \left(R^2 - (2a)^2 \right)^{1/2}$$

See Figure 5

Compute 45 values $i = 0, \dots, 14$

$$x_i = 2a - b' + z_0 \sin \theta \sin \omega t_i + (x_0 - 2a \cos \omega t_i$$

$$y_i = (R - h \cos \theta \sin \omega t_i$$

$$z_i = b' + (x_0 - 2a) \sin \theta \sin \omega t_i + (-b' + z_0) \cos \omega t_i$$

B 4 2 Velocity

Compute the two values

$$x_0 = \omega (-b' + z_0 \sin \theta$$

$$z_0 = \omega (x_0 - 2a) \sin \theta$$

where $x_0 = x(x_0, z_0)$

B 5 Generation of Range Sums

Let ρ_{ij} denote range-sum. Compute the 56 values

$$\rho_{ij} = \left[x_i^2 + y_i^2 + z_i^2 \right]^{1/2} + \left[(x_i - x_j)^2 + y_i^2 + (z_i - z_j)^2 \right]^{1/2}$$

B 3

Compute the 5 values

$$r_0 = \left[x_0^2 + z_0^2 \right]^{1/2} \quad (x_0, 0, z_0) \text{ is a grid point}$$

$$r_j = \left[(x_0 - x_j)^2 + (z_0 - z_j)^2 \right]^{1/2} \quad 1 \leq j \leq 4$$

B 6 Range Sum Difference

Let

$$\Delta_{ij} = \rho_{ij} - \rho_{0j}$$

B 6.1 Introduction of Error into "true" Range-Sum Differences

In order to simulate realistic conditions, errors in Δ_{ij} may be introduced. This is usually done either by means of fixed bias errors or random error generation.

In any case let

$$M_{ij} = \Delta_{ij} + \text{error}_{ij}$$

In the errorless case, of course,

$$\Delta_{ij} = M_{ij}$$

APPENDIX C
ILLUSTRATIONS

PHILCO

GOVERNMENT & INDUSTRIAL GROUP
WESTERN DEVELOPMENT LABORATORIES

APPENDIX C

LIST OF ILLUSTRATIONS

<u>Figure Number</u>	<u>Title</u>
1	Flow Chart: Synthetic Data Generation
2a	Flow Chart. Data Reduction - Position
2b	Flow Chart. Data Reduction - Velocity
3	Flow Chart. Test Case
4	Beam Configuration
5	Station Configuration
6abcd to 14abcd	A plot of $\frac{\sigma_x}{\sigma_M}, \frac{\sigma_z}{\sigma_M}, \frac{\sigma_x}{\sigma_M}, \frac{\sigma_z}{\sigma_M}$ vs Beamwidth for fixed x and \emptyset , for constant contours of z.
15ab to 20ab	A plot of $\frac{\sigma_x}{\sigma_M}, \frac{\sigma_z}{\sigma_M}$ vs z for fixed x and Beamwidth, for constant contours of \emptyset
21ab to 28ab	A plot of $\frac{\sigma_x}{\sigma_M}, \frac{\sigma_z}{\sigma_M}$ vs x for fixed Beamwidth and \emptyset , for constant contours of z
29ab to 34 ab	A plot of $\frac{\sigma_x}{\sigma_M}, \frac{\sigma_z}{\sigma_M}, \frac{\sigma_x}{\sigma_M}, \frac{\sigma_z}{\sigma_M}$ vs z for fixed x and \emptyset , for constant contours of Beamwidth.
35abcd	A plot of $\frac{\sigma_x}{\sigma_M}, \frac{\sigma_z}{\sigma_M}, \frac{\sigma_x}{\sigma_M}, \frac{\sigma_z}{\sigma_M}$ vs z for fixed x and \emptyset , for constant contours independent of Beamwidth.

FLOW CHART: GENERATION OF SYNTHETIC ORBIT DATA

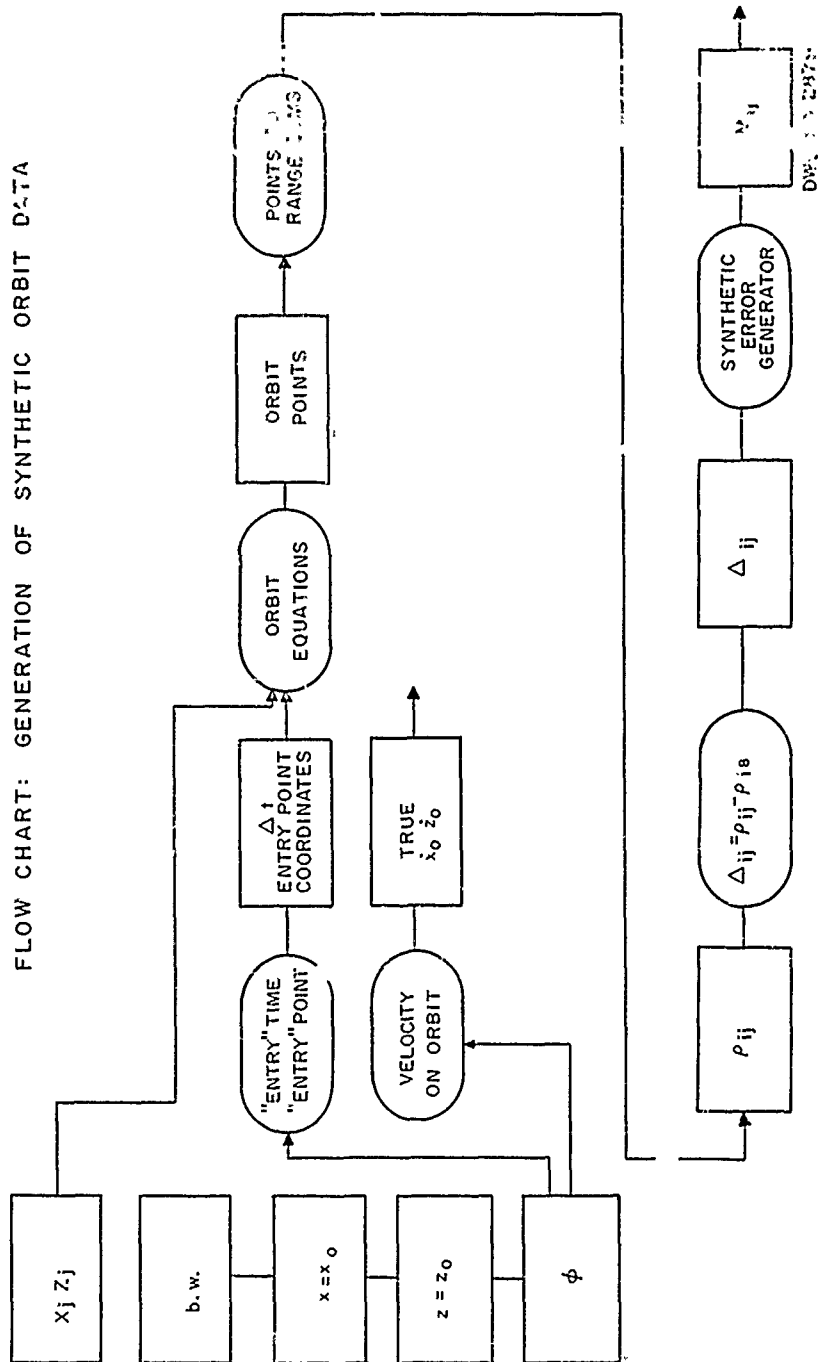


FIGURE 1

FLOW CHART: POSITION DETERMINATION

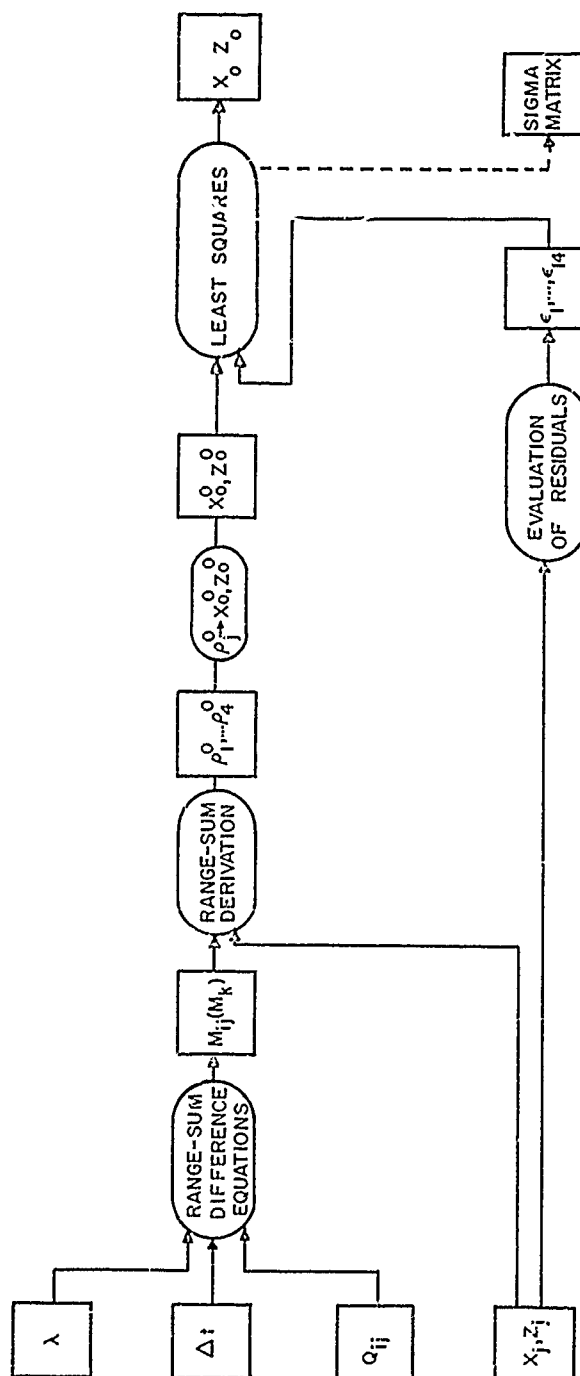


FIGURE 2a

FLOW CHART: VELOCITY DETERMINATION

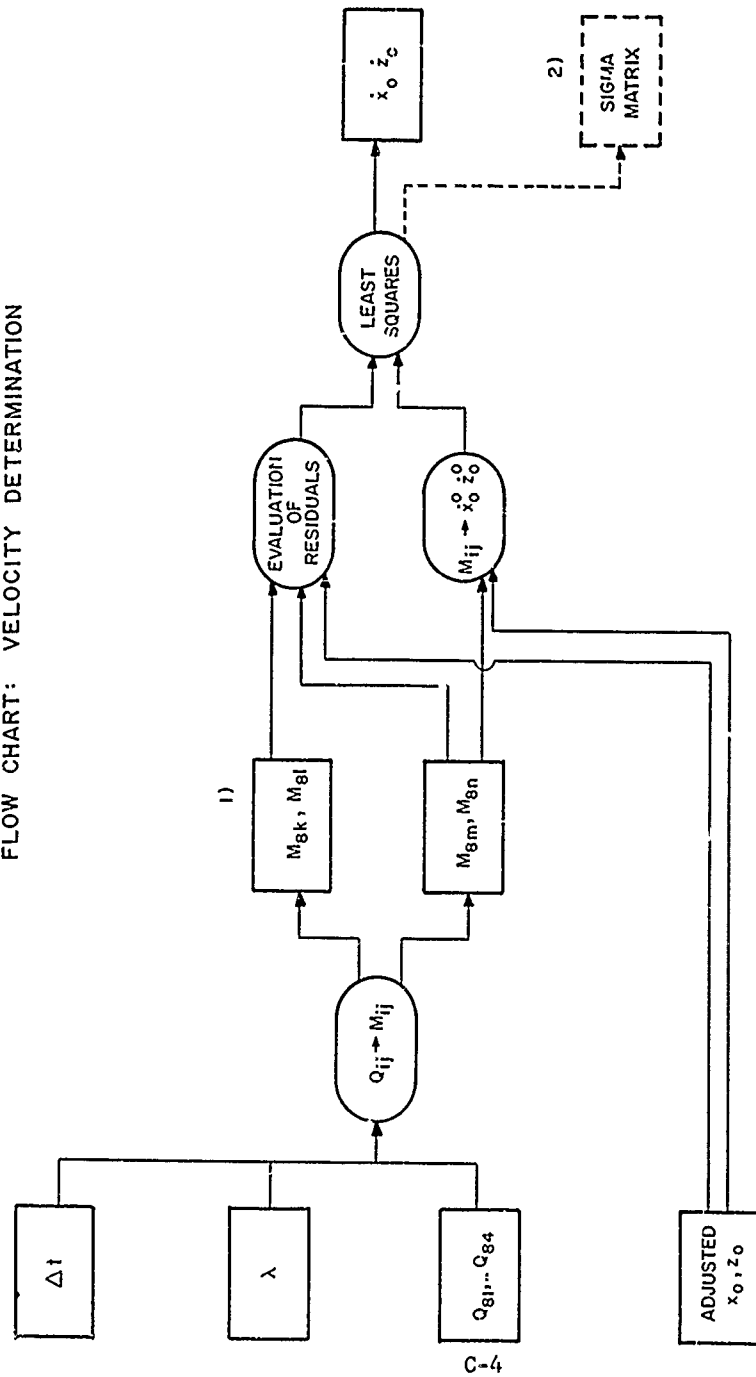


FIGURE 2 b

FLOW CHART: TEST CASE

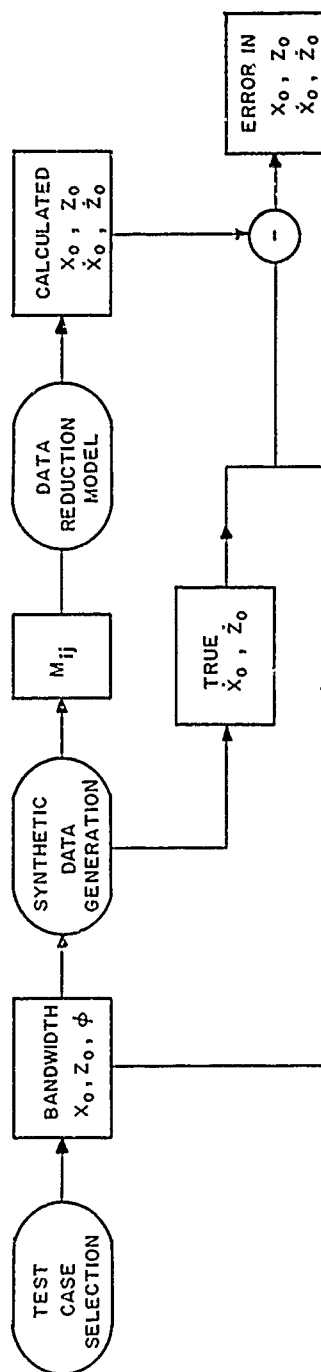
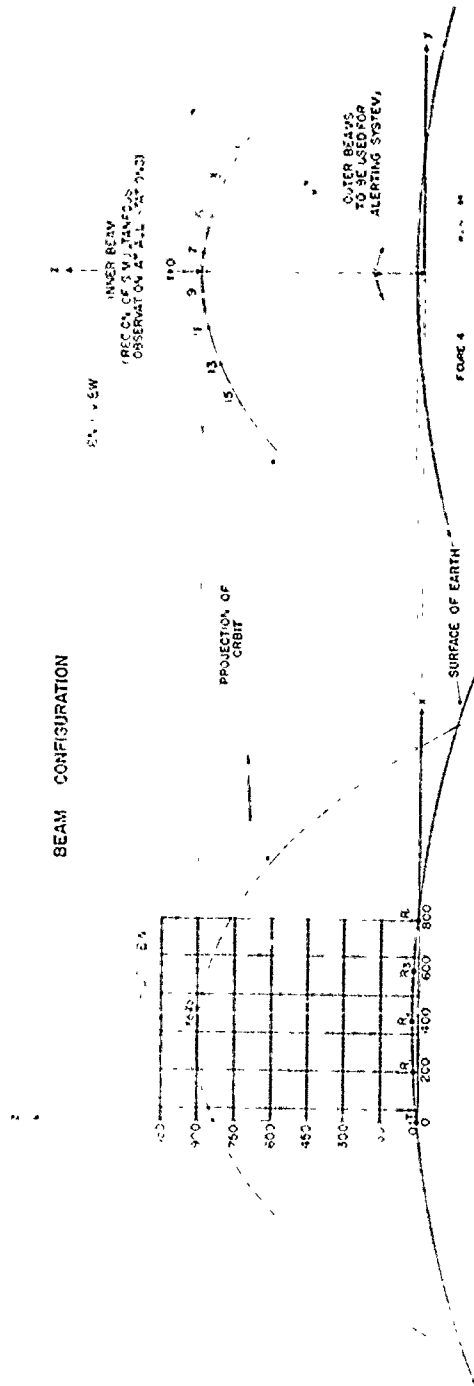


FIGURE 3

C-5

BEAM CONFIGURATION



PHILCO

GOVERNMENT & INDUSTRIAL GROUP
WESTERN DEVELOPMENT LABORATORIES

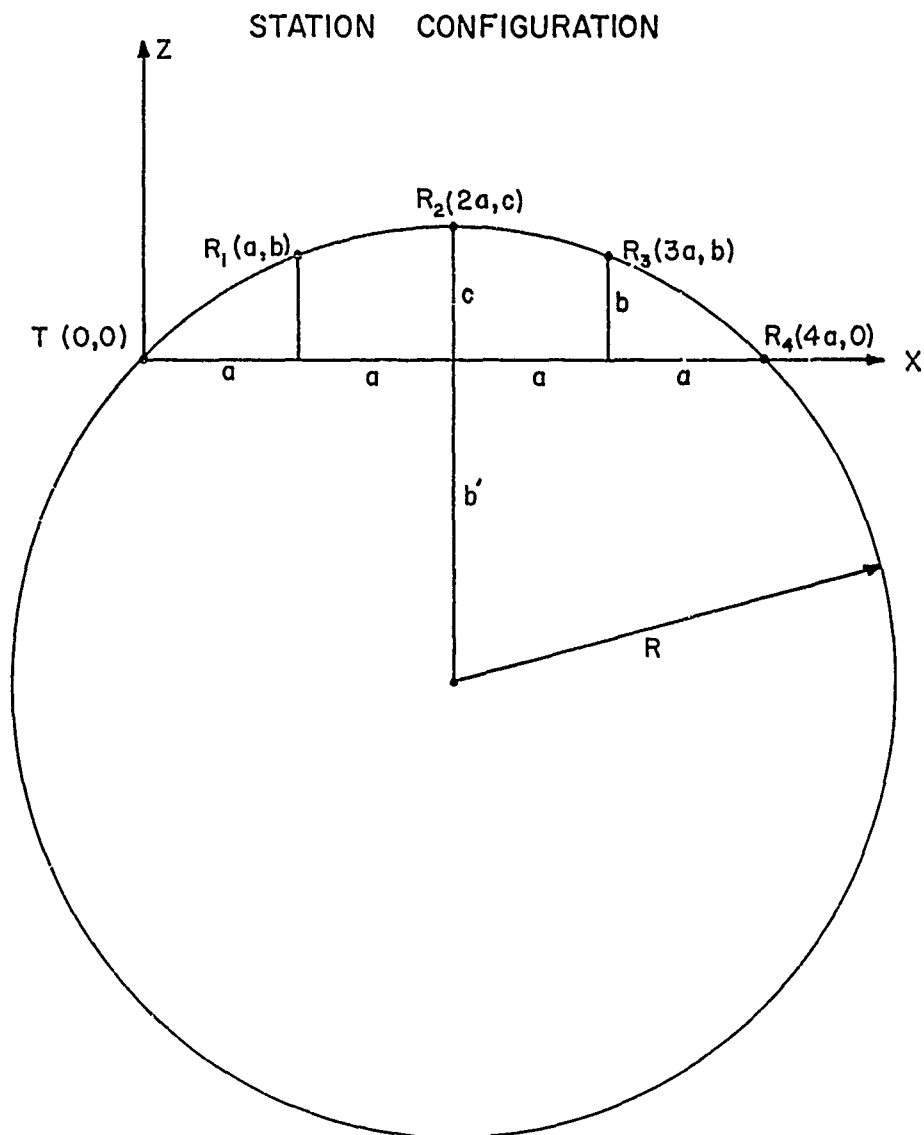


FIGURE 5

C-7

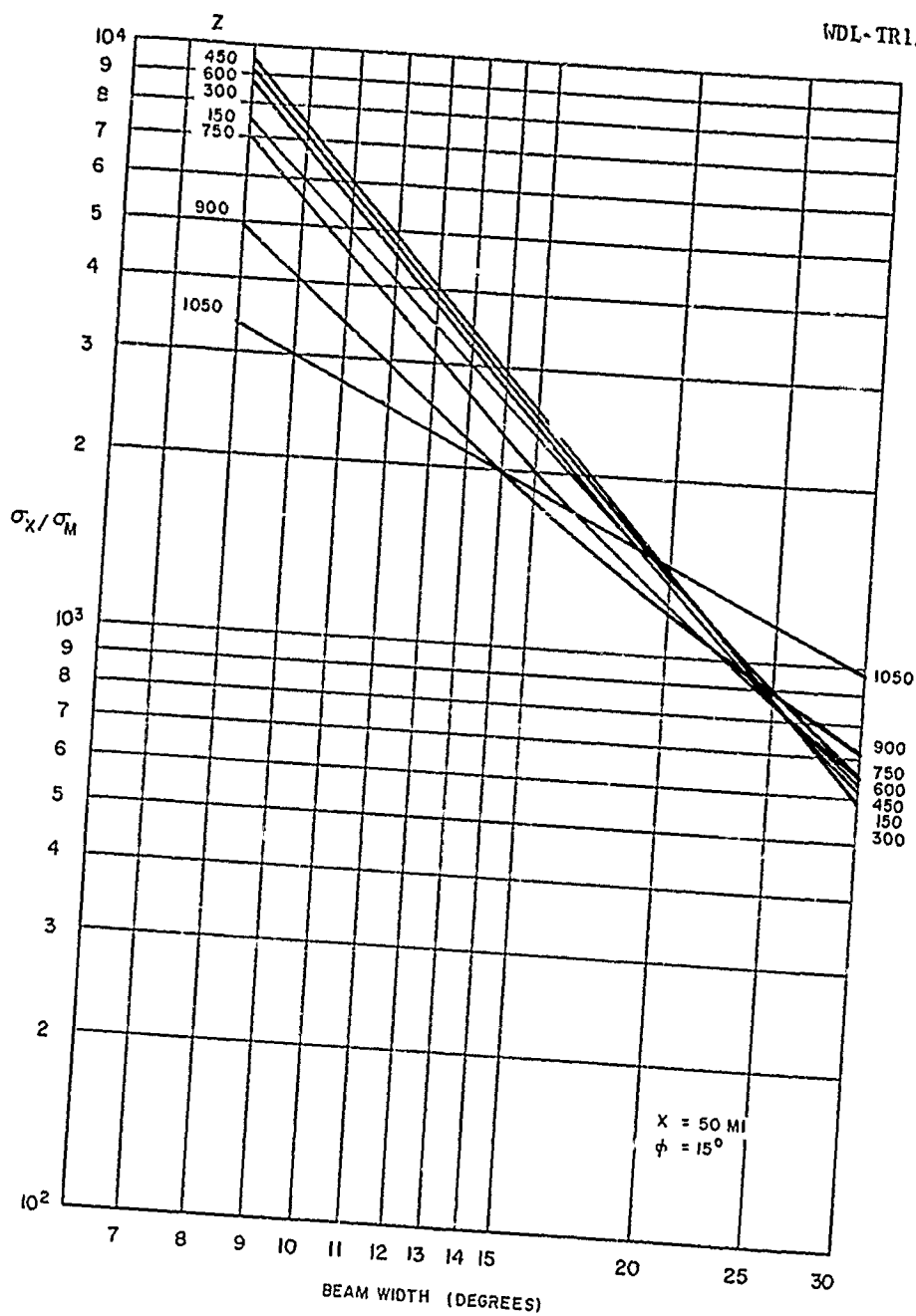


Figure 6a

C-8

DWG NO. 2804

PHILCO

GOVERNMENT & INDUSTRIAL GROUP
WESTERN DEVELOPMENT LABORATORIES

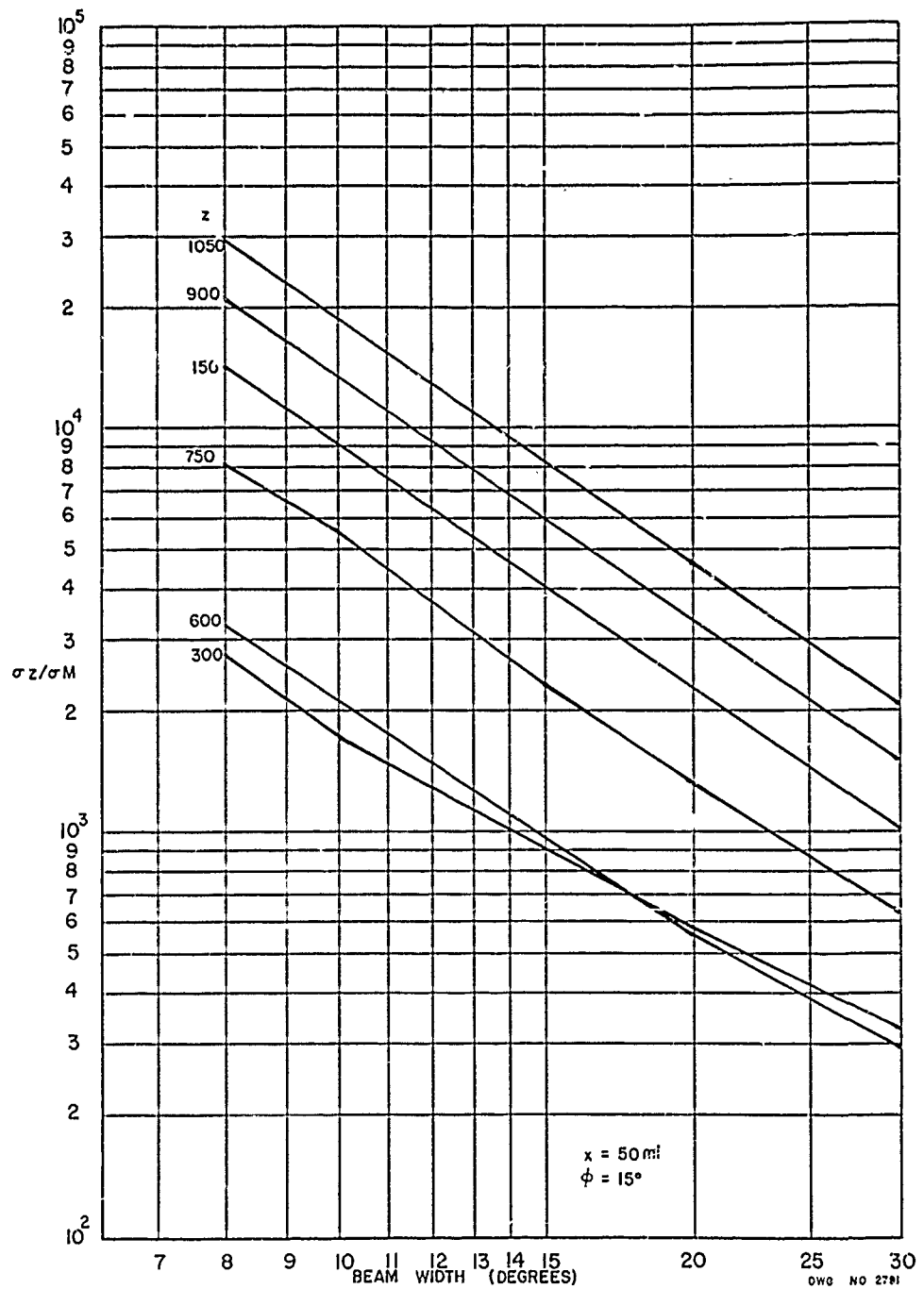


Figure 6b
c 9

EDL-JR1778

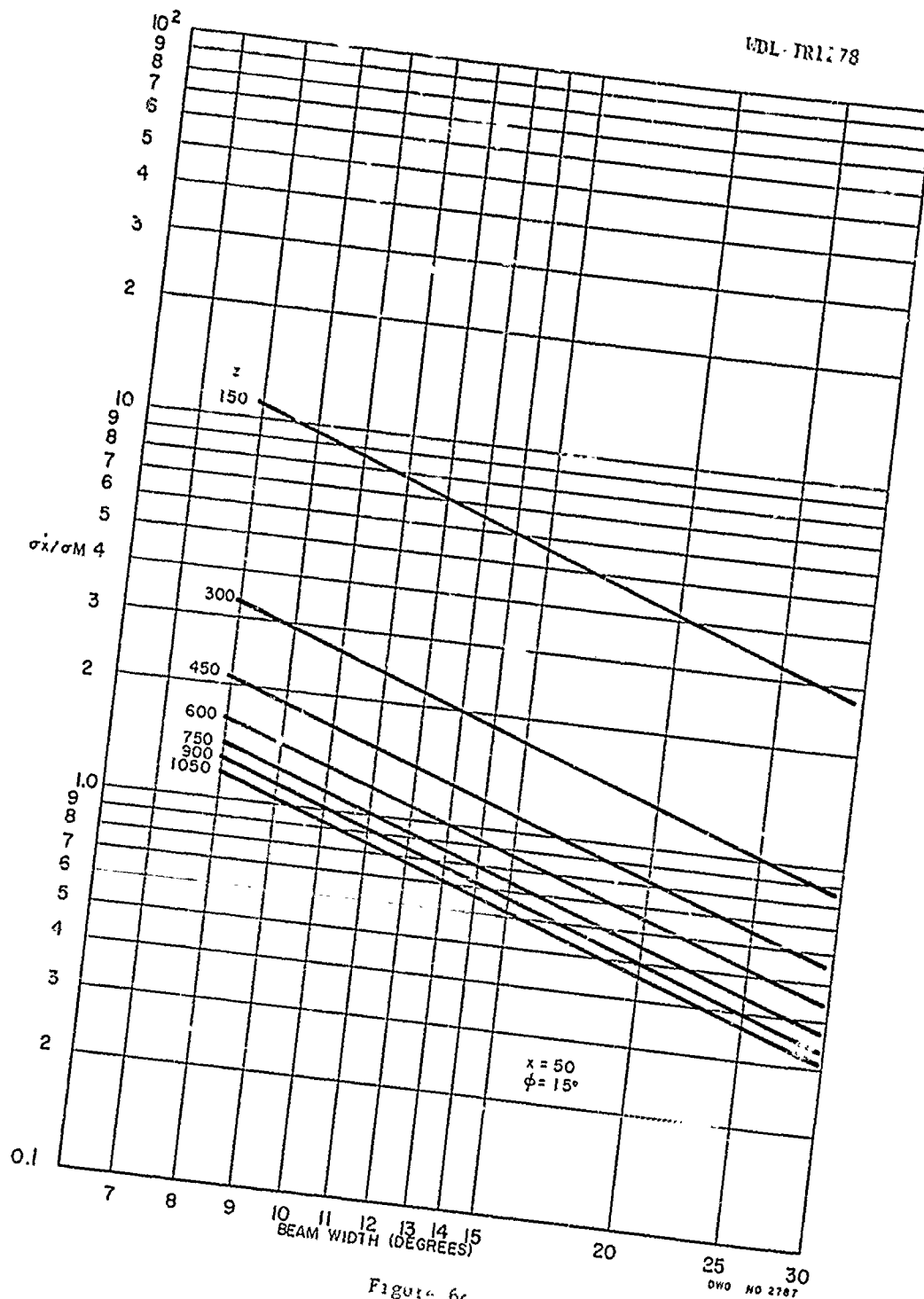


Figure 6c

10

PHILCO

GOVERNMENT & INDUSTRIAL GROUP
WESTERN DEVELOPMENT LABORATORIES

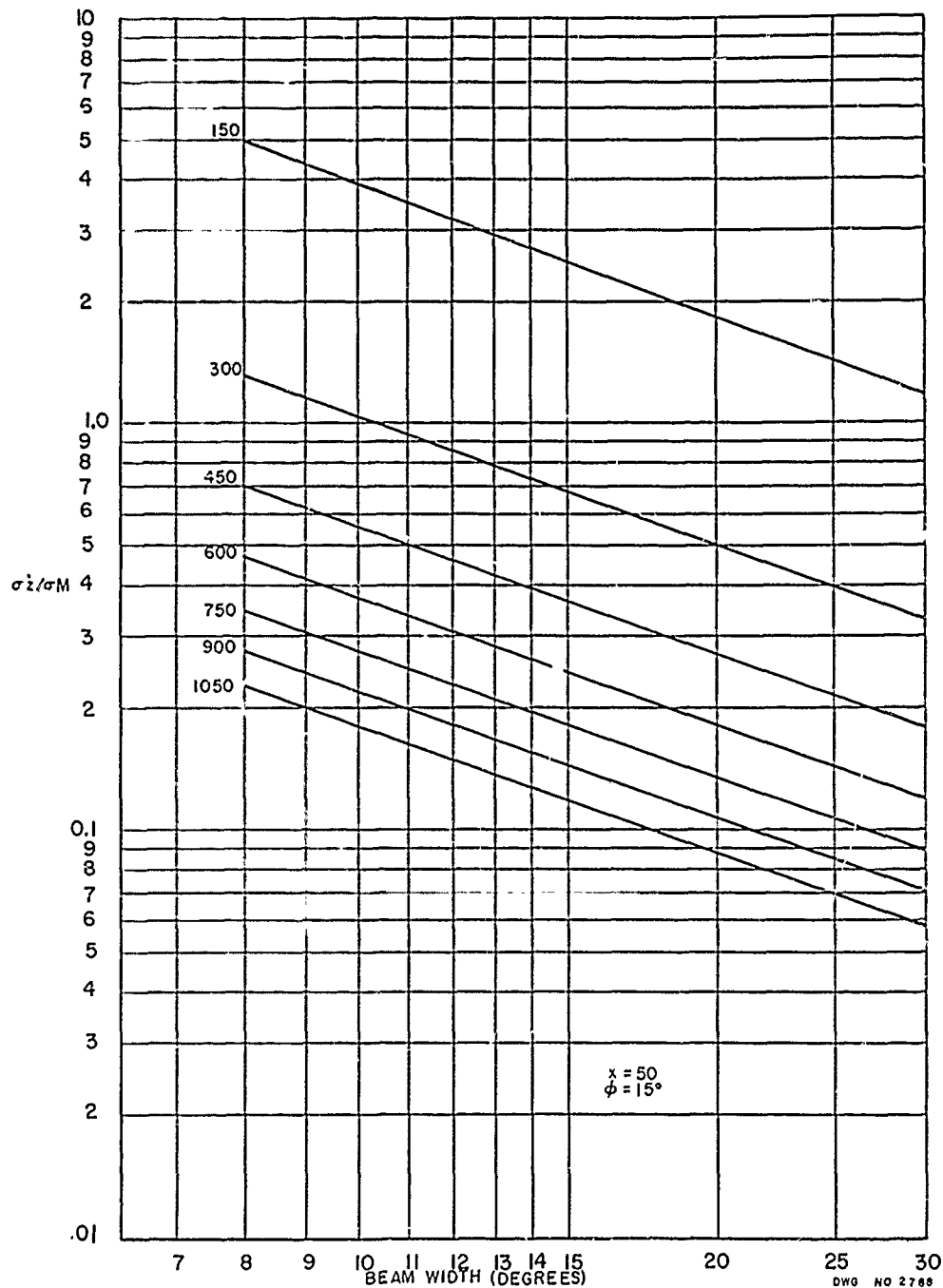


Figure 6d

C 11

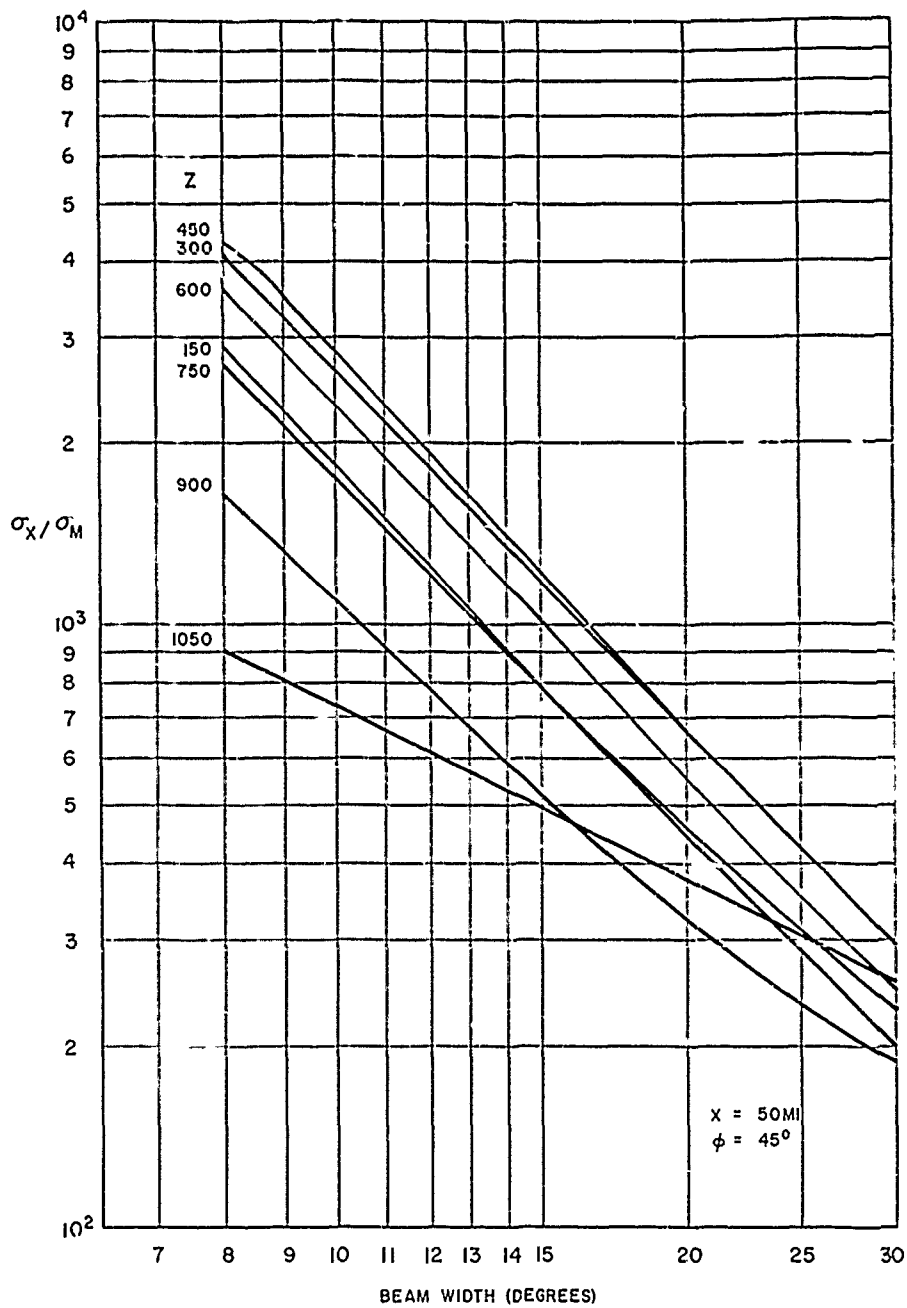


Figure 1a
C-12

OWO NO 2808

PHILCO

GOVERNMENT & INDUSTRIAL GROUP
WESTERN DEVELOPMENT LABORATORIES

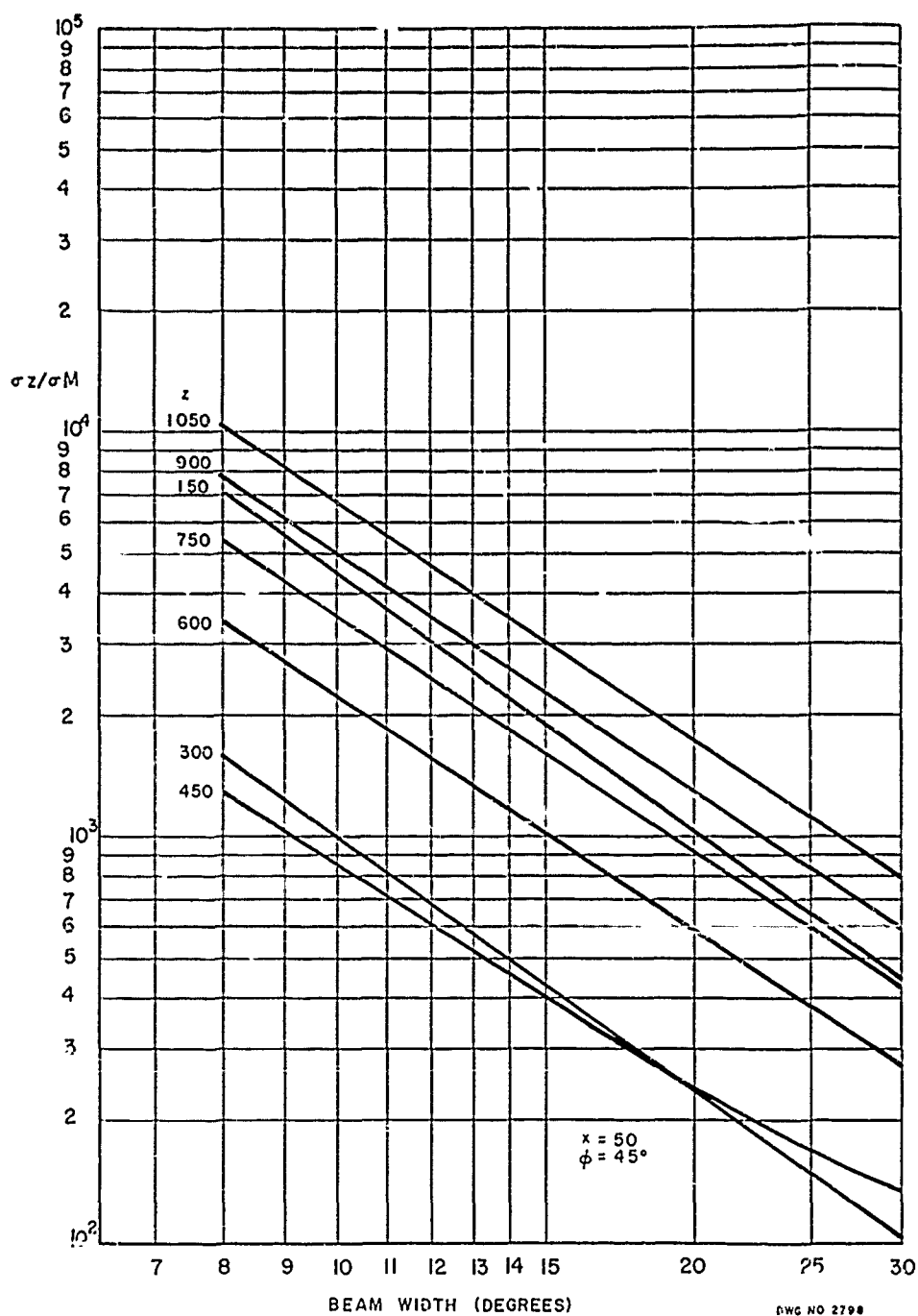


Figure 7b

C-13

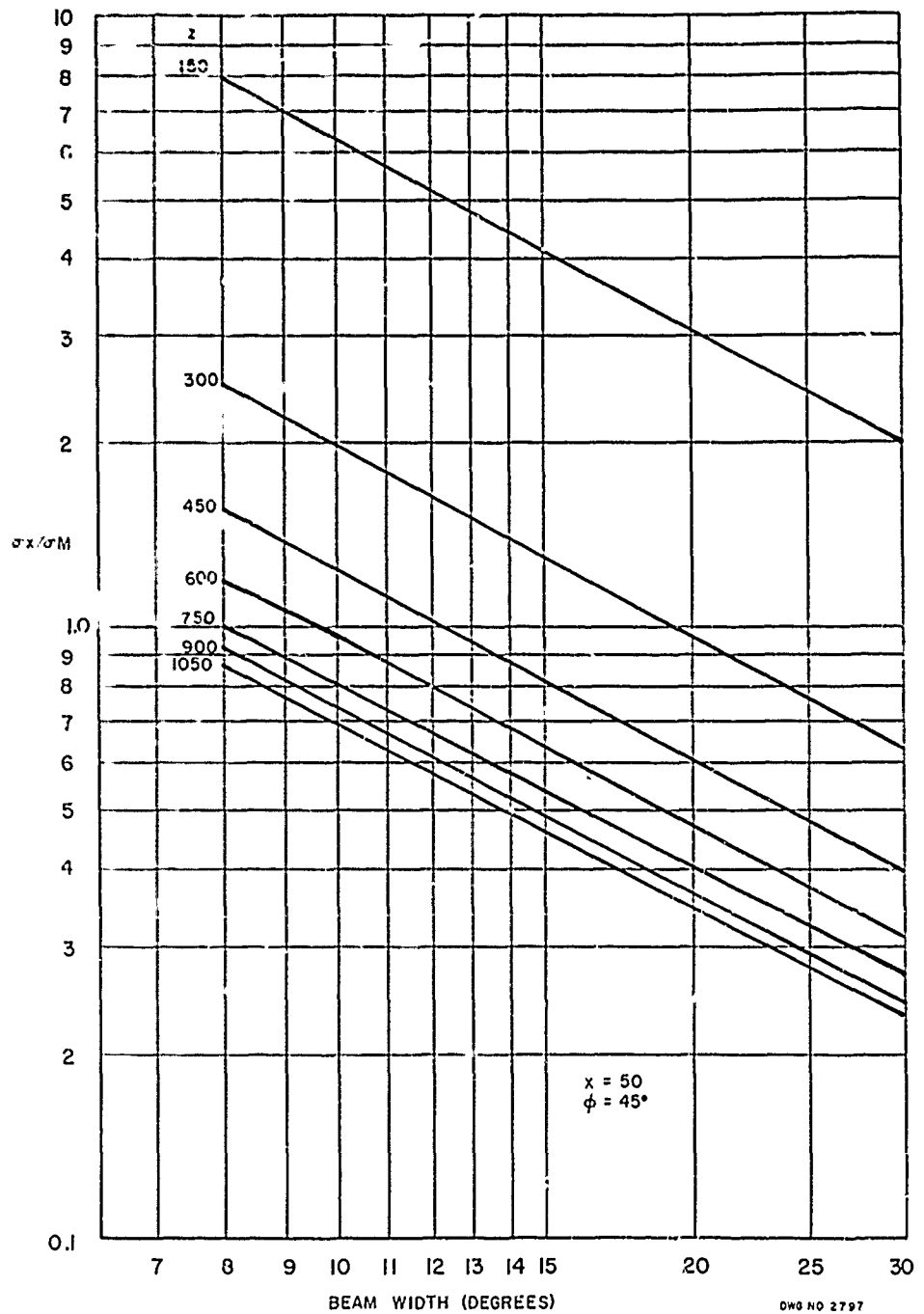


Figure 7c

C-14

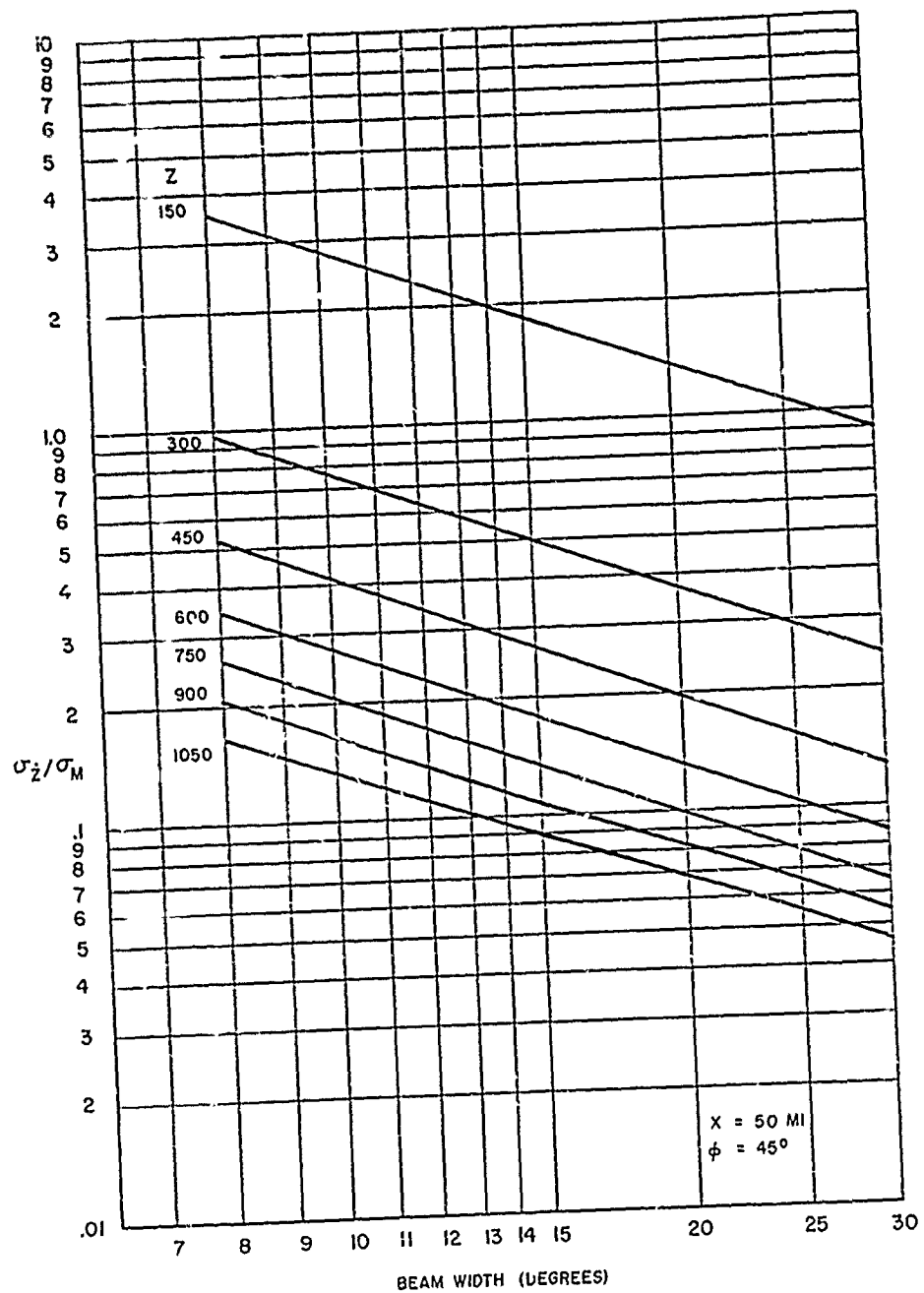


Figure 7d

DWG NO 2807

C-15

PHILCO

GOVERNMENT & INDUSTRIAL GROUP
WESTERN DEVELOPMENT LABORATORIES

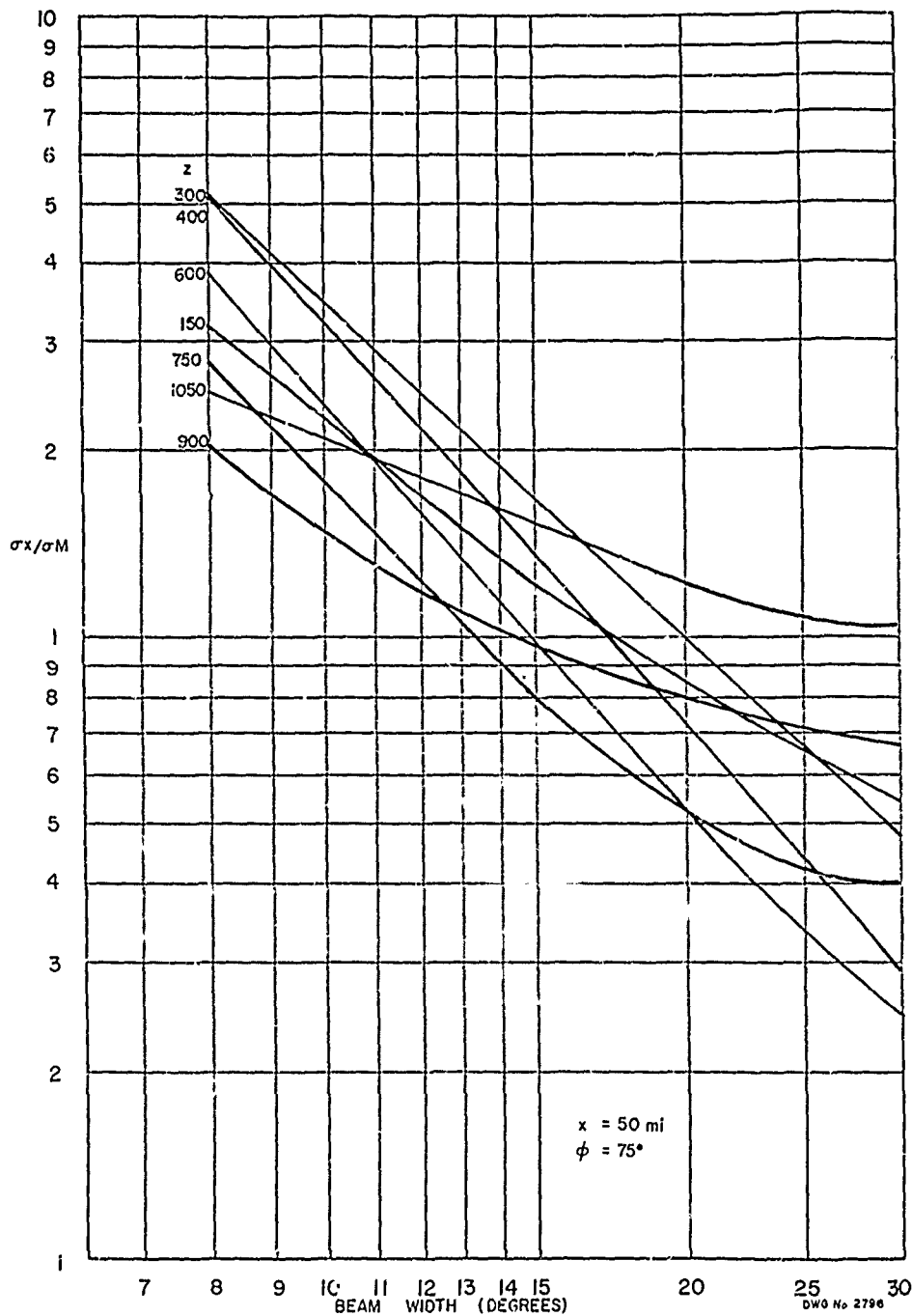


Figure 8a

C 16

PHILCO

GOVERNMENT & INDUSTRIAL GROUP
WESTERN DEVELOPMENT LABORATORY

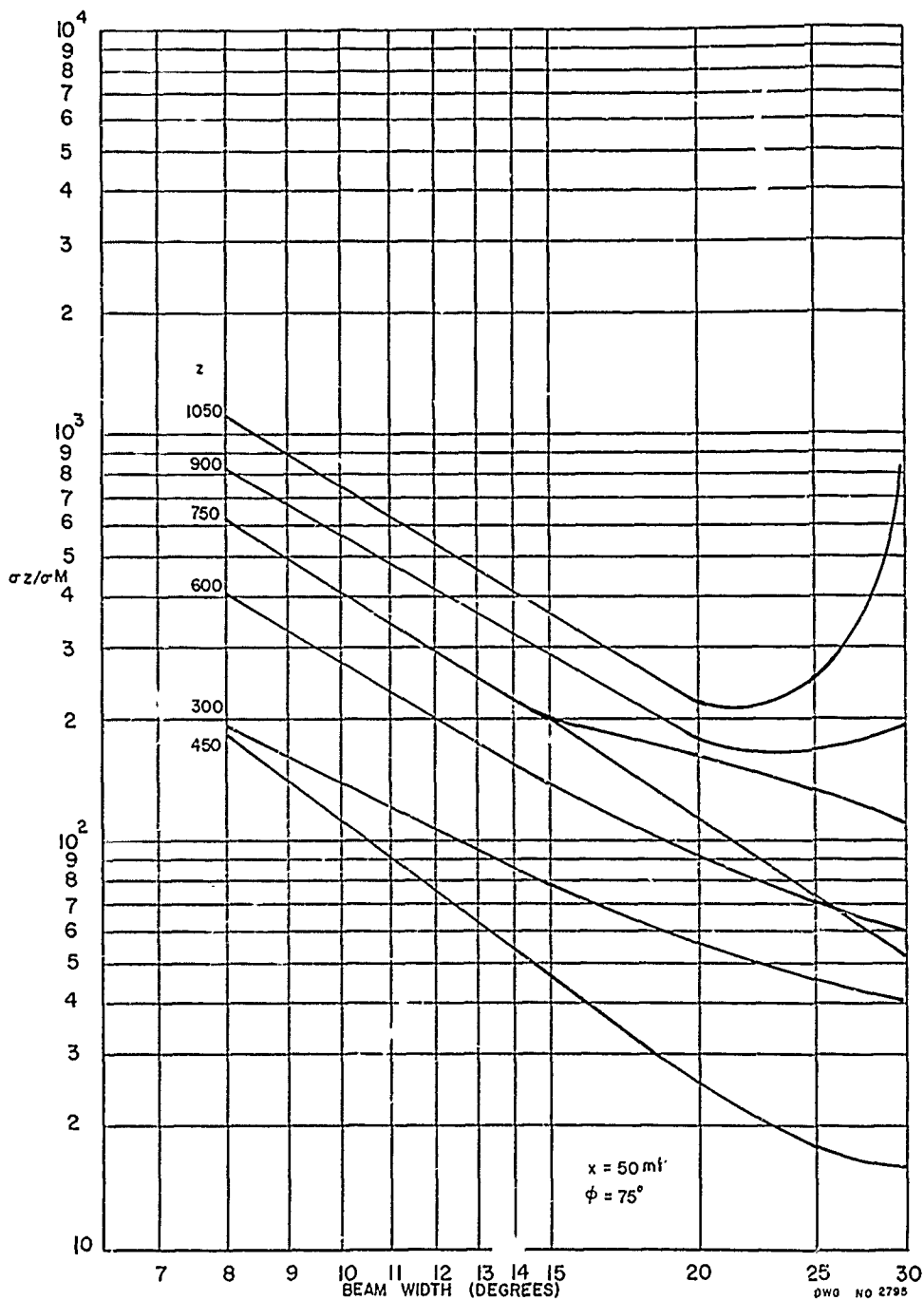


Figure 8b

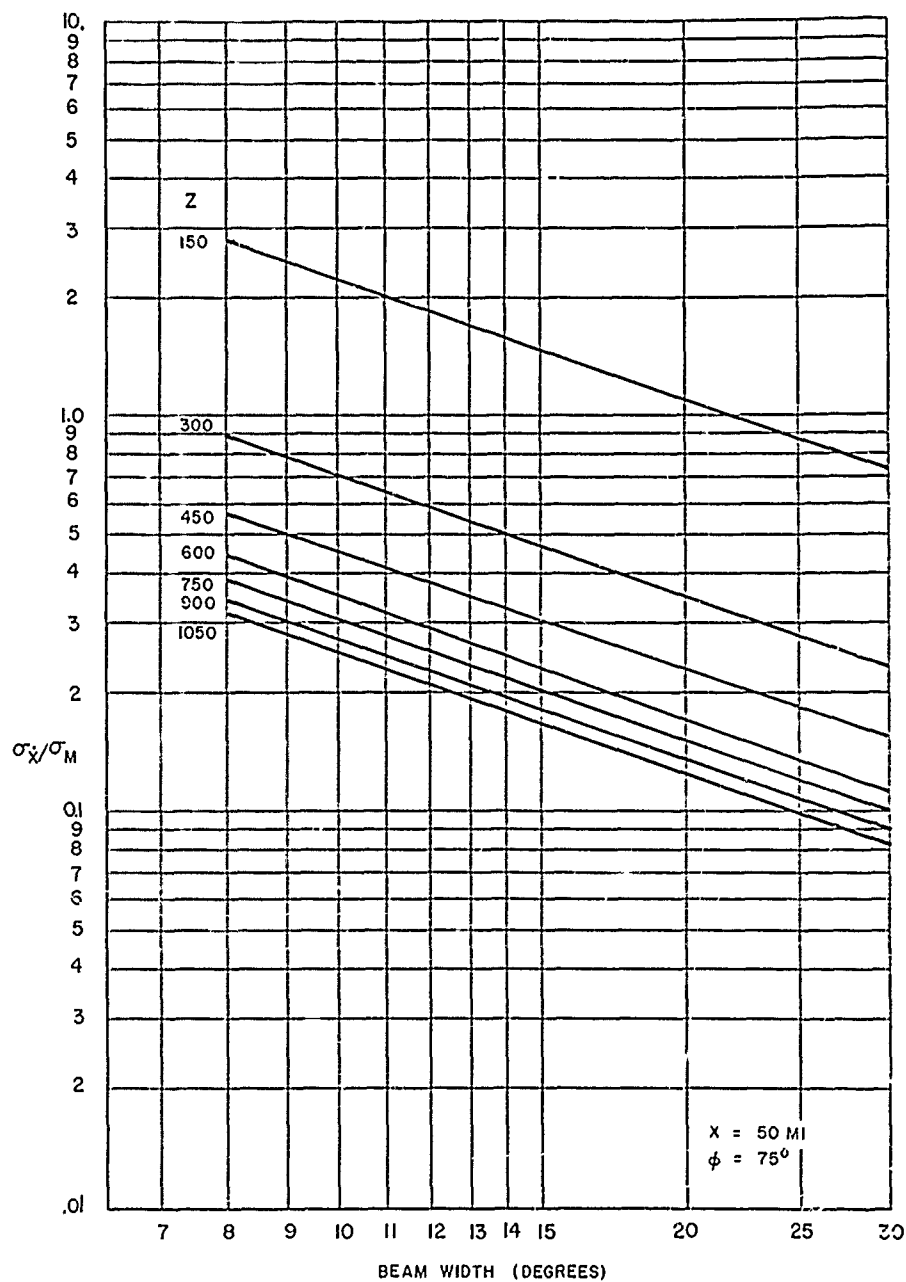


Figure 8c

C-18

DWG NO 2805

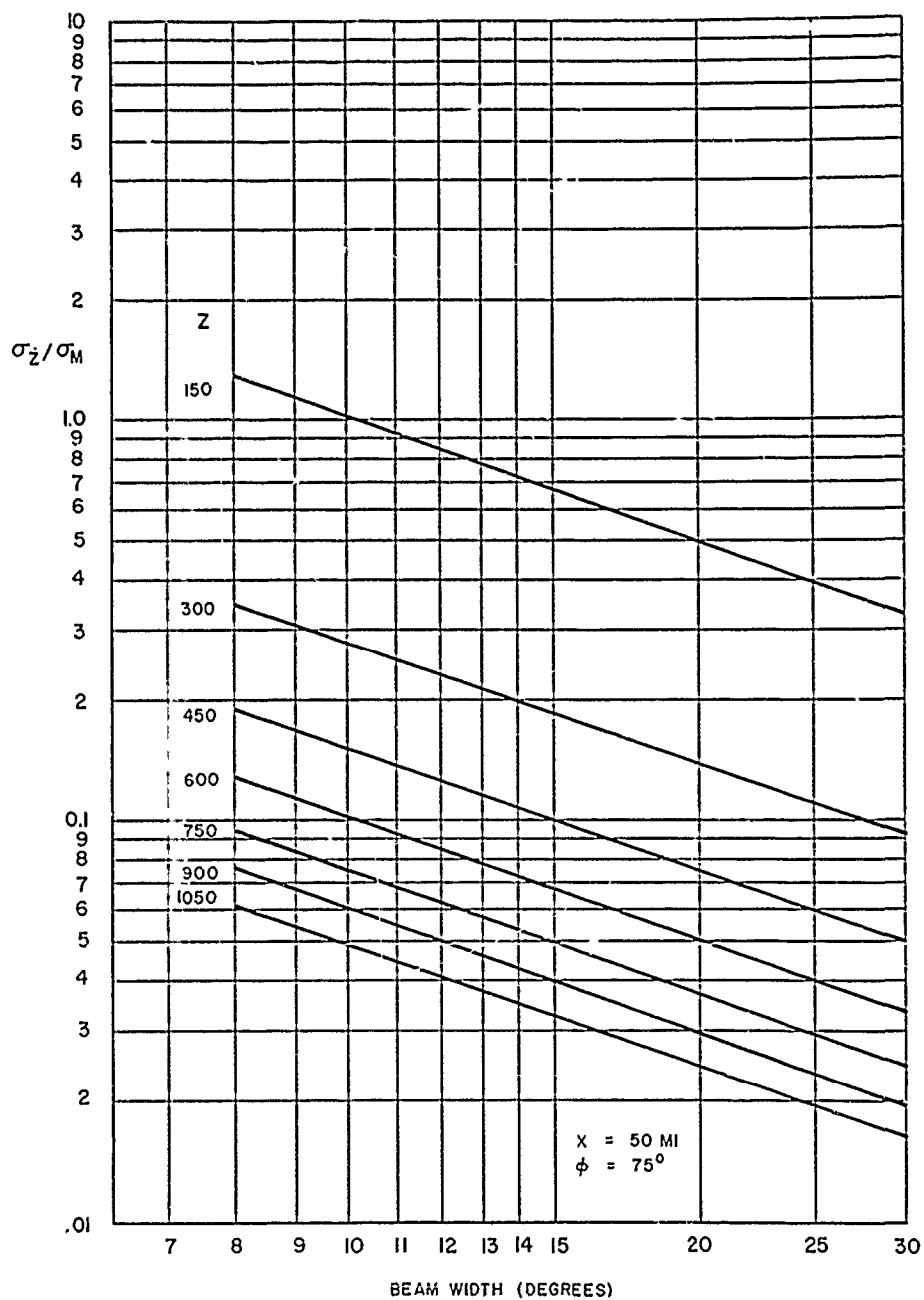


Figure 8d

c 19

DWO NO. 2806

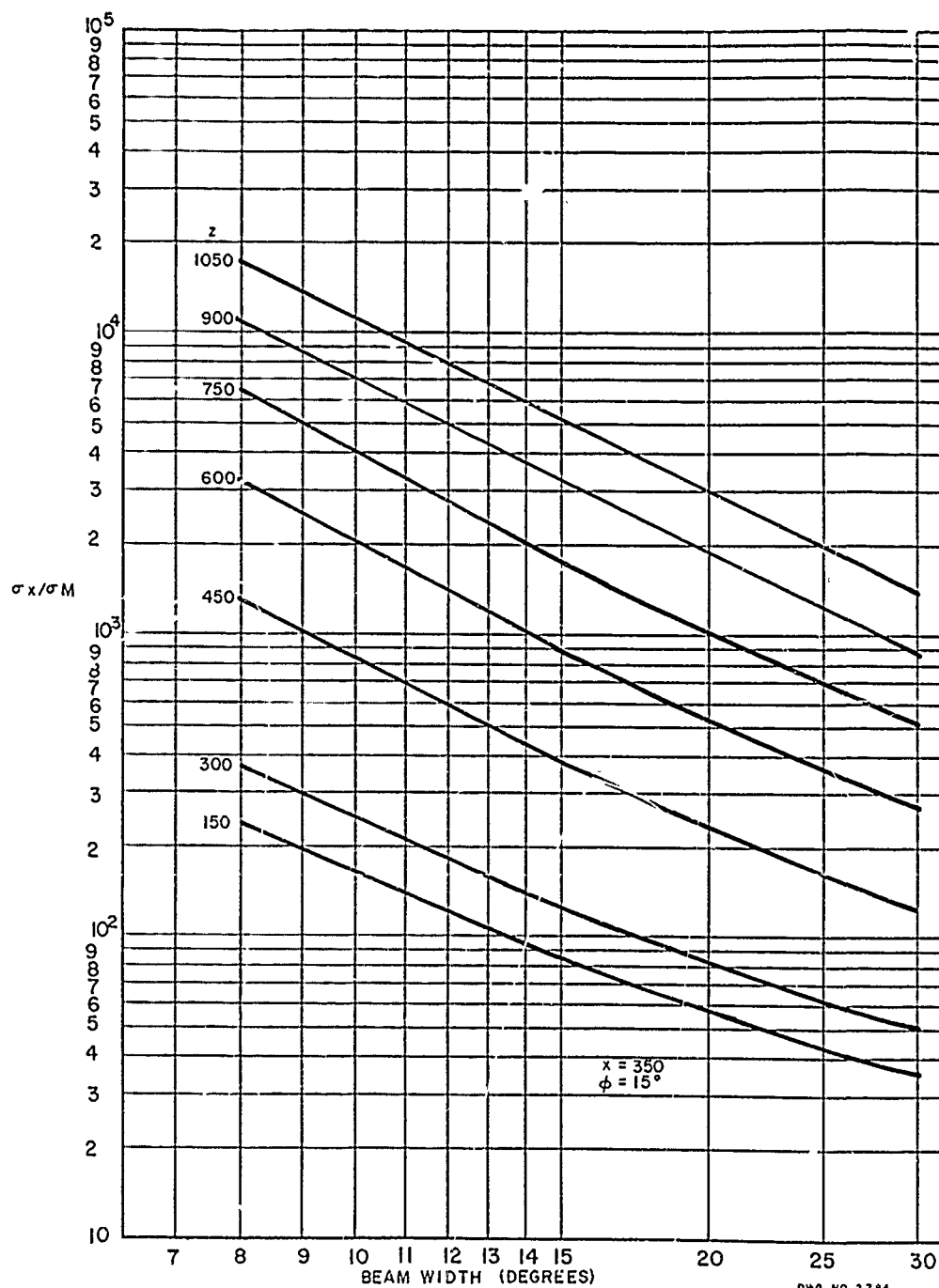


Figure 9a

C-20

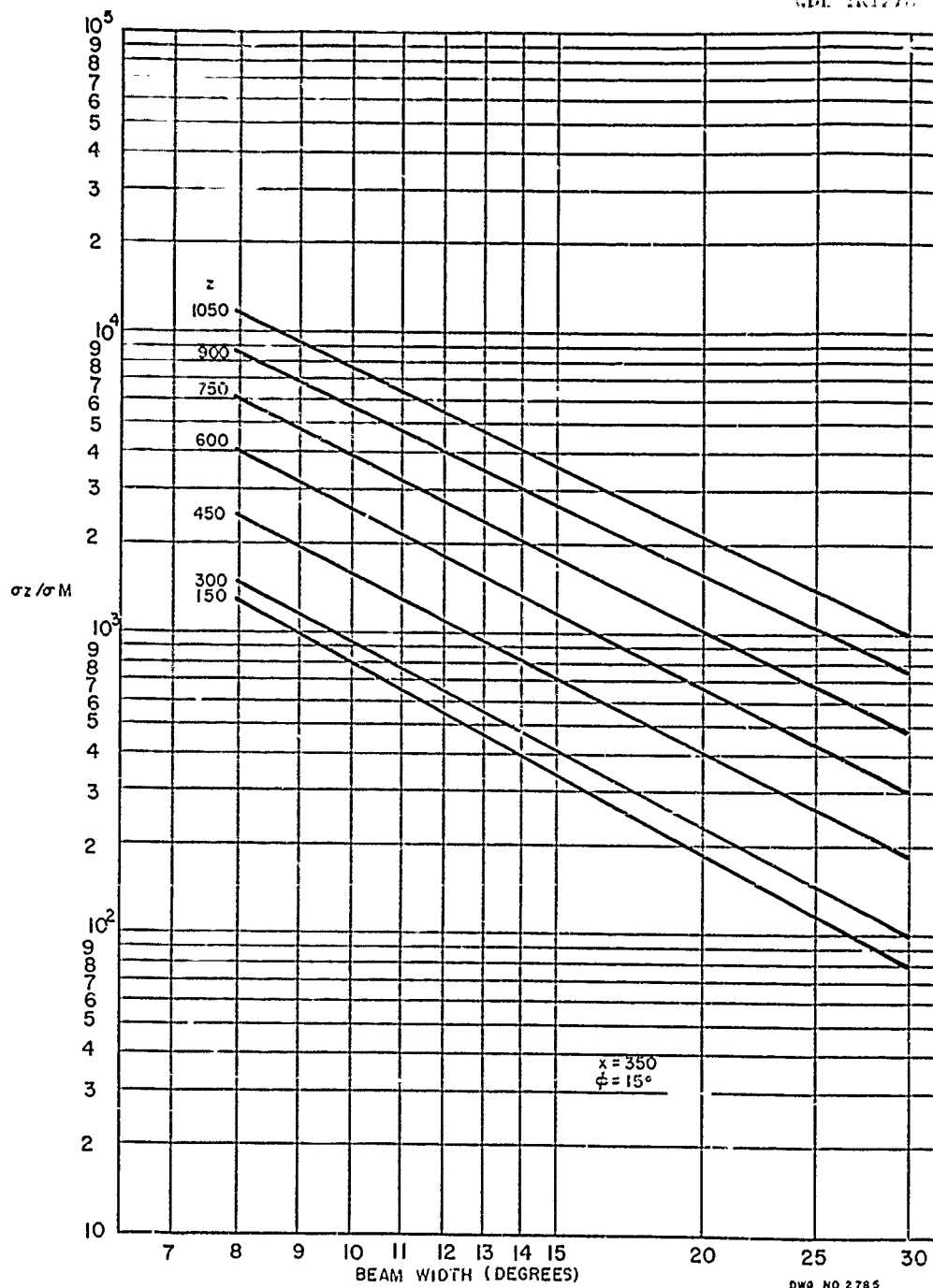


Figure 9b

C 21

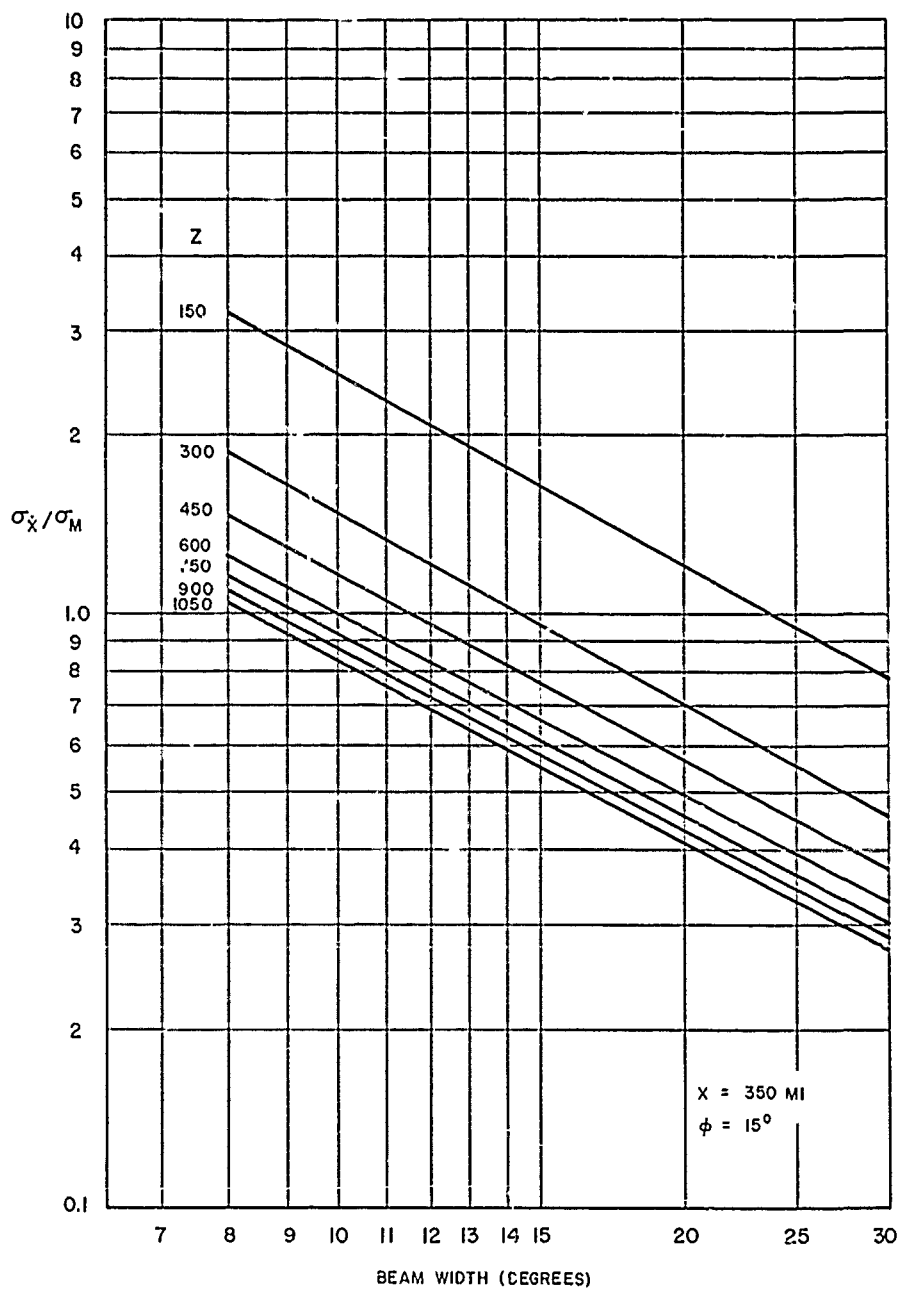


Figure 9c

C-22

DWG NO. 2810

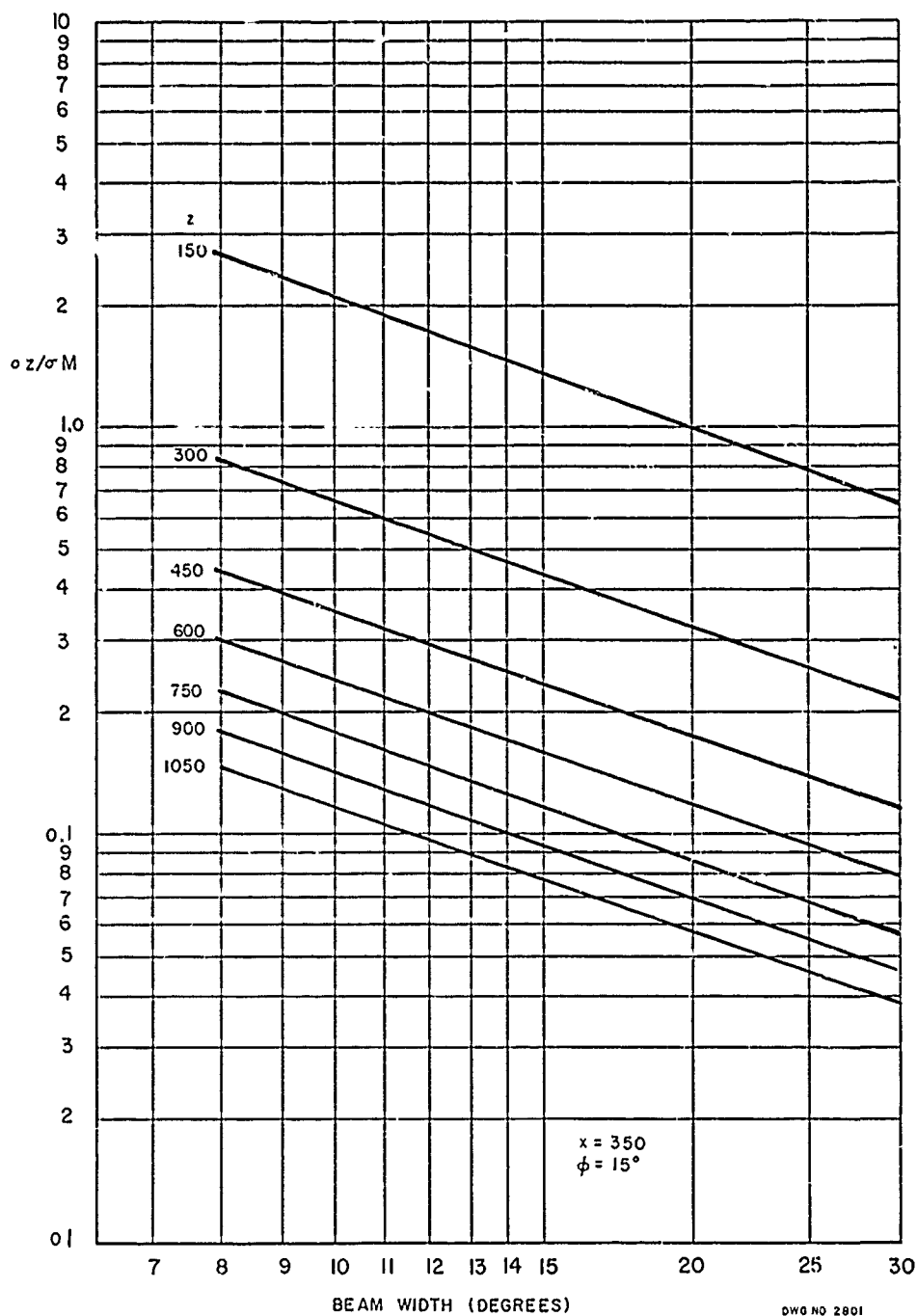
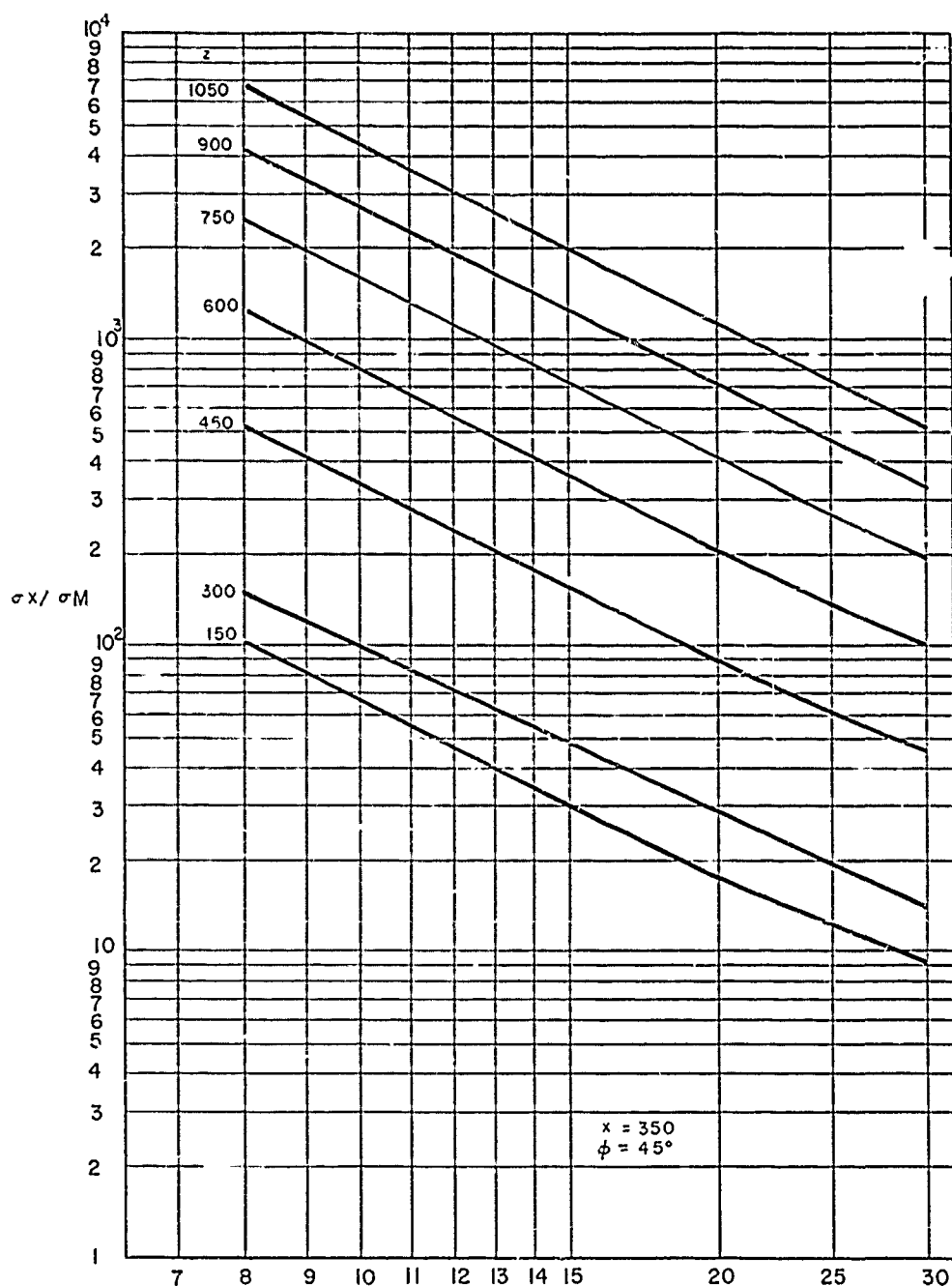


Figure 9d

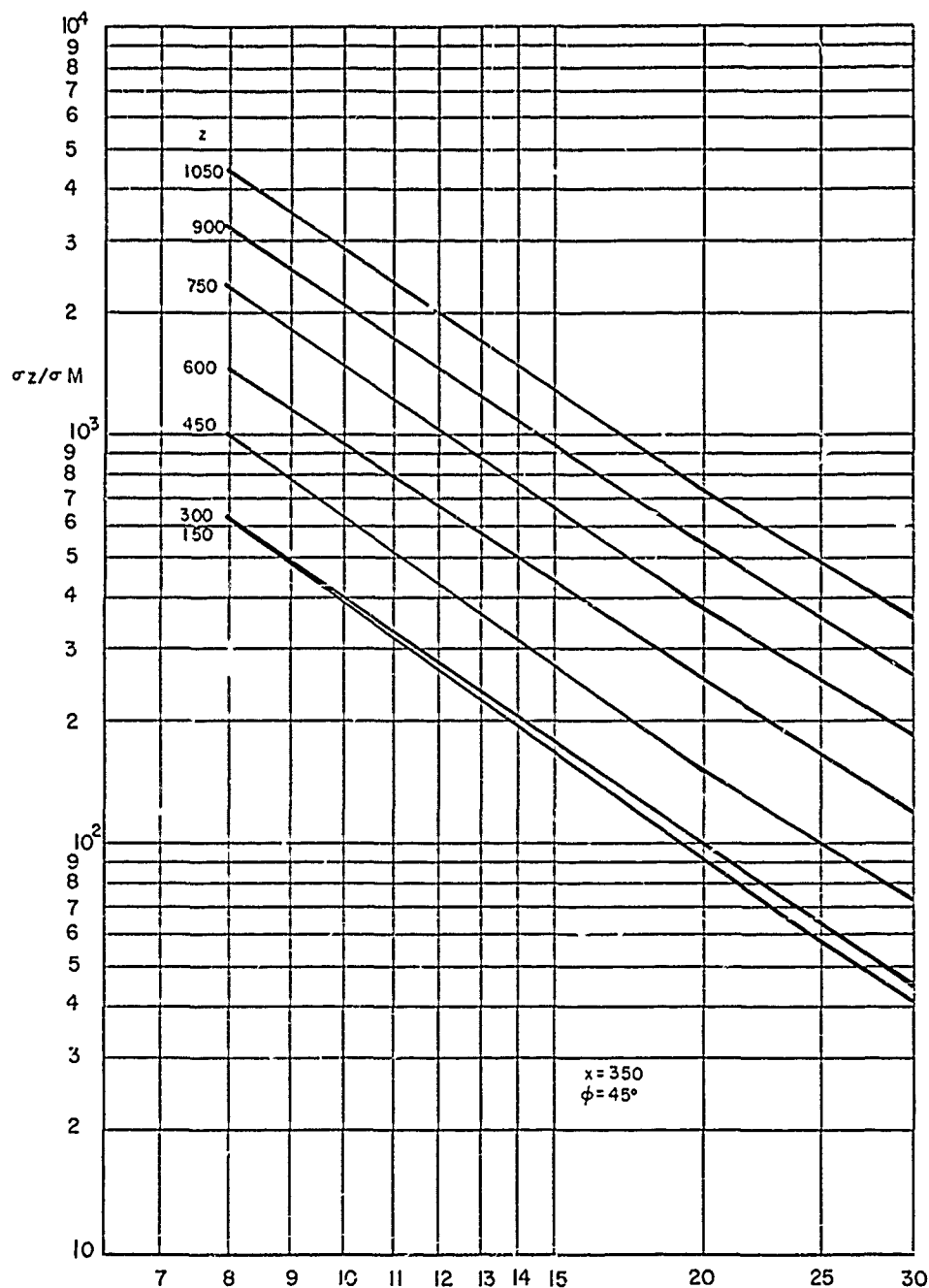
C-23



DWG NO 2786

Figure 10a

(-24



BEAM WIDTH (DEGREES)

Figure 10b

C-23

DWG NO 2800

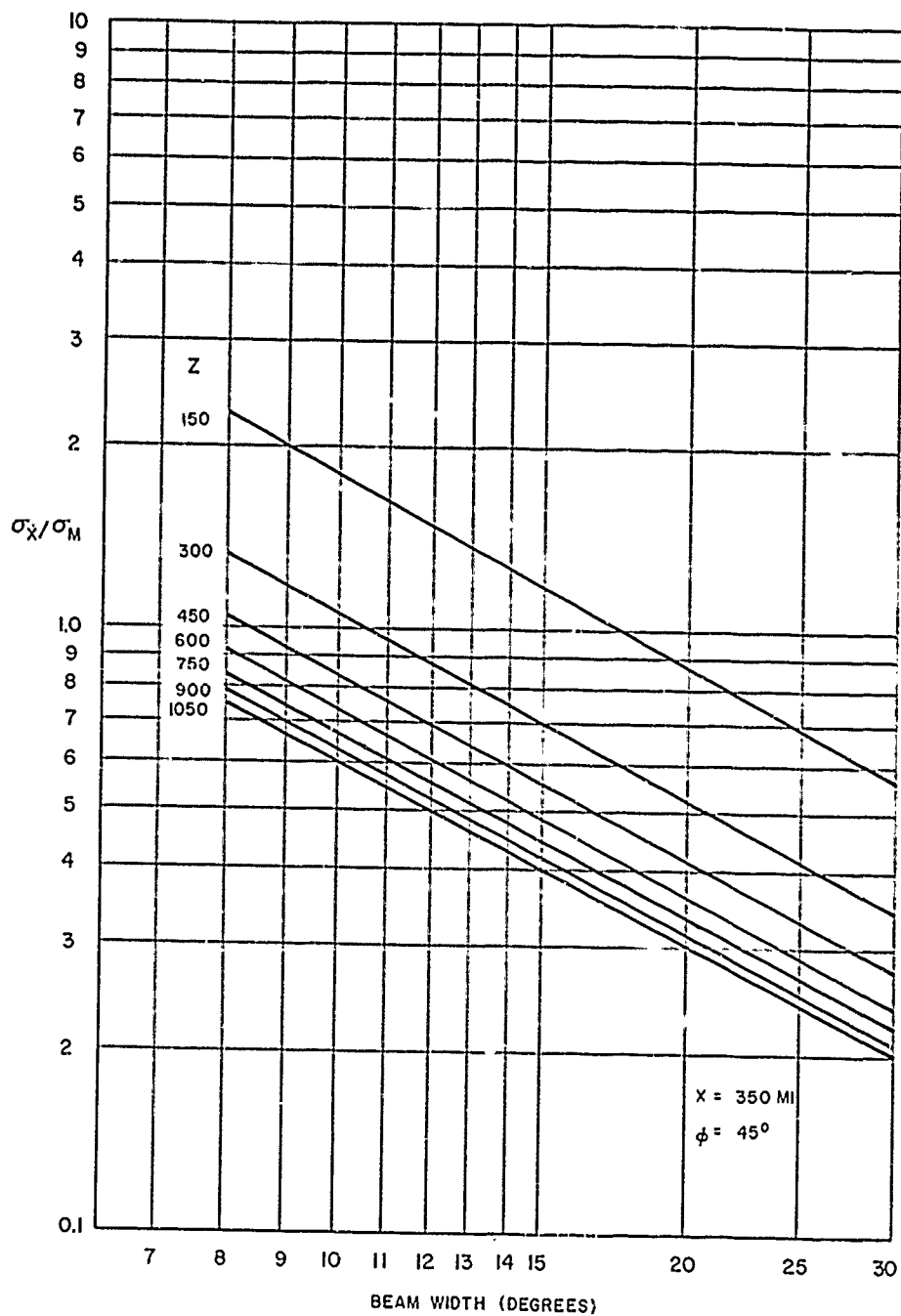


Figure 10c

DWO No 2809

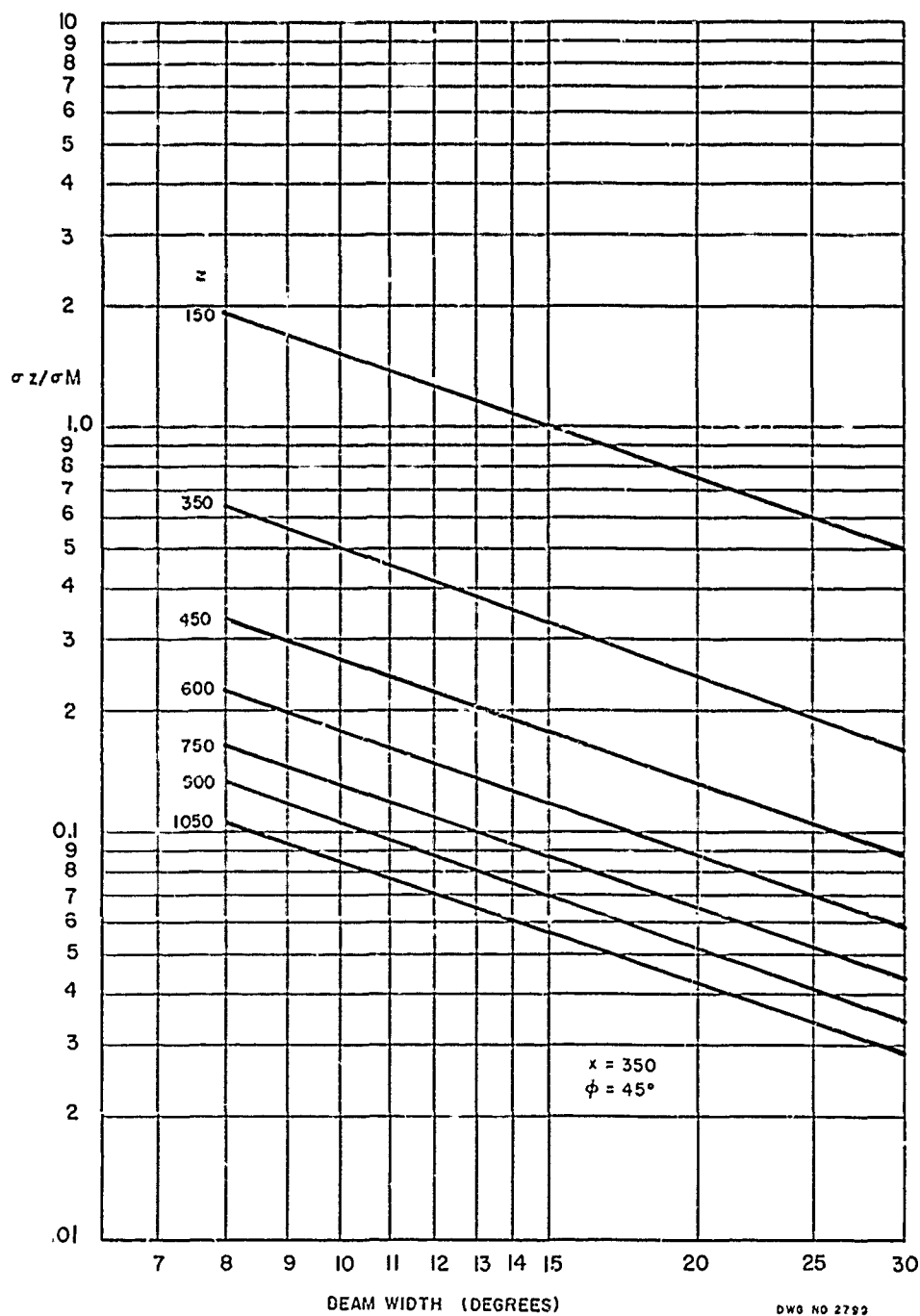
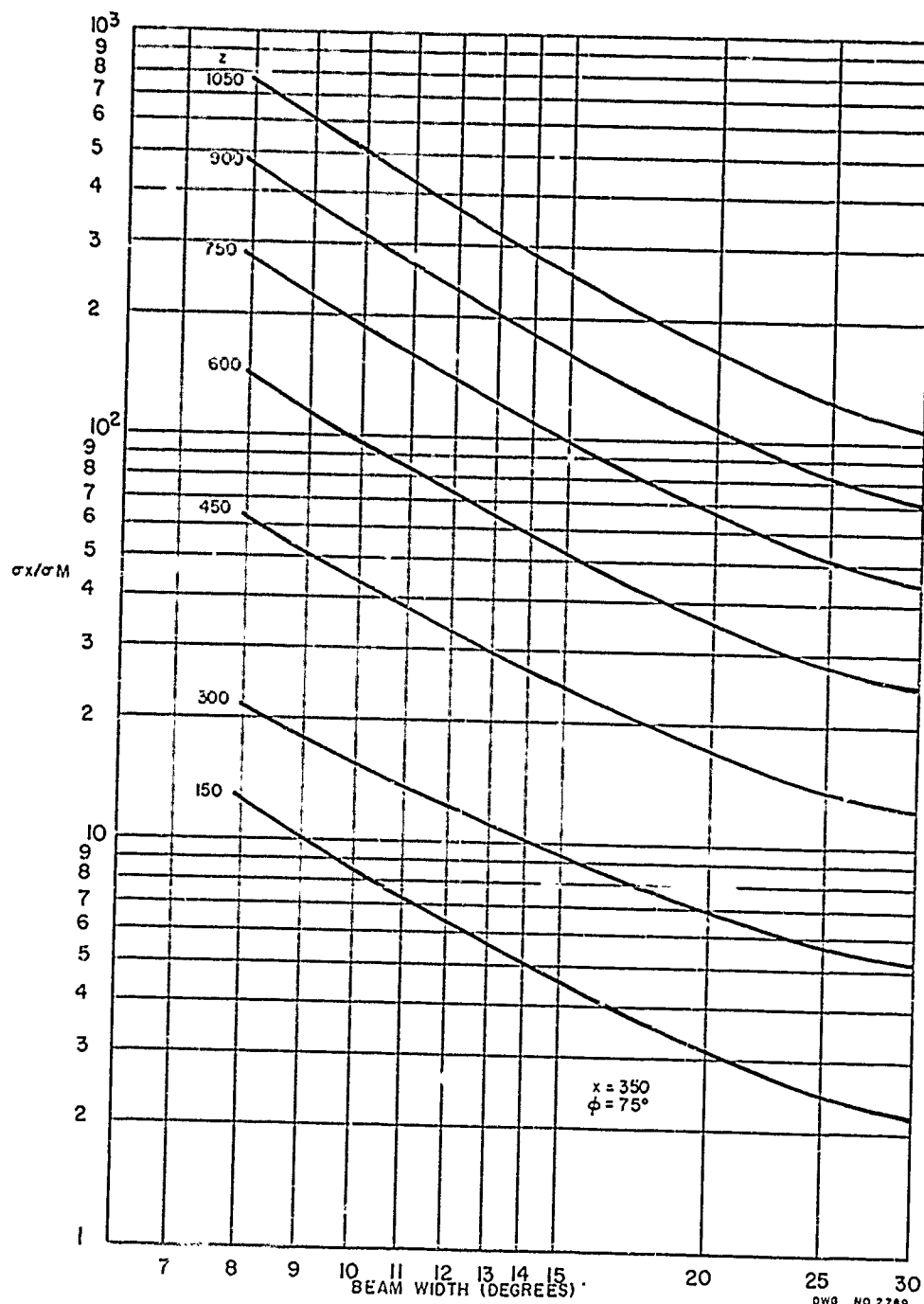


Figure 10d

C-27



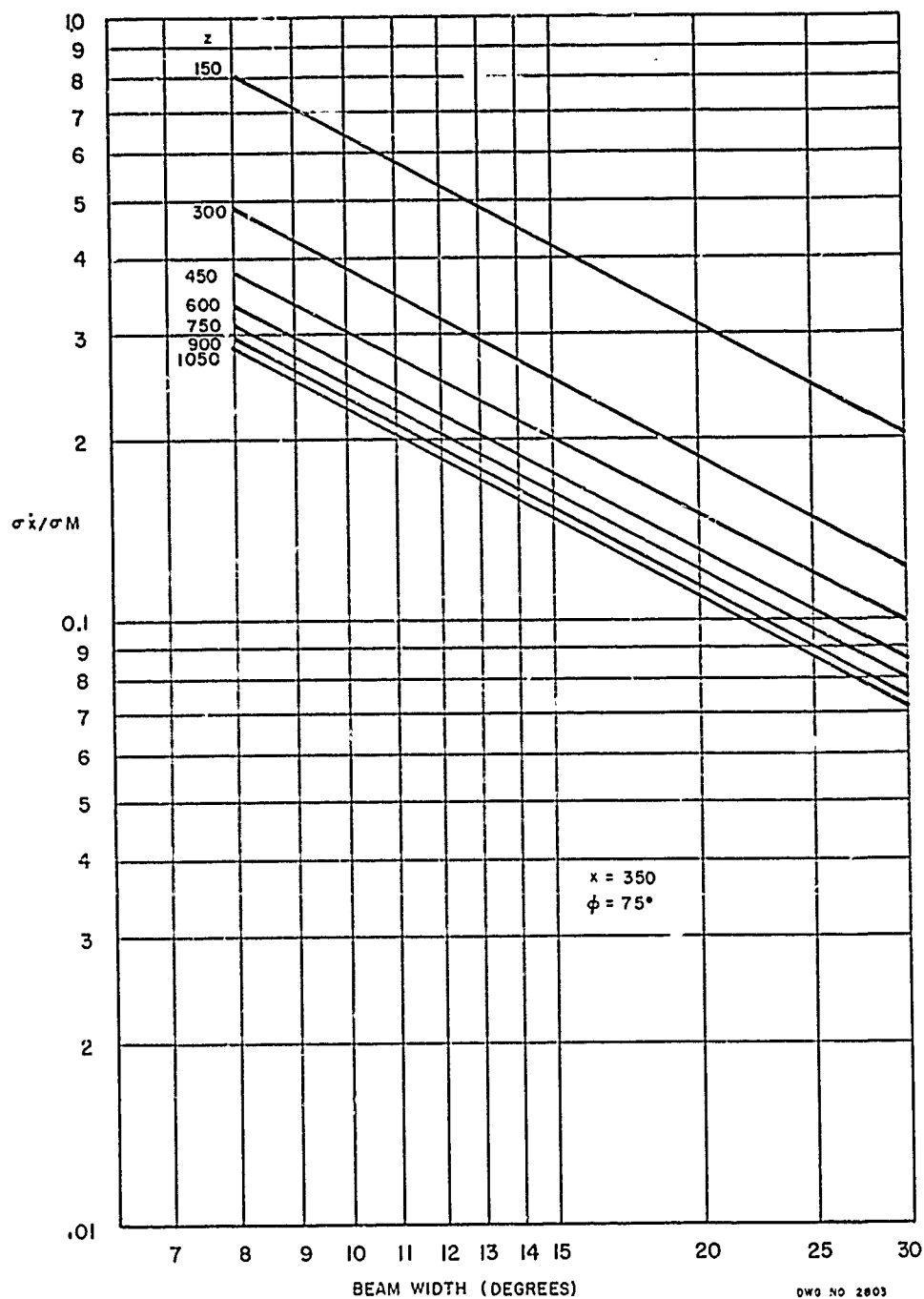


Figure 11c

C 30

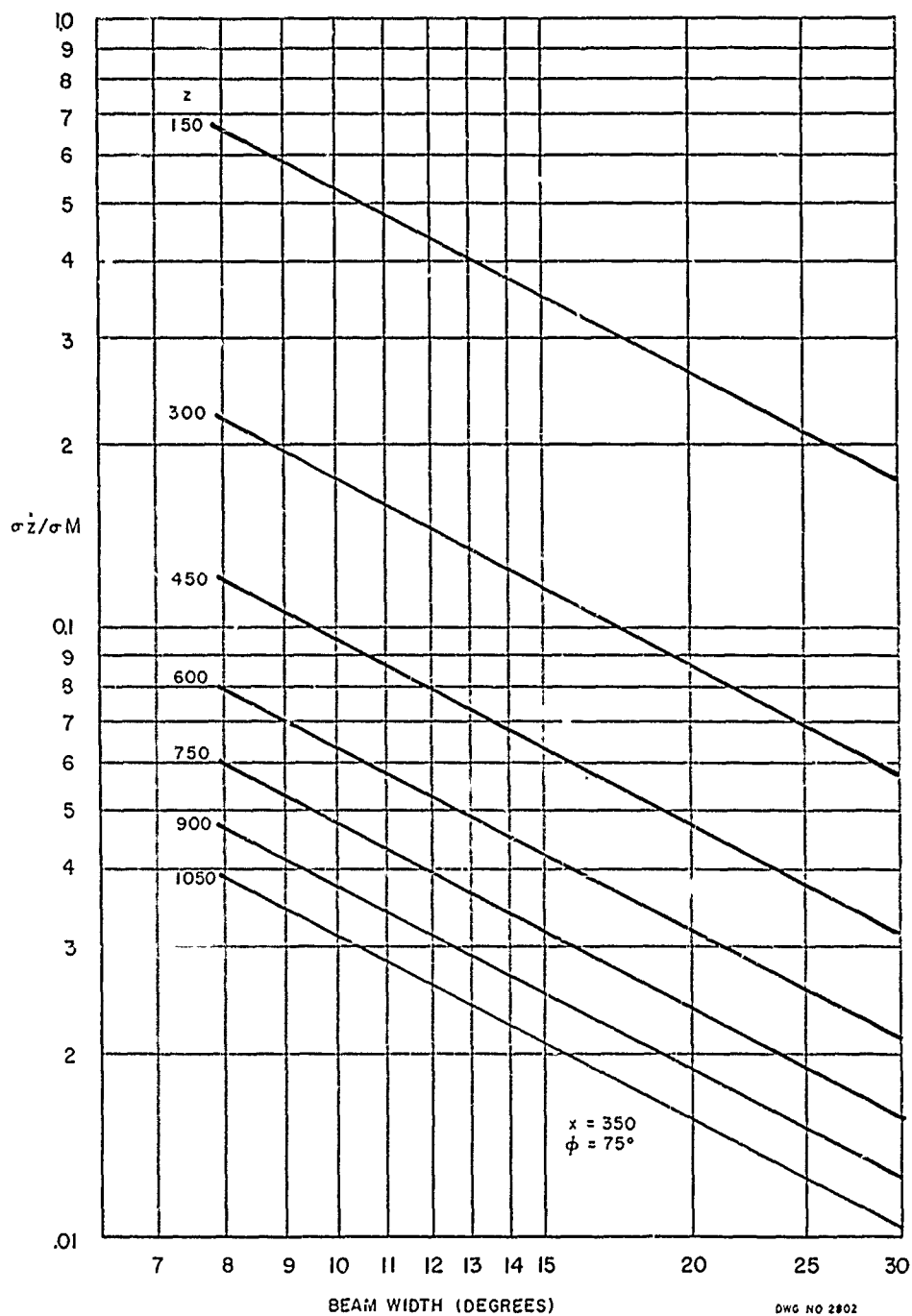


Figure 11d

C 31

PHILCO

GOVERNMENT & INDUSTRIAL GROUP
WESTERN DEVELOPMENT LABORATORIES

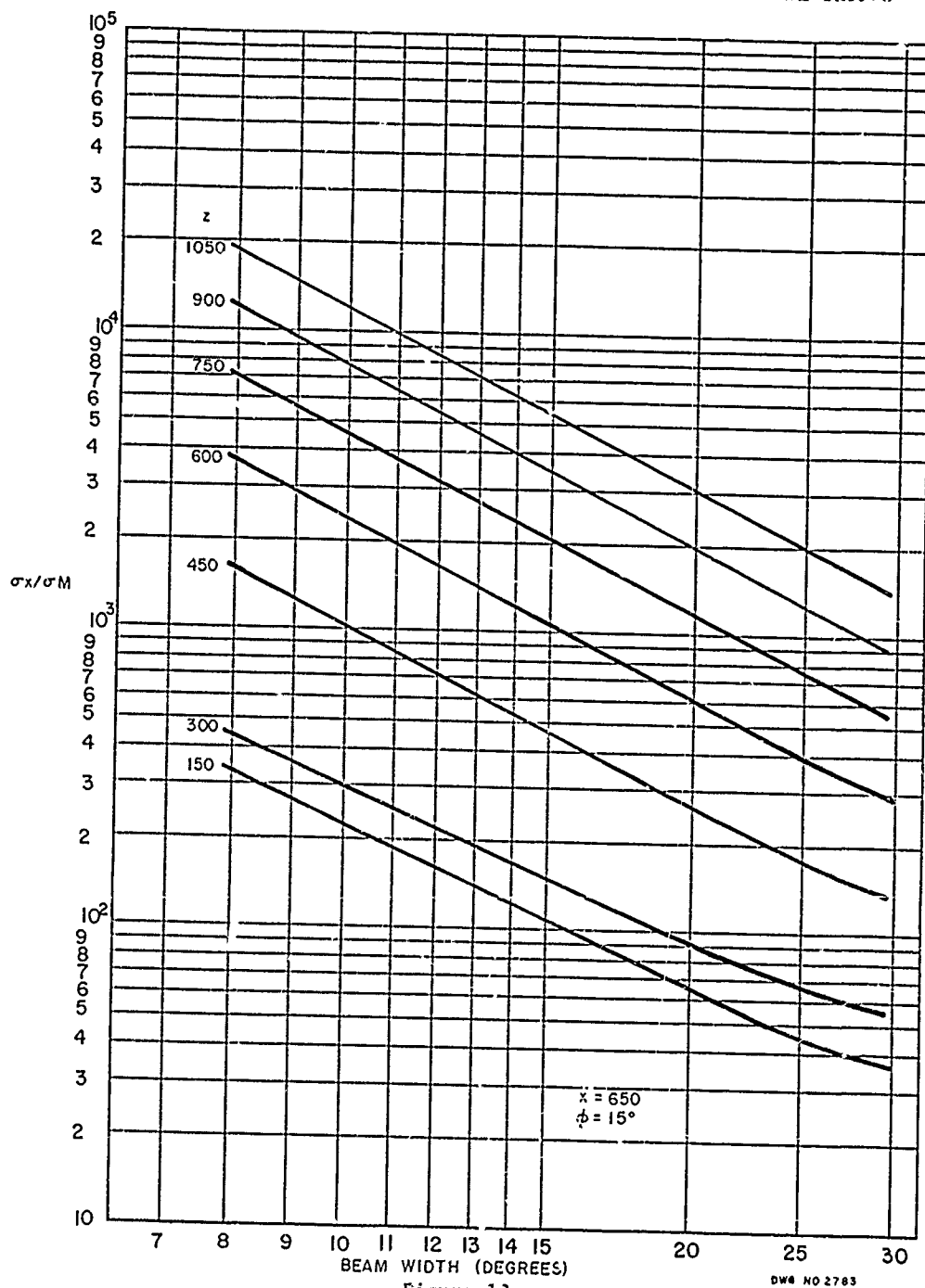


Figure 12a

C-32

PHILCO

GOVERNMENT & INDUSTRIAL GROUP
WESTERN DEVELOPMENT LABORATORIES

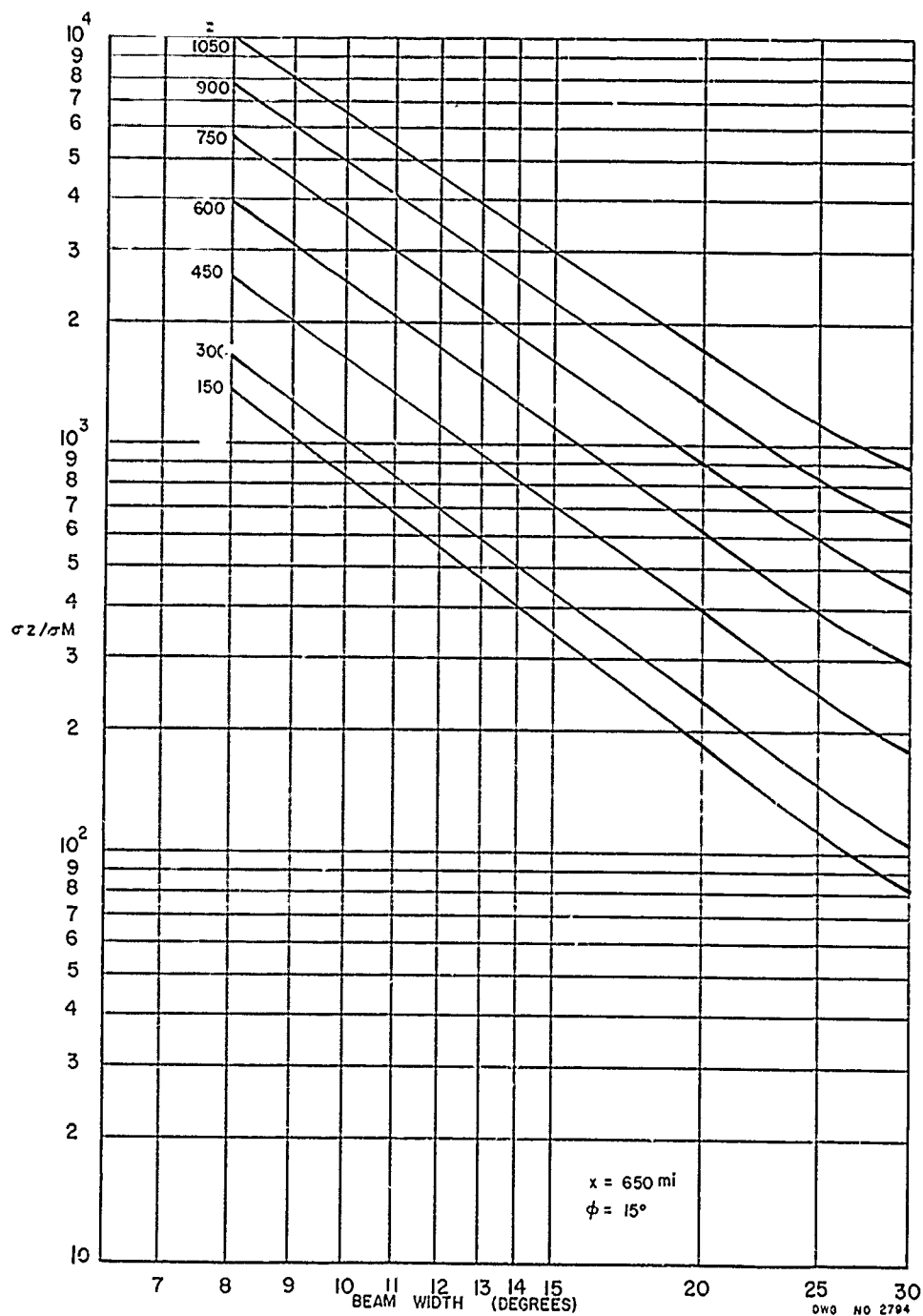


Figure 12b

C-33

PHILCO

GOVERNMENT & INDUSTRIAL GROUP
WESTERN DEVELOPMENT LABORATORIES

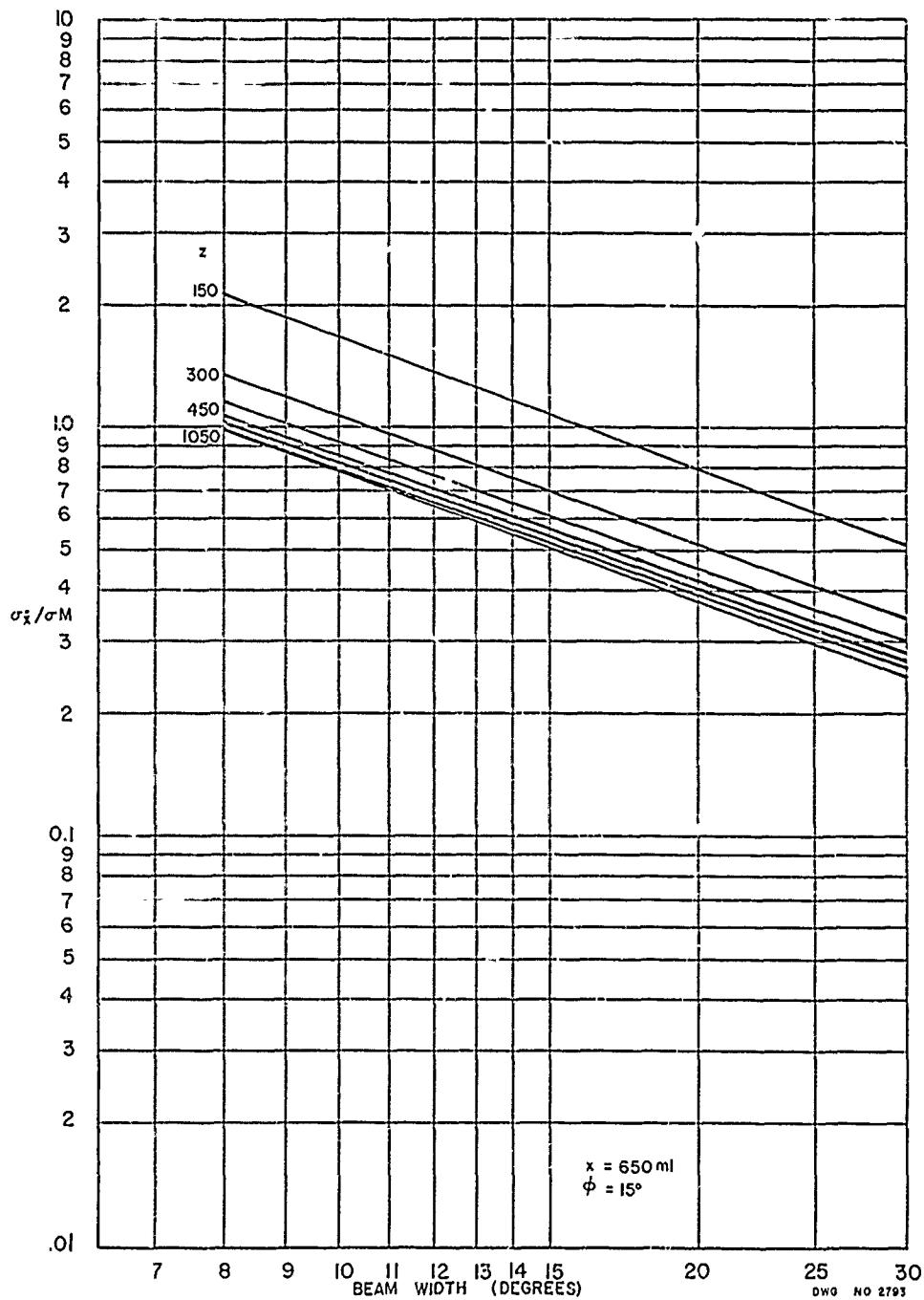


Figure 12c
C-34

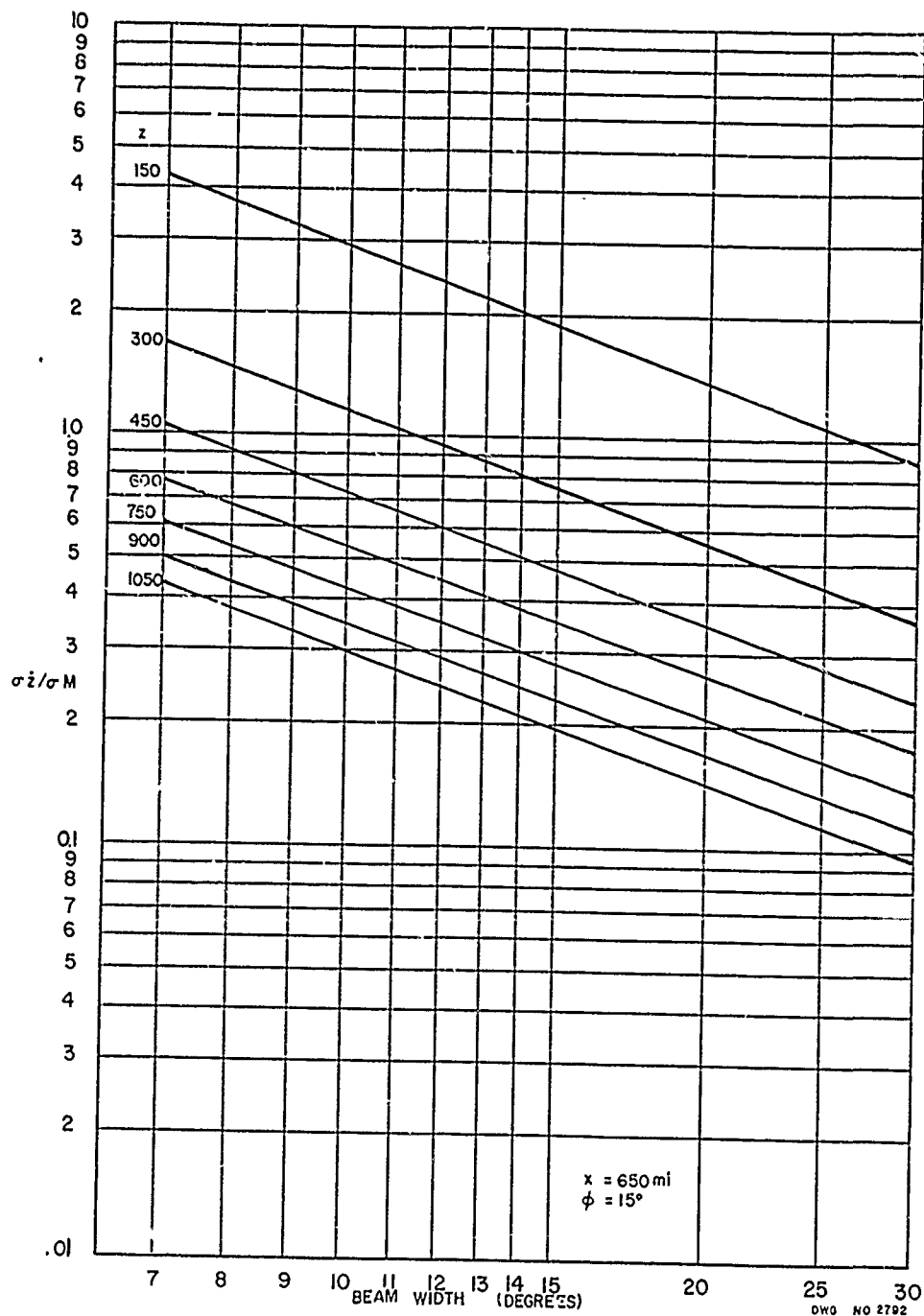


Figure 12d
 C-35

PHILCO

GOVERNMENT & INDUSTRIAL GROUP
 WESTERN DEVELOPMENT LABORATORIES

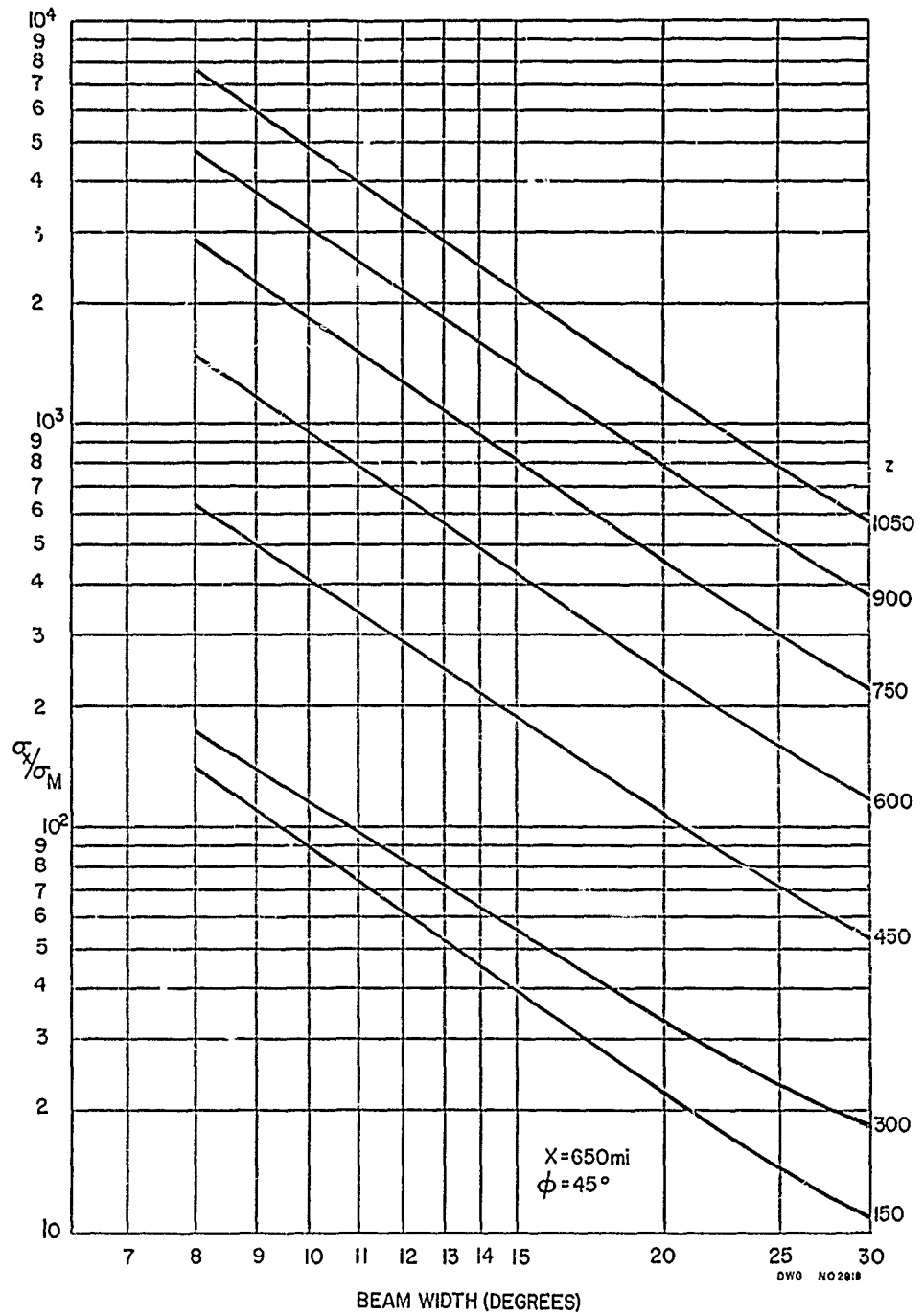


Figure 13a

C-36

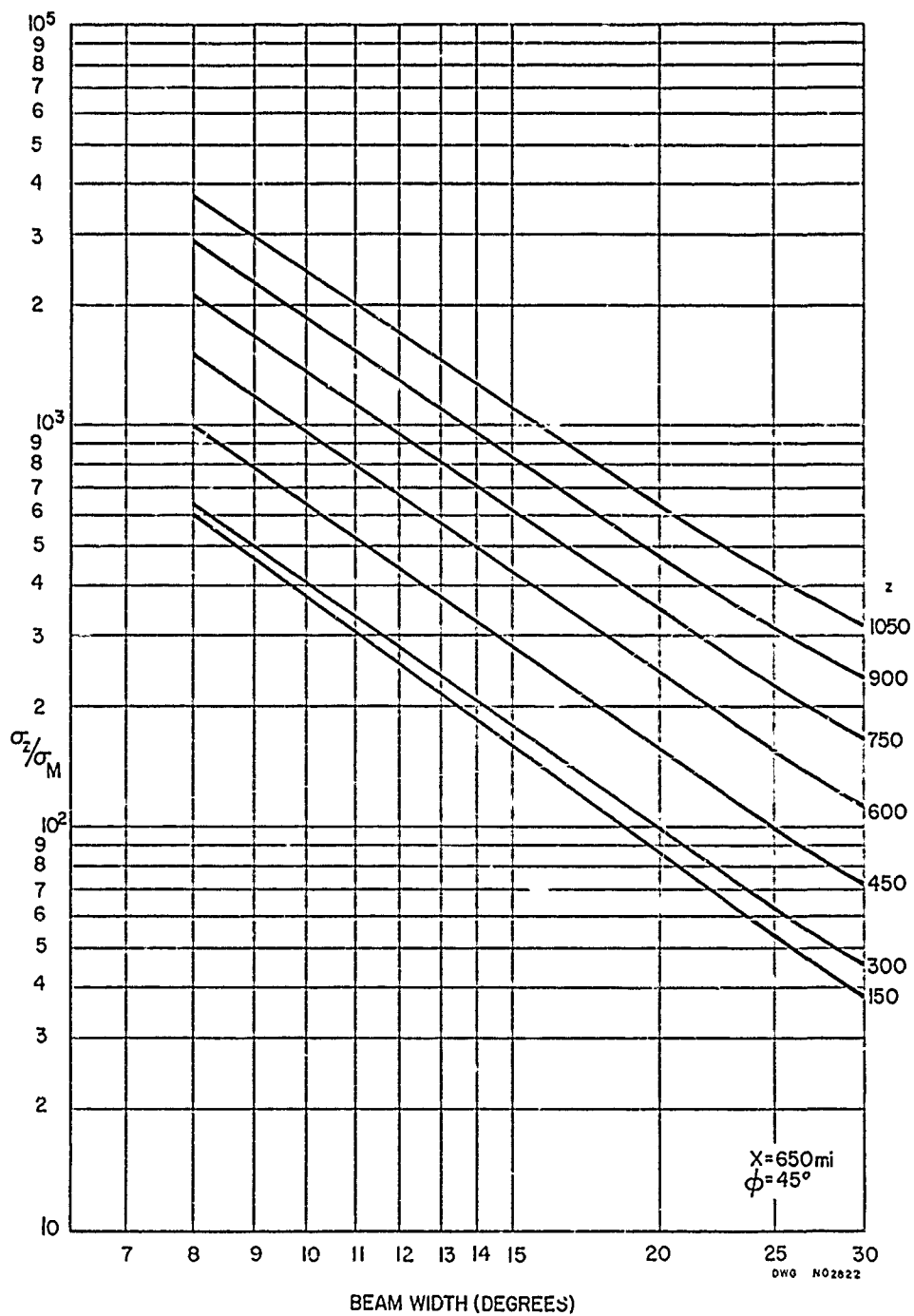


Figure 13b

C-37

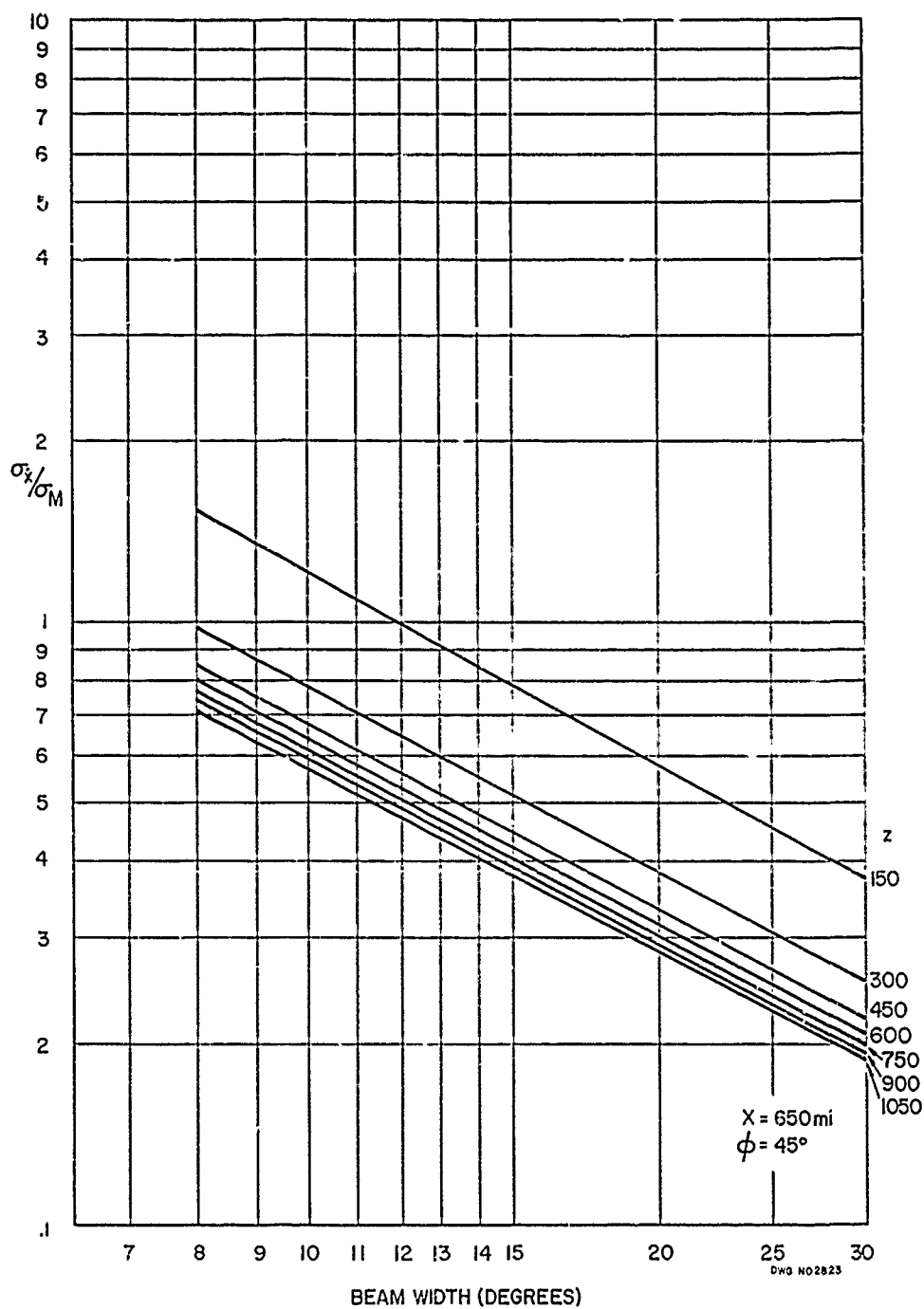
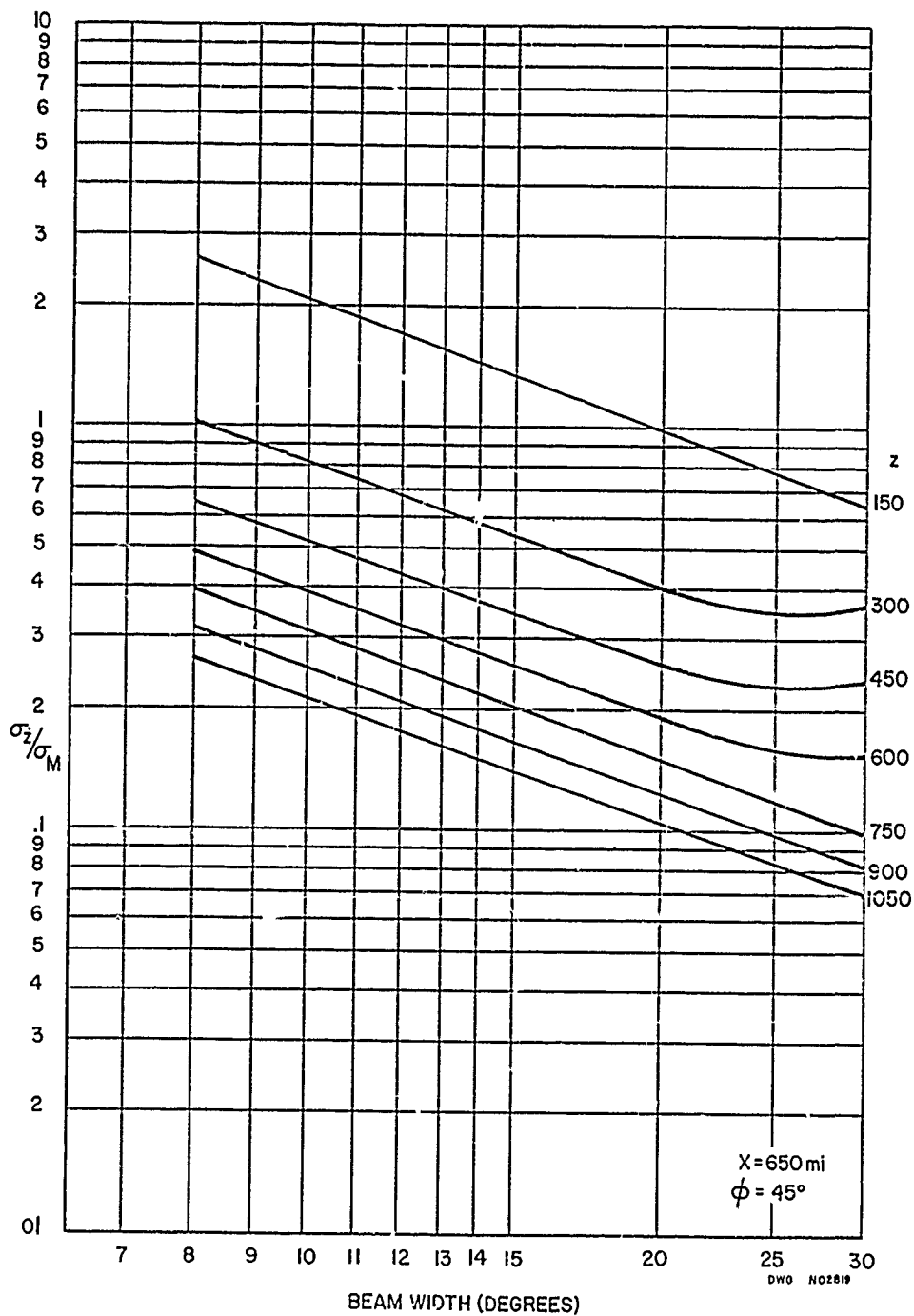


Figure 13c

C-38

PHILCO

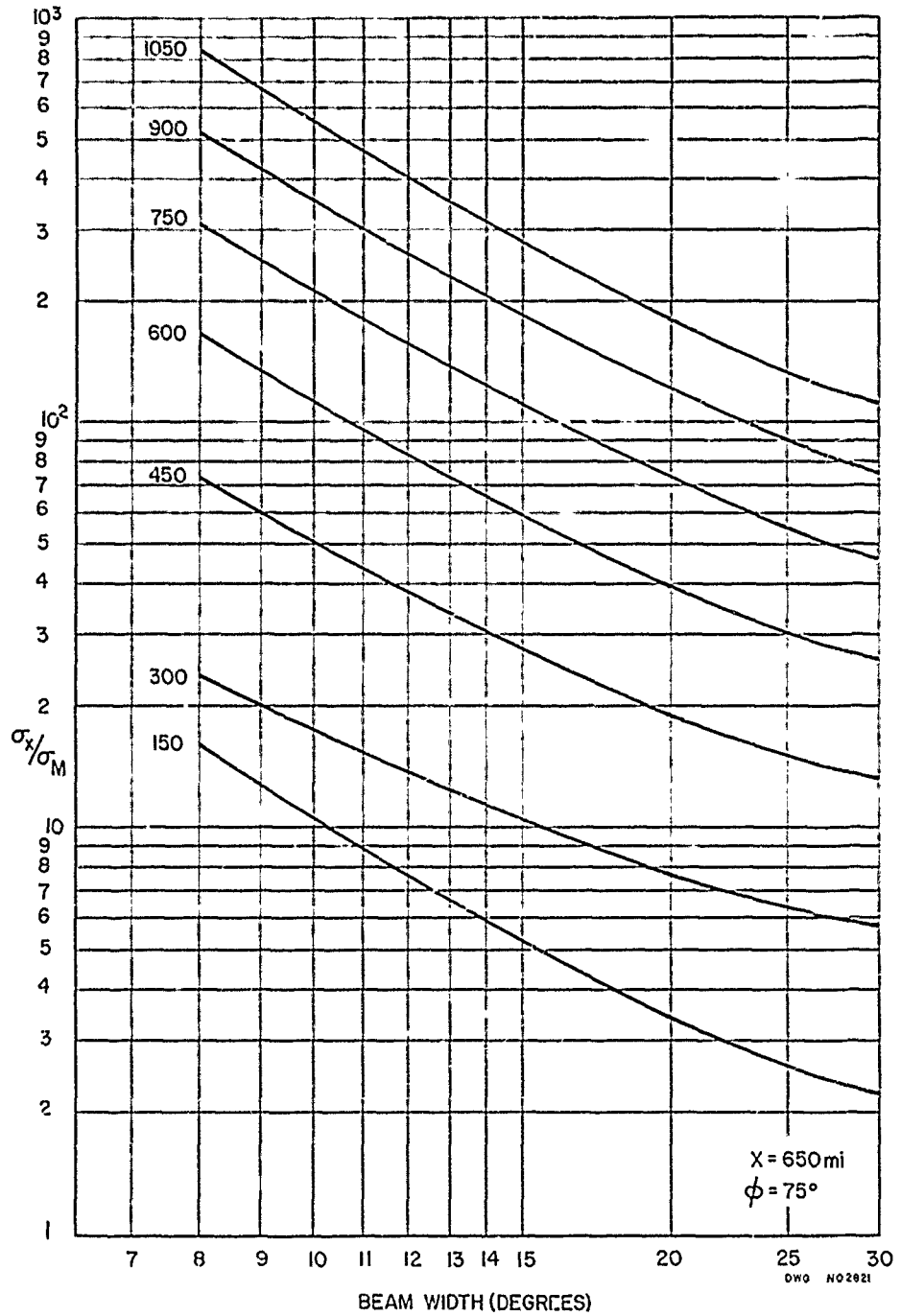
GOVERNMENT & INDUSTRIAL DIVISION
WESTERN DEVELOPMENT LABORATORIES



BEAM WIDTH (DEGREES)

Figure 13d

C-39



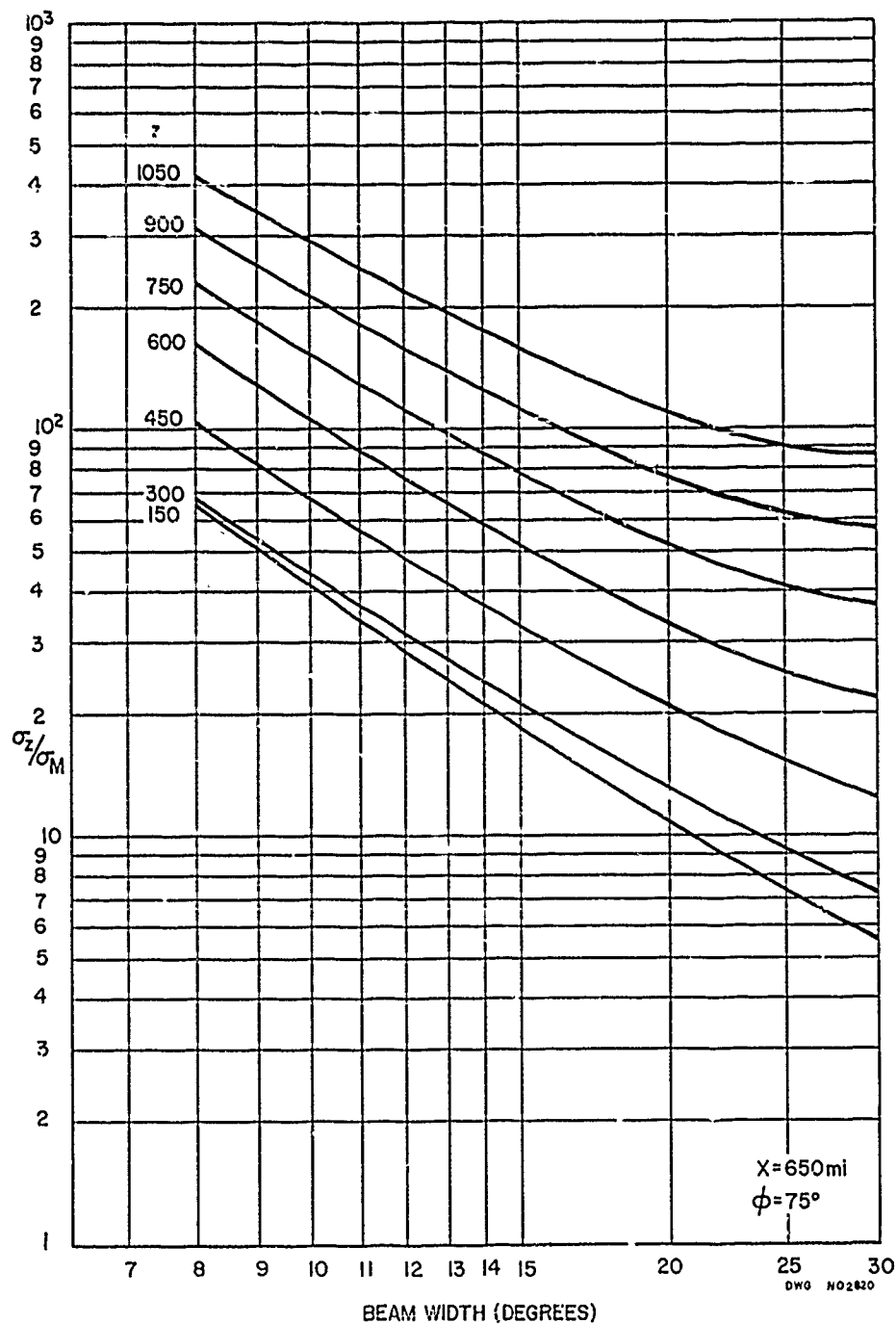


Figure 14b

C-41

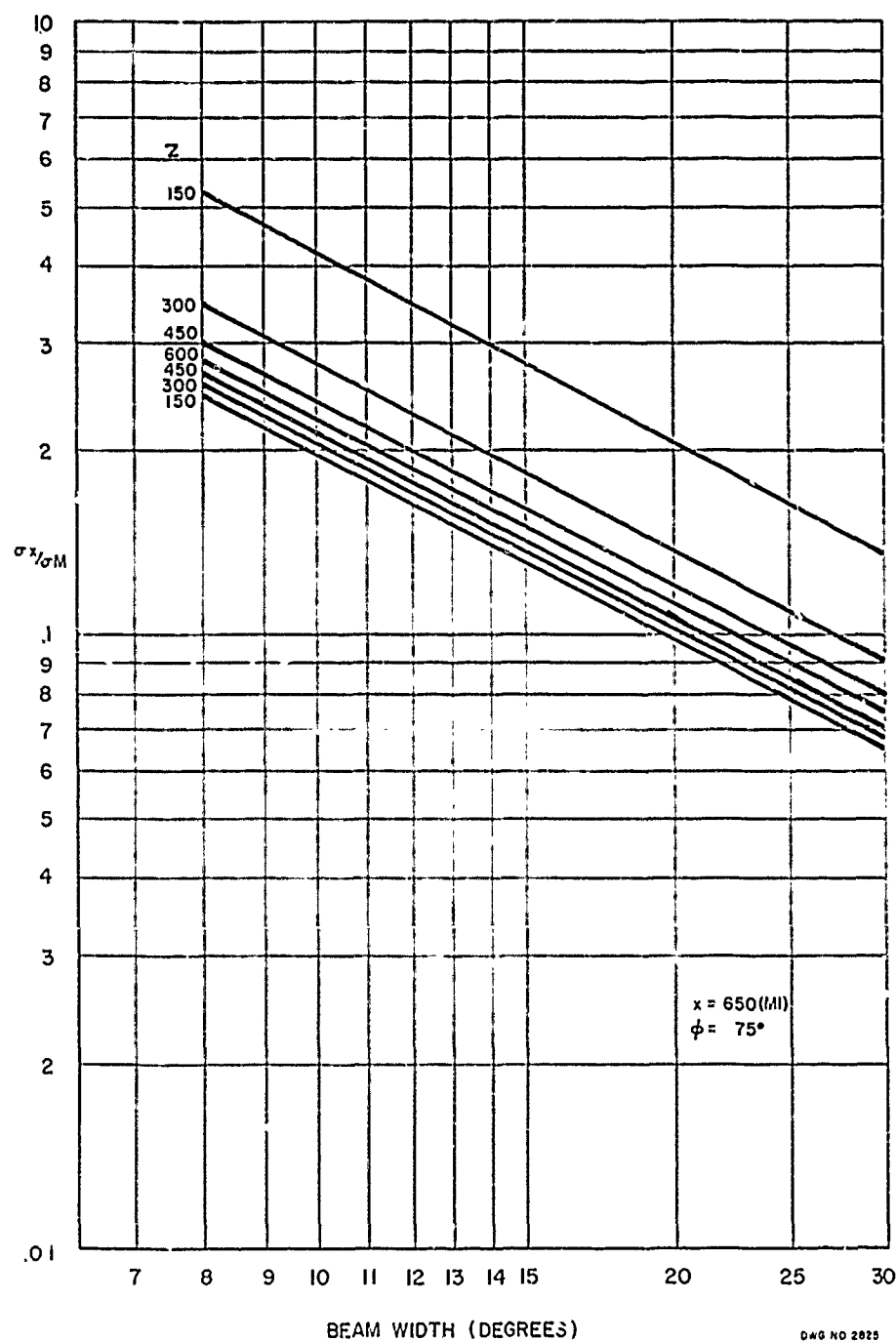
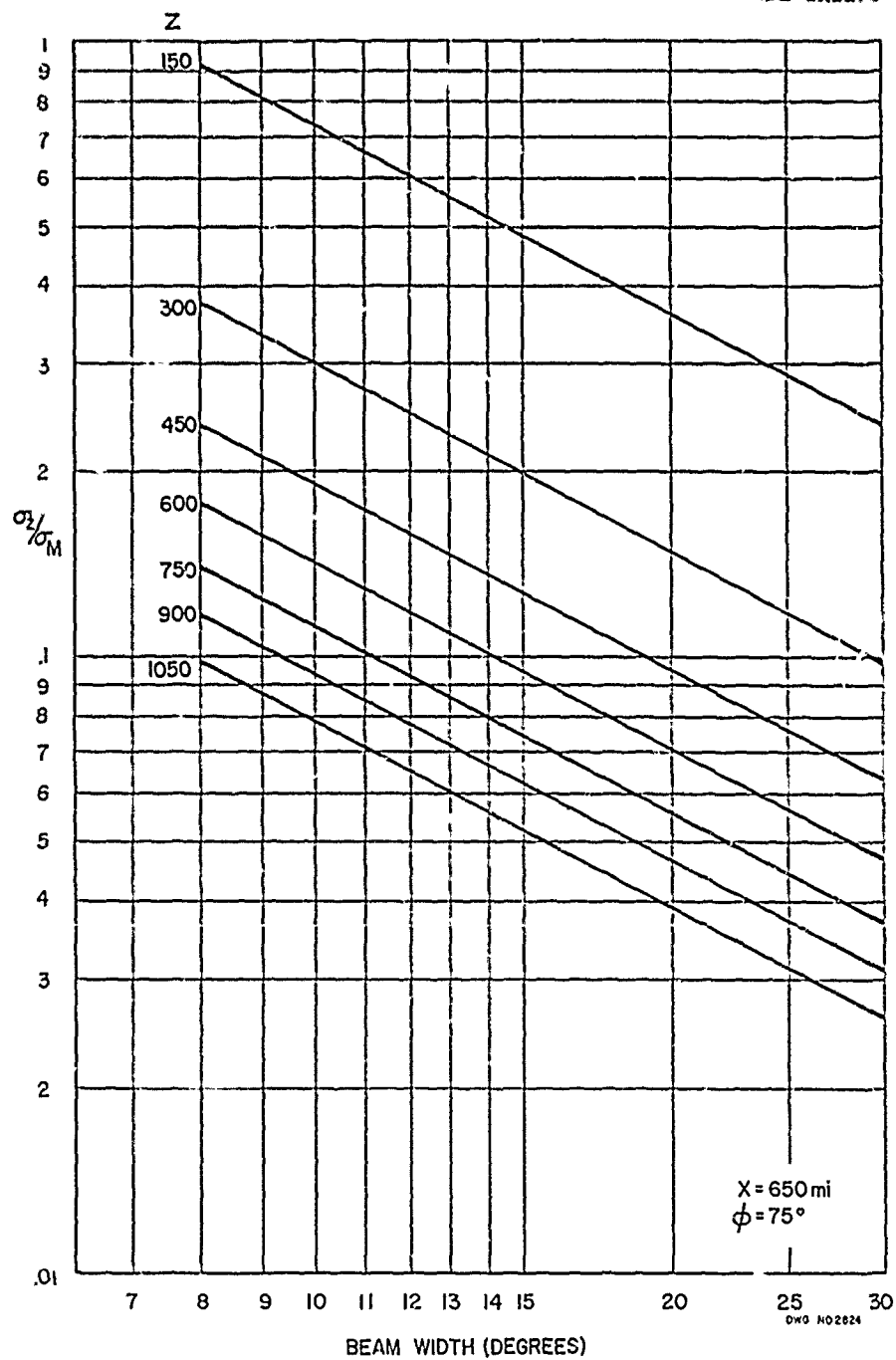


Figure 14c
42



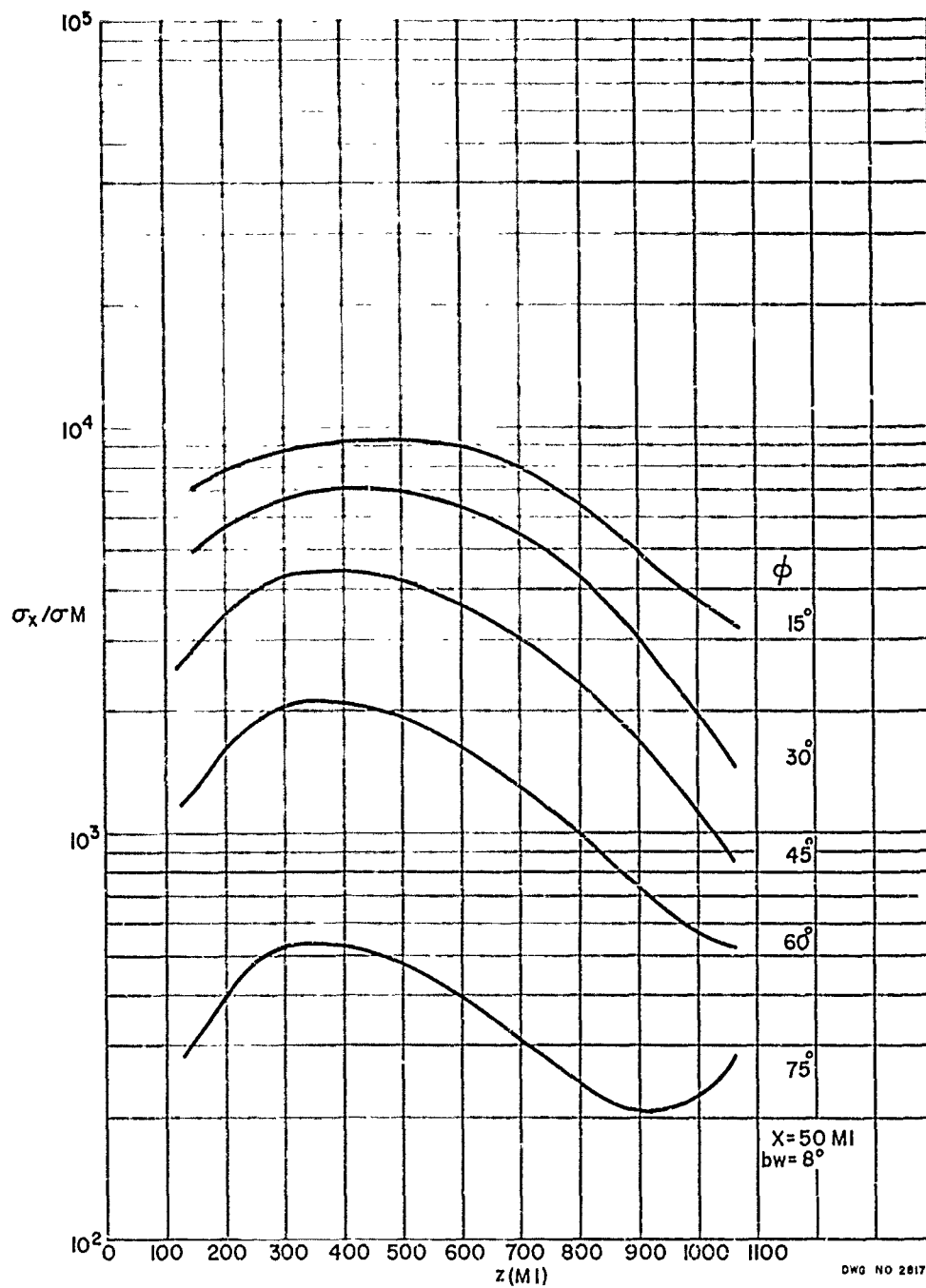


Figure 2a

44

PHILCO

GOVERNMENT & INDUSTRIAL DIVISION
WESTERN DEVELOPMENT LABORATORIES

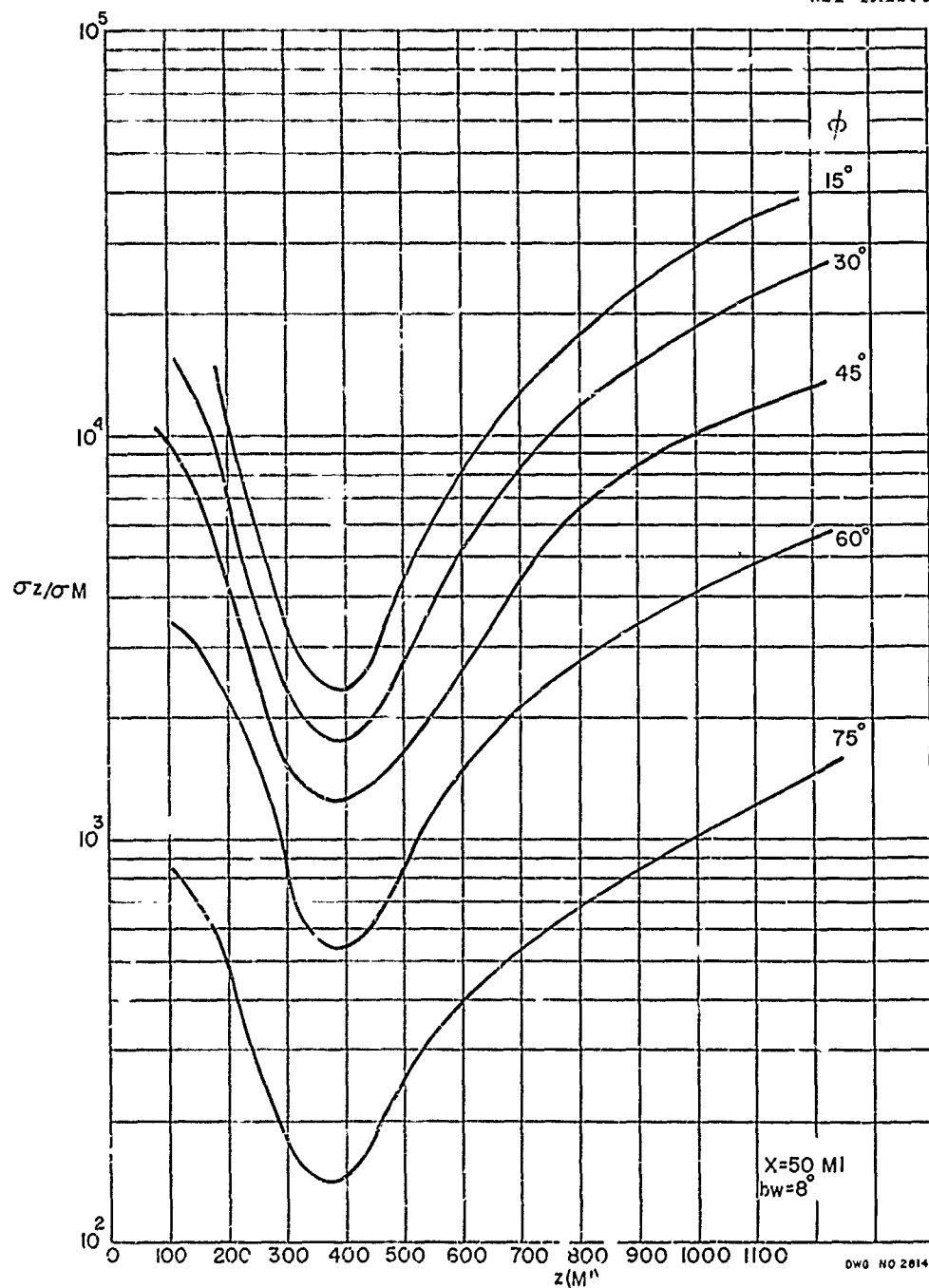


Figure 150

• 4 •

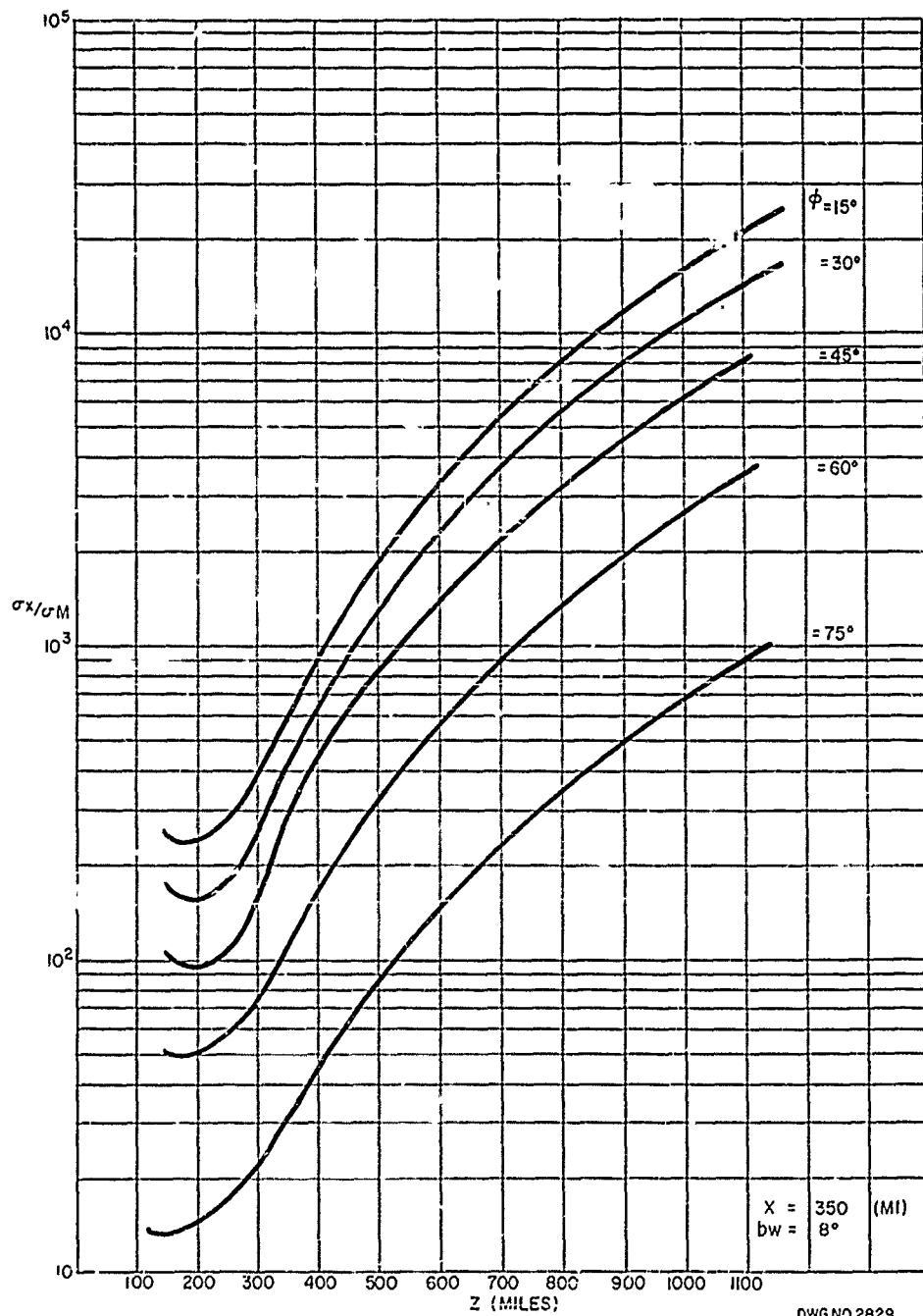


Figure 16a

C-46

PHILCO

GOVERNMENT & INDUSTRIAL GROUP
WESTERN DEVELOPMENT LABORATORIES

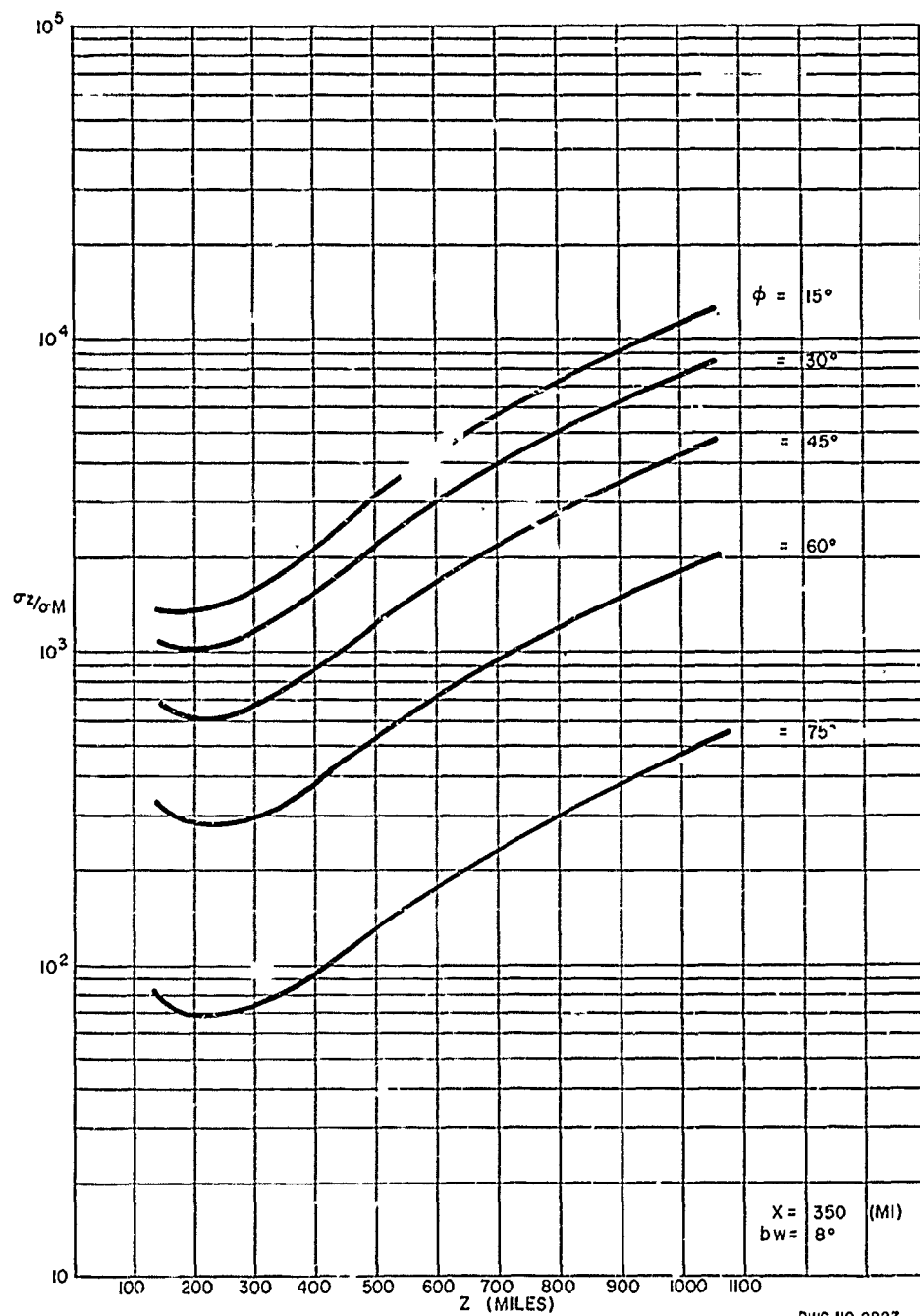


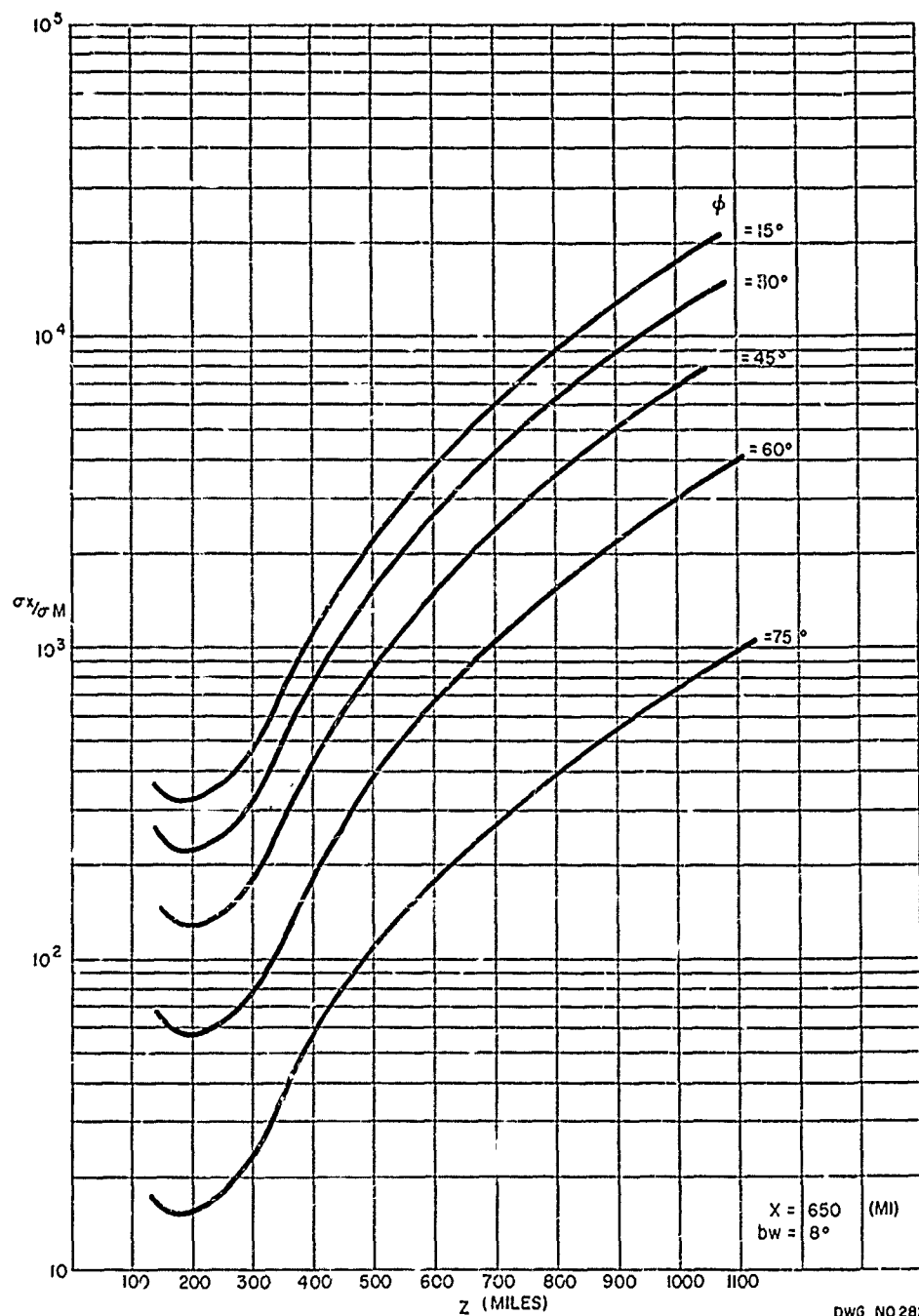
Figure 16b

C-47

DWG NO 2827

PHILCO

GOVERNMENT & INDUSTRIAL GROUP
WESTERN DEVELOPMENT LABORATORIES



DWG NO 2826

Figure 17a

6-45

PHILCO

GOVERNMENT & INDUSTRIAL GROUP
WESTERN DEVELOPMENT LABORATORIES

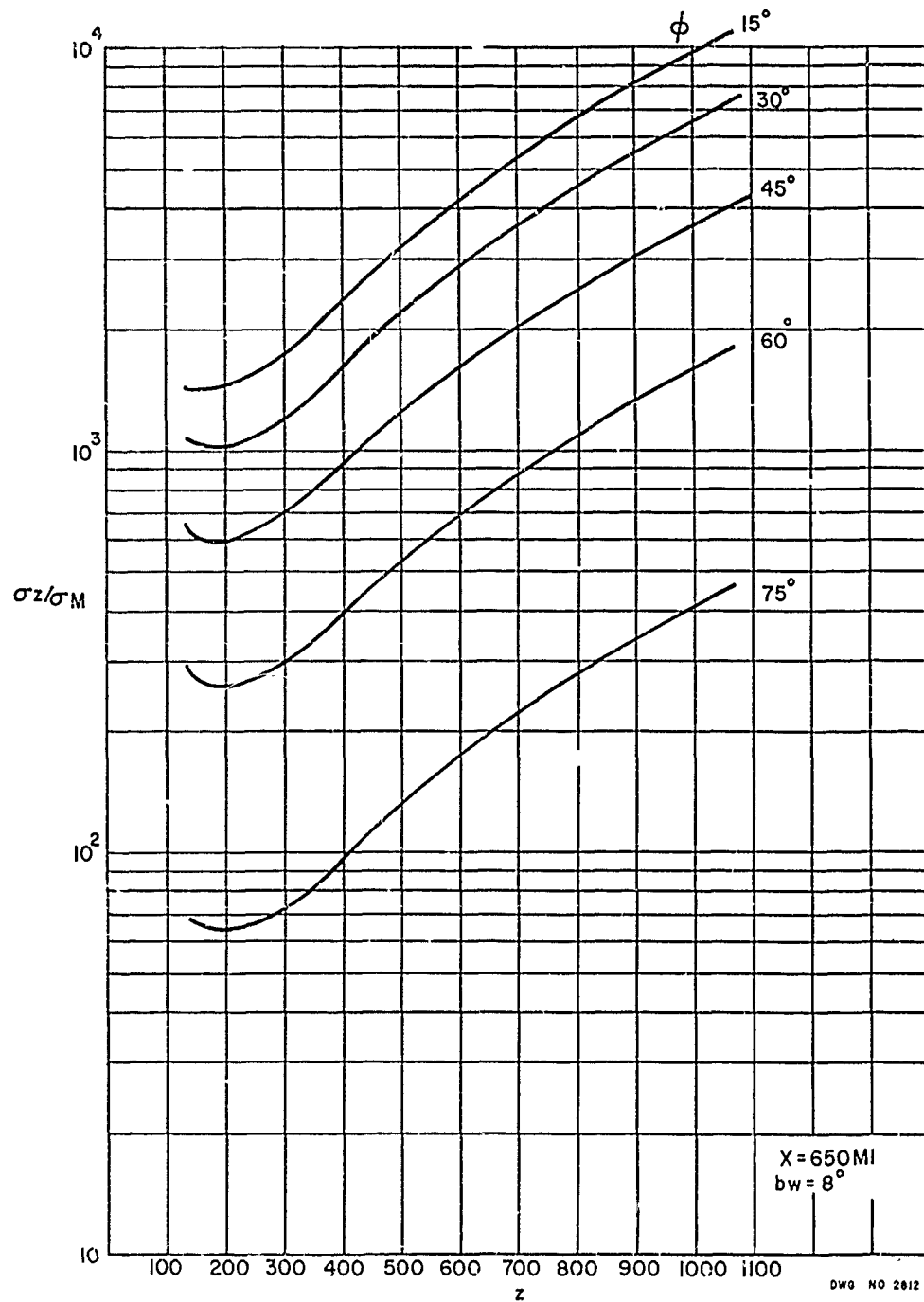


Figure 17b

C-49

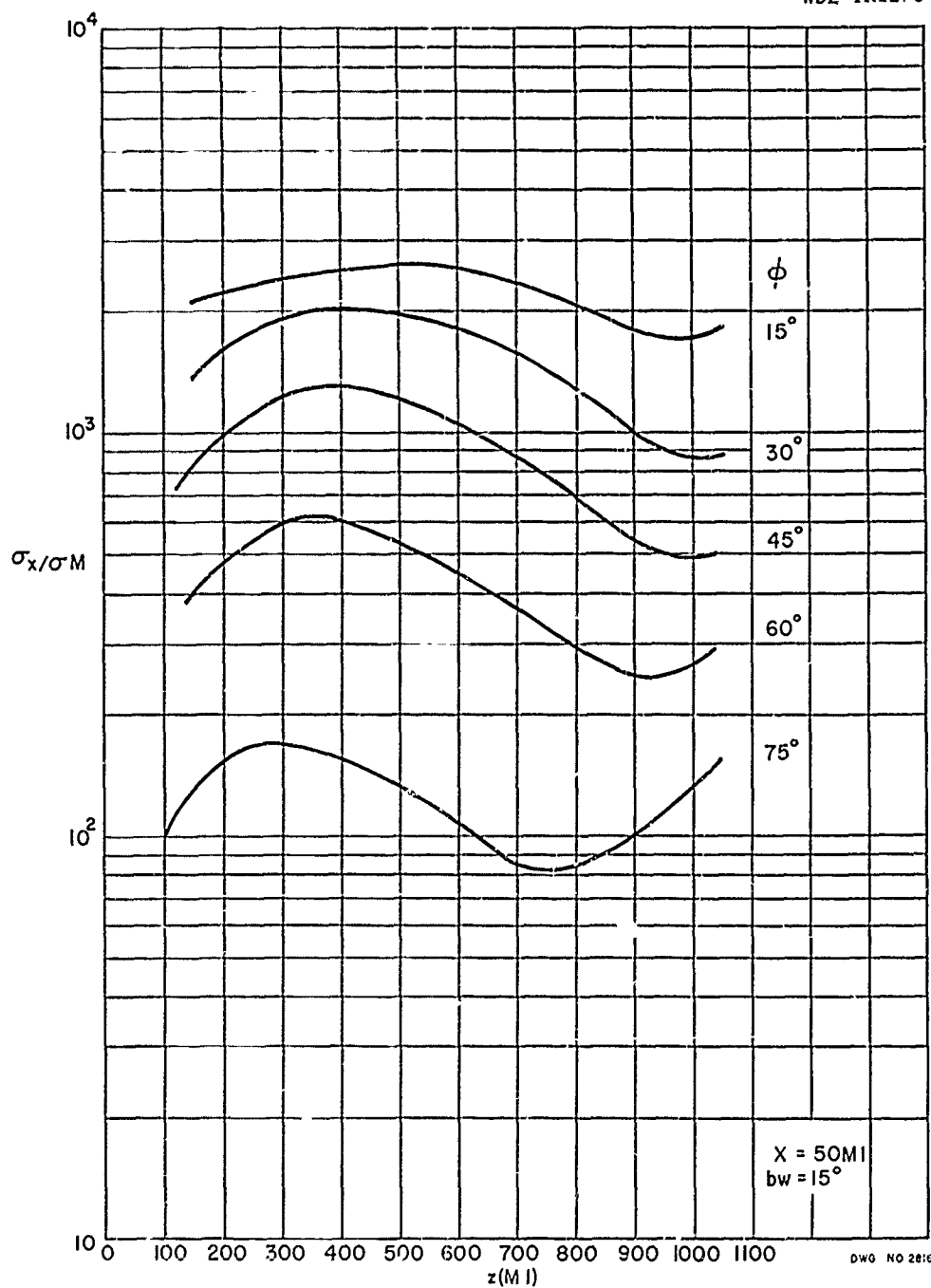


Figure 18a

6 20

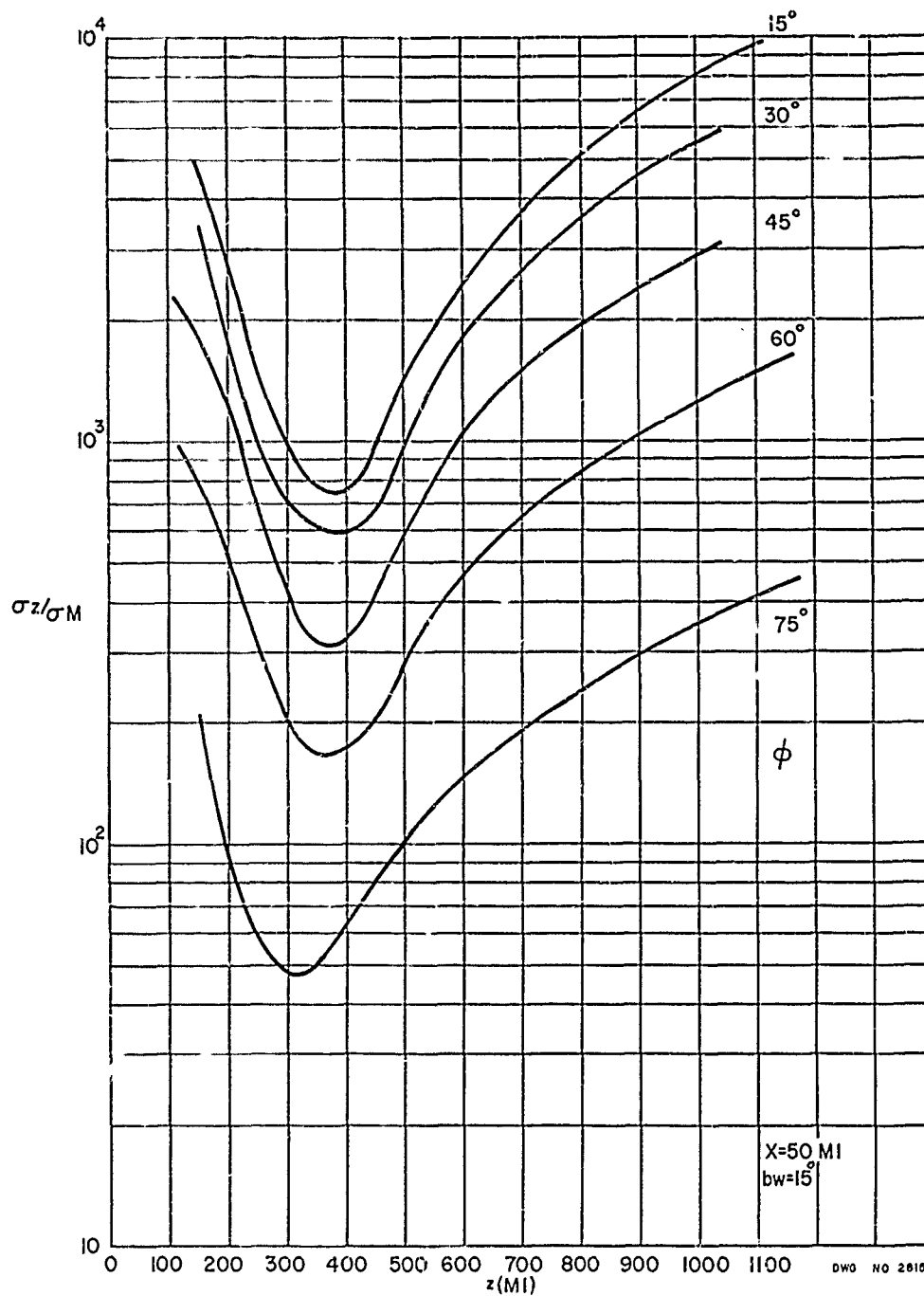
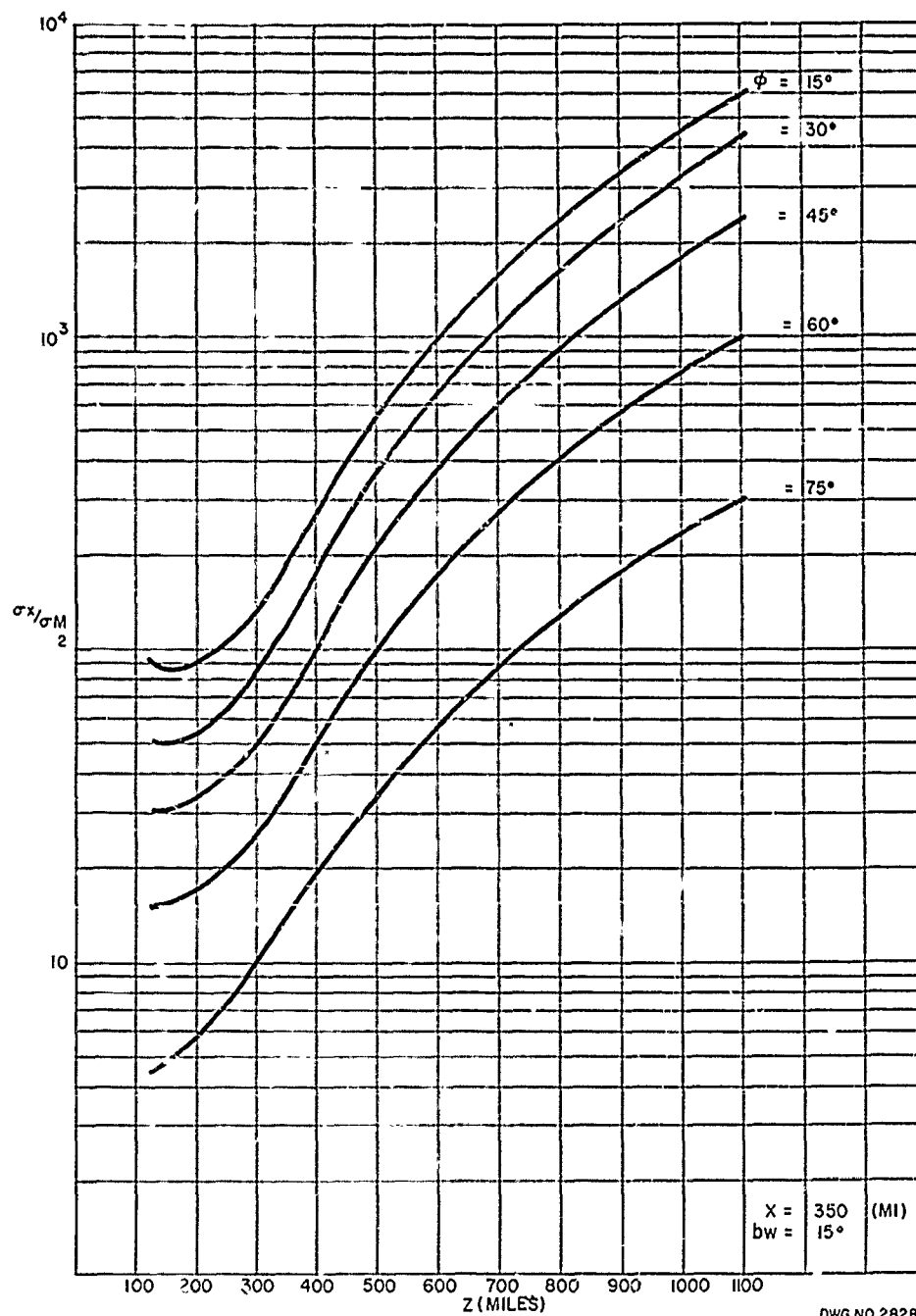


Figure 18b
C 51



DWG NO 2828

Figure 19a

C-2

PHILCO

GOVERNMENT & INDUSTRIAL GROUP
WESTERN DEVELOPMENT LABORATORIES

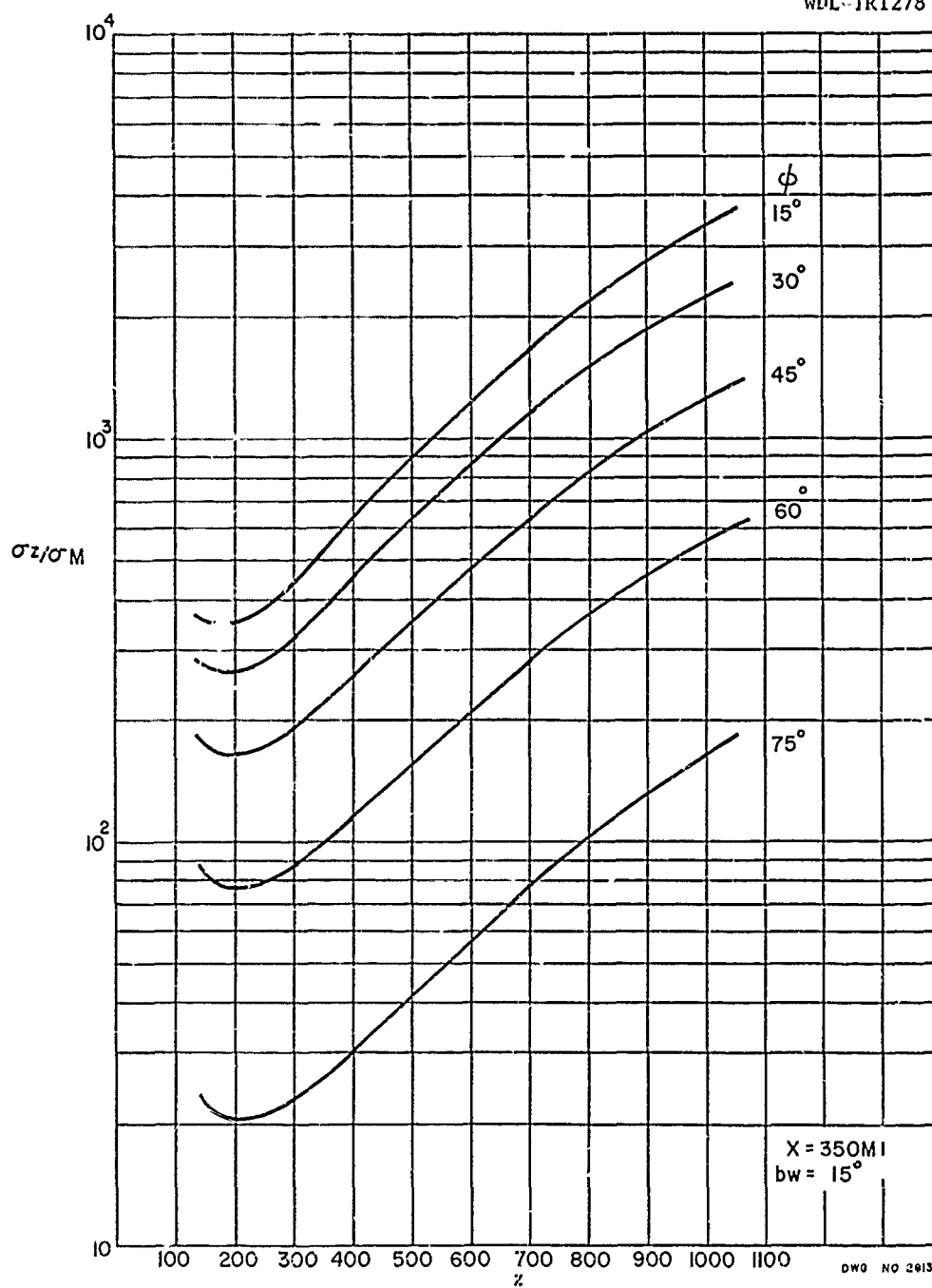
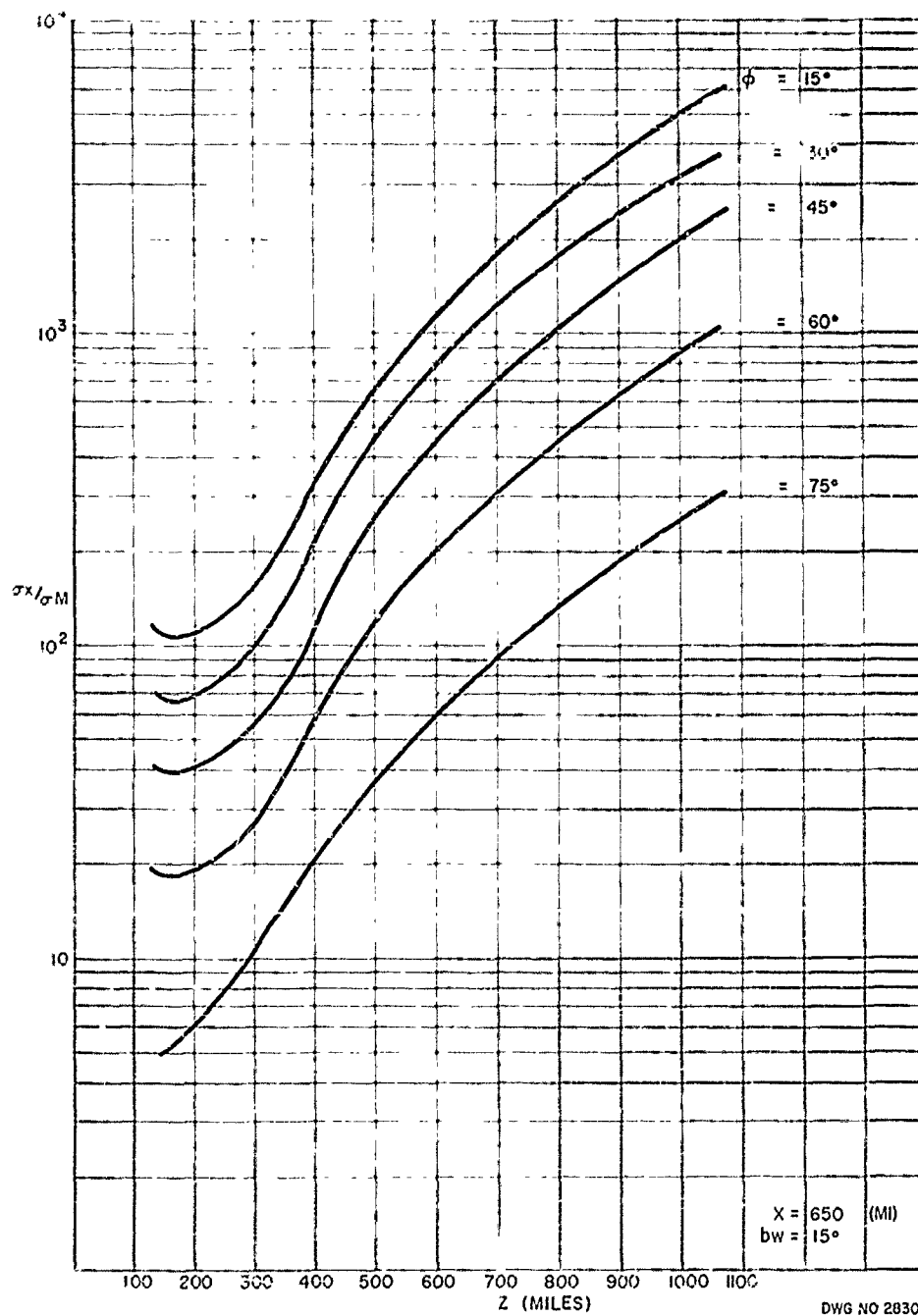


Figure 19b

C 53

PHILCO

GOVERNMENT & INDUSTRIAL GROUP
WESTERN DEVELOPMENT LABORATORIES



PHILCO

GOVERNMENT & INDUSTRIAL GROUP
WESTERN DEVELOPMENT LABORATORIES

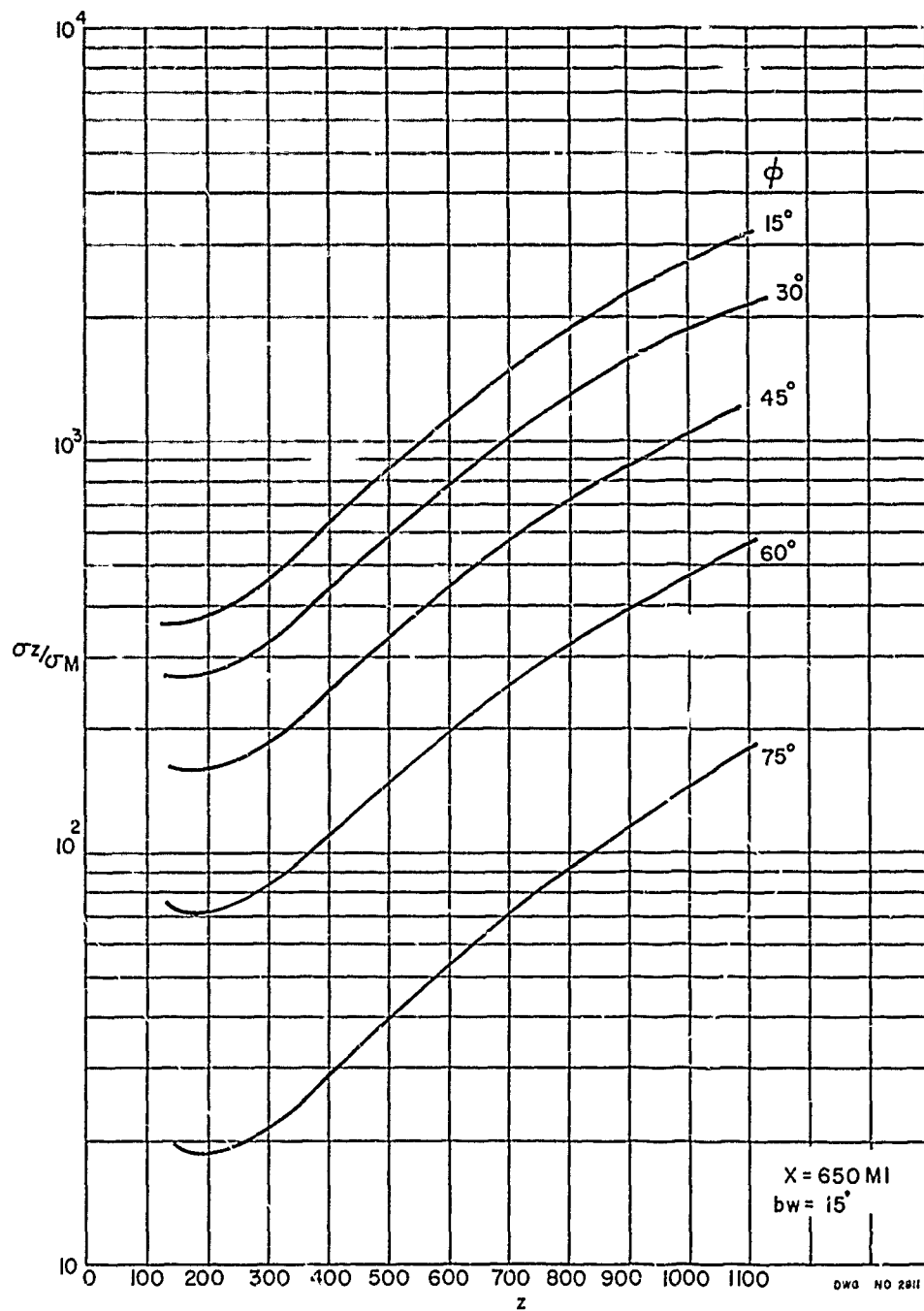


Figure 20b

C-53

PHILCO

GOVERNMENT & INDUSTRIAL GROUP
WESTERN DEVELOPMENT LABORATORIES

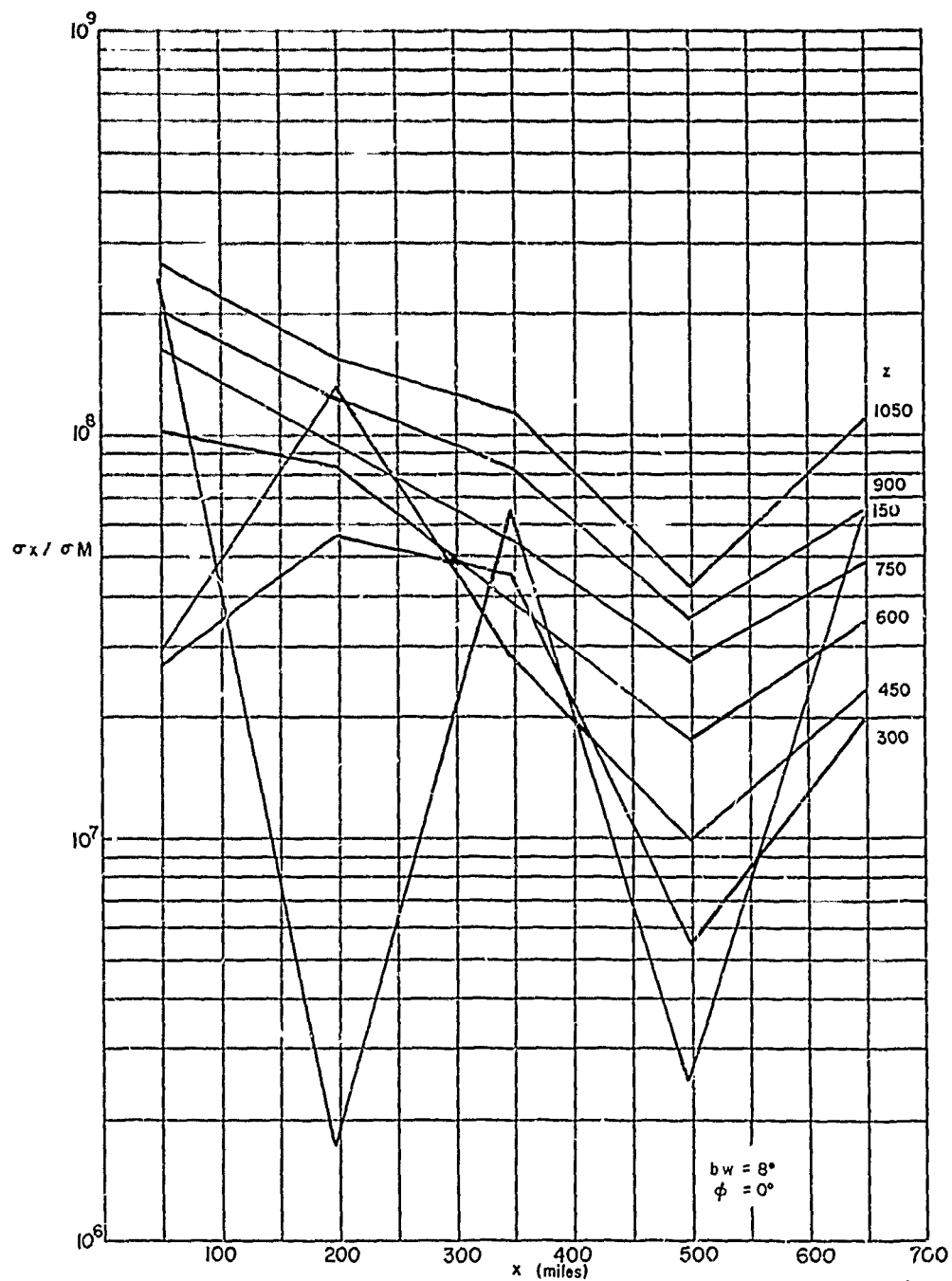
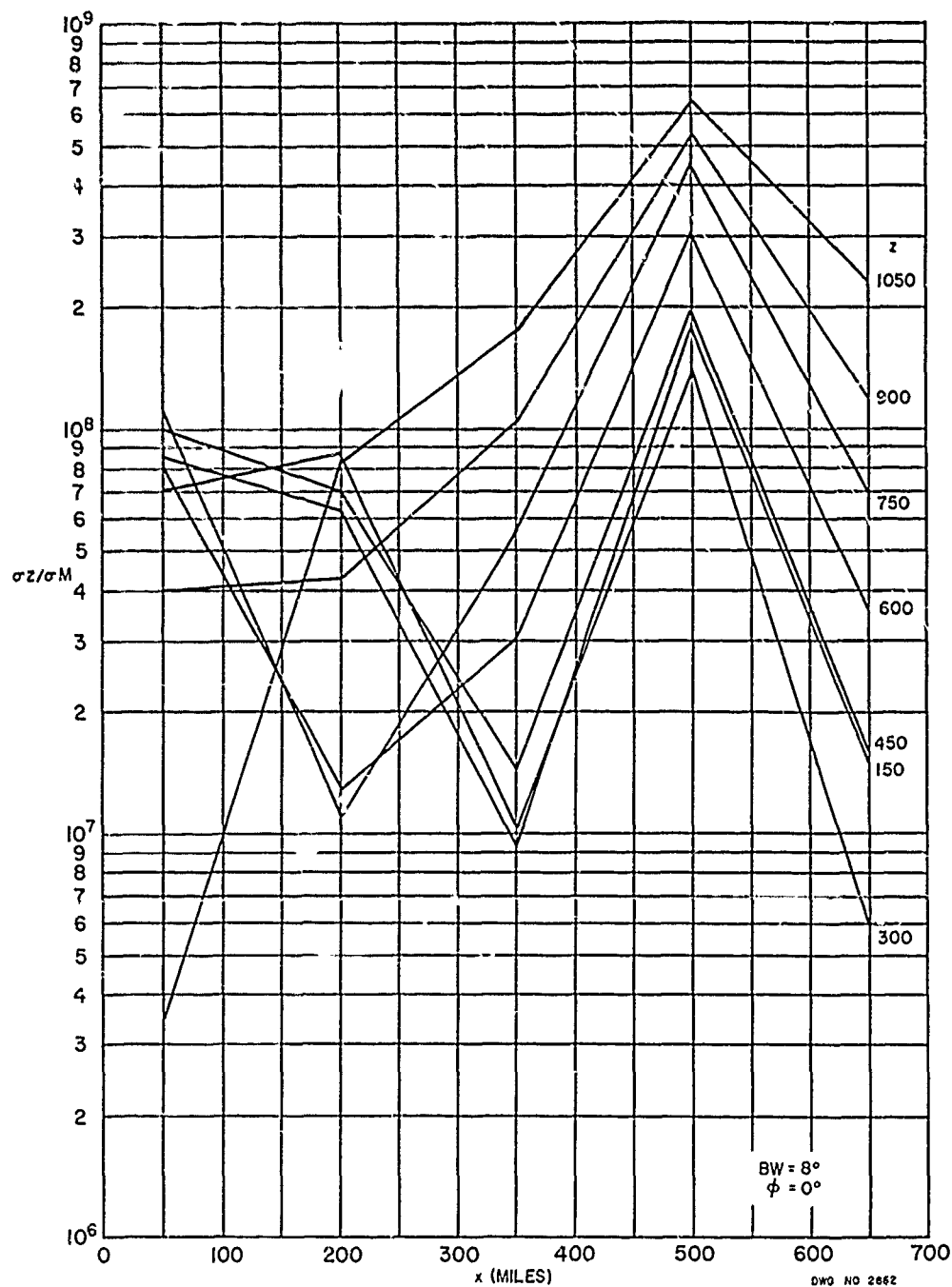


Figure 21a

C-56

PHILCO

GOVERNMENT & INDUSTRIAL GROUP
WESTERN DEVELOPMENT LABORATORIES



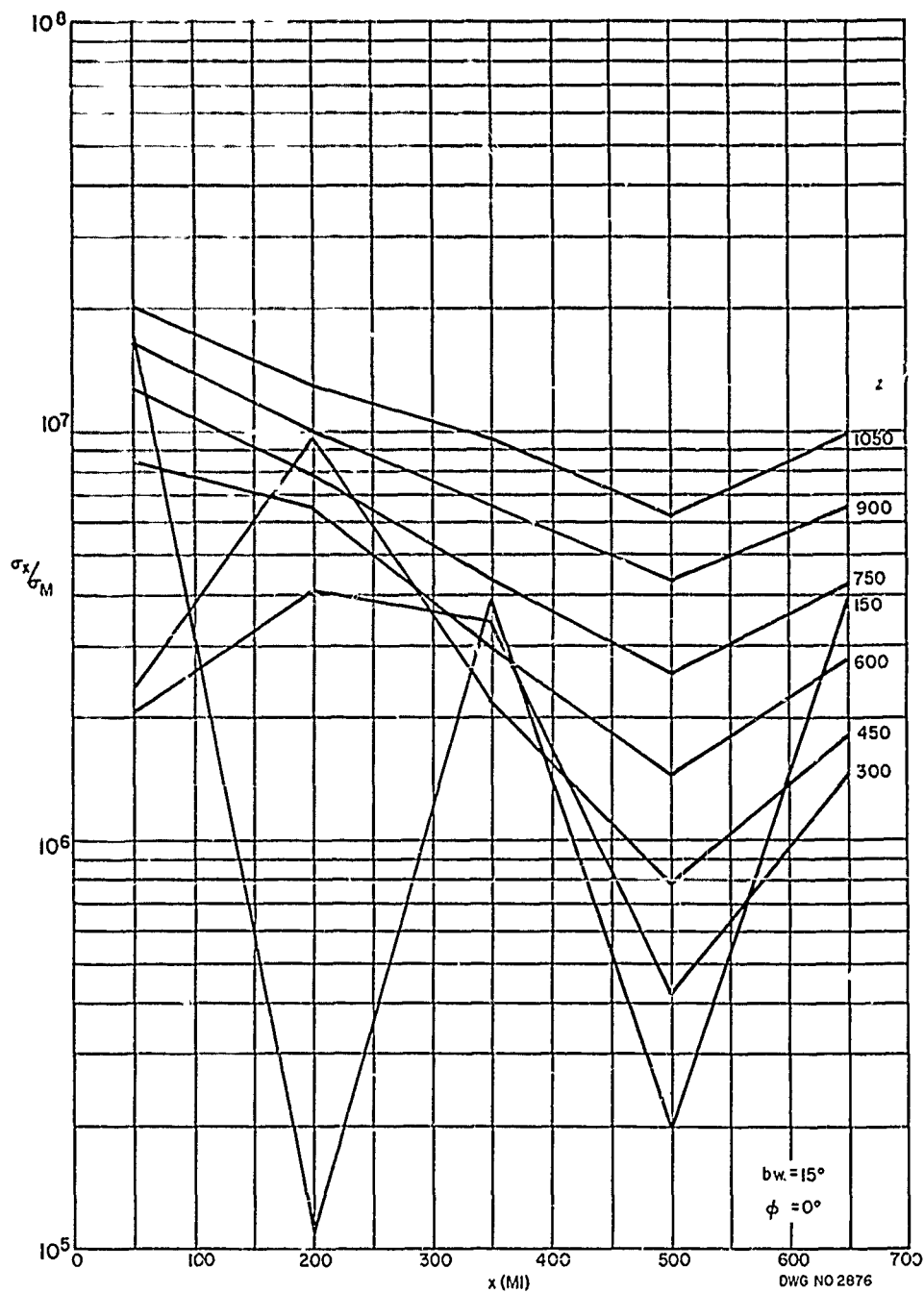


Figure 22a

C-58

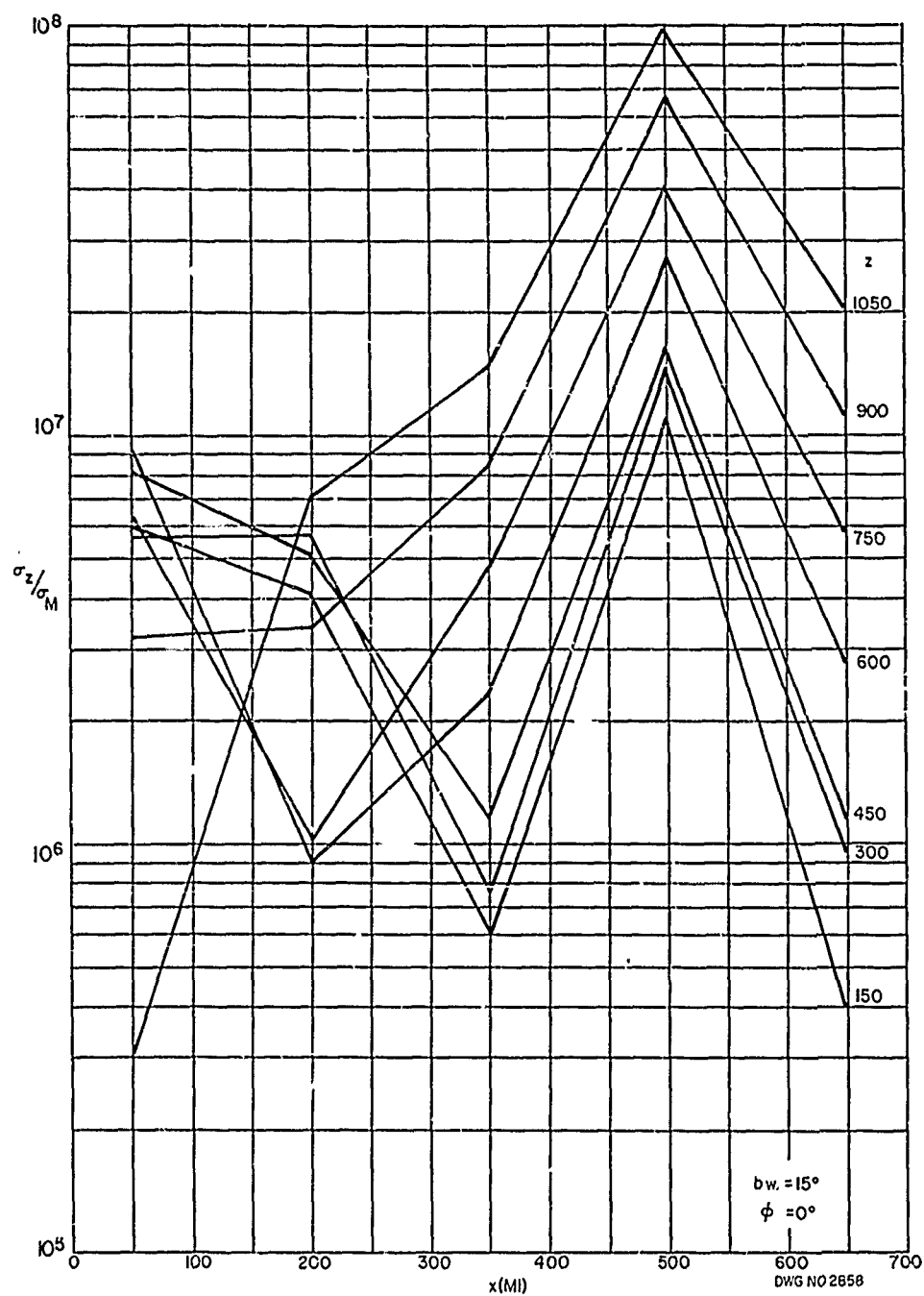


Figure 22b
C-59

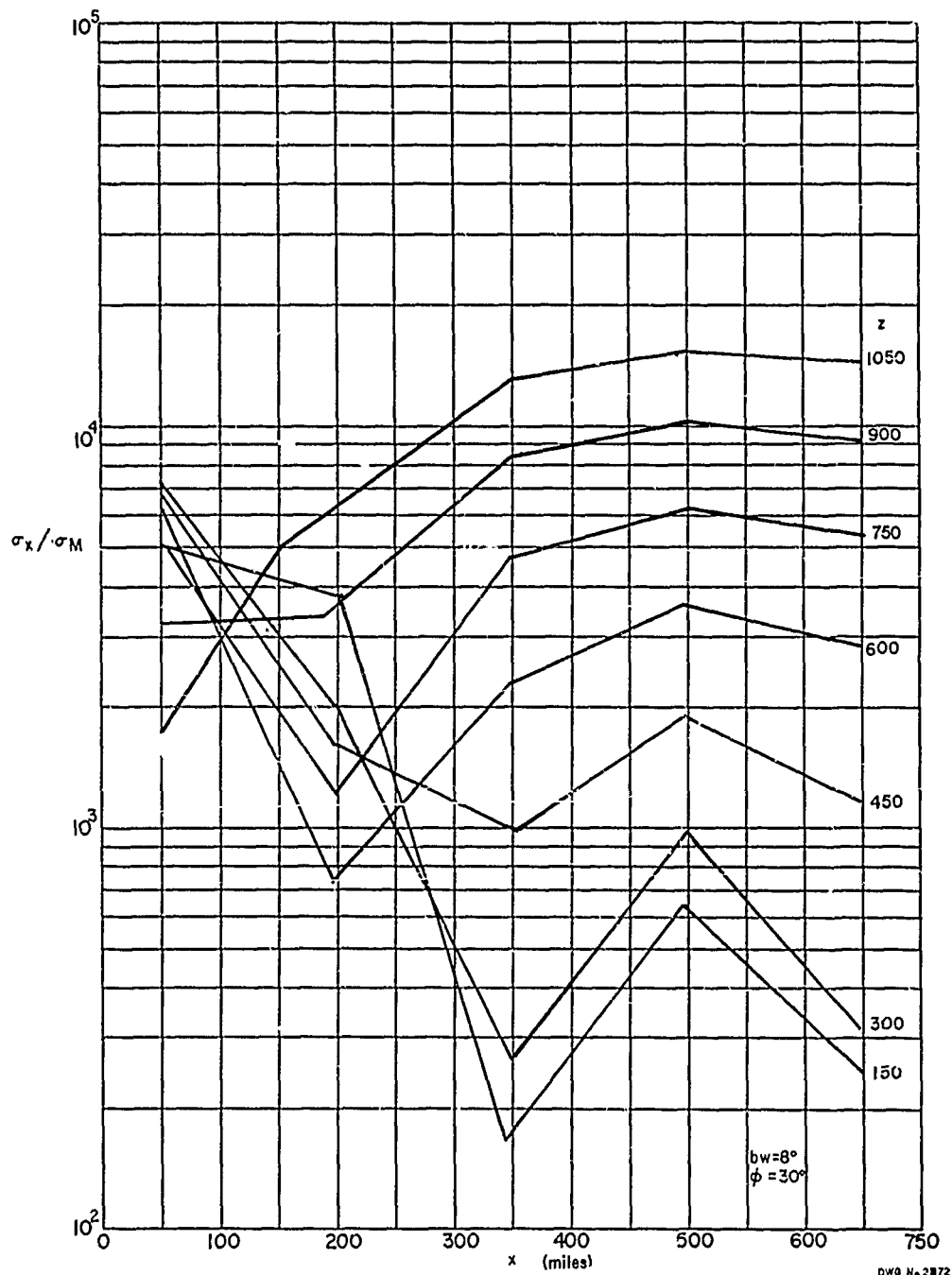
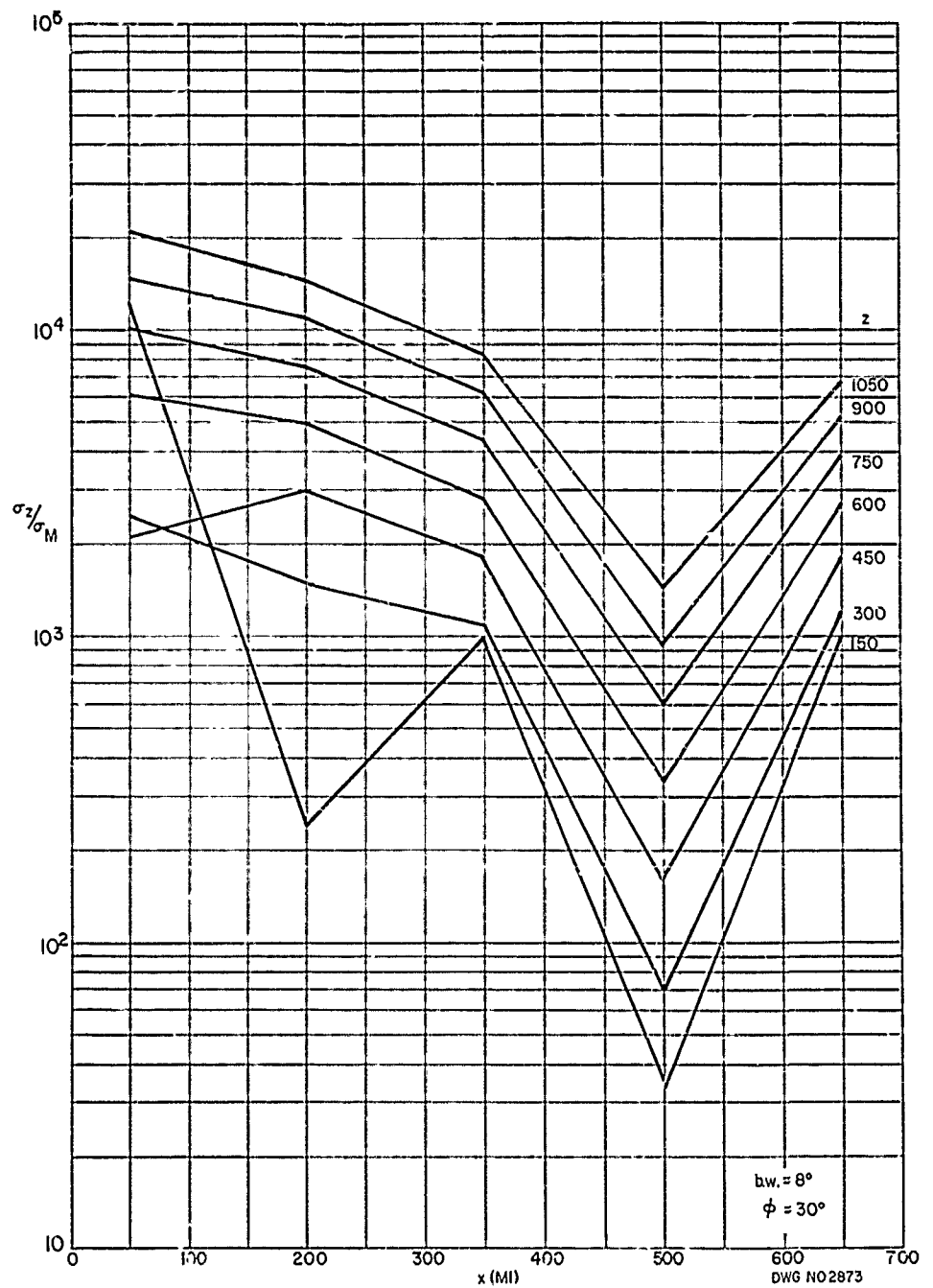


Figure 23a

C-60

PHILCO

GOVERNMENT & INDUSTRIAL GROUP
WESTERN DEVELOPMENT LABORATORIES



PHILCO

GOVERNMENT & INDUSTRIAL GROUP
WESTERN DEVELOPMENT LABORATORIES

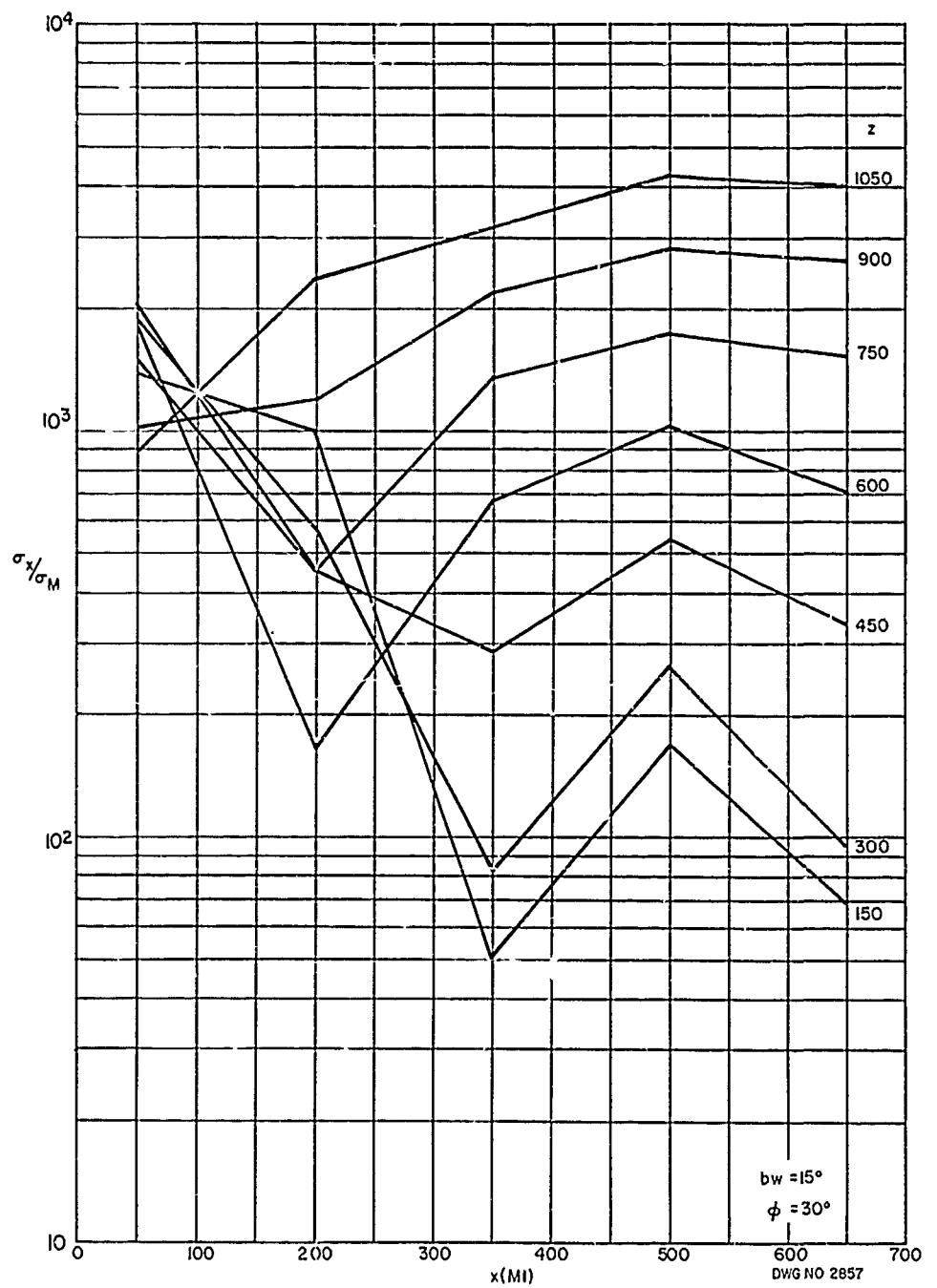


Figure 24a
C-62

PHILCO

GOVERNMENT & INDUSTRIAL GROUP
WESTERN DEVELOPMENT LABORATORIES

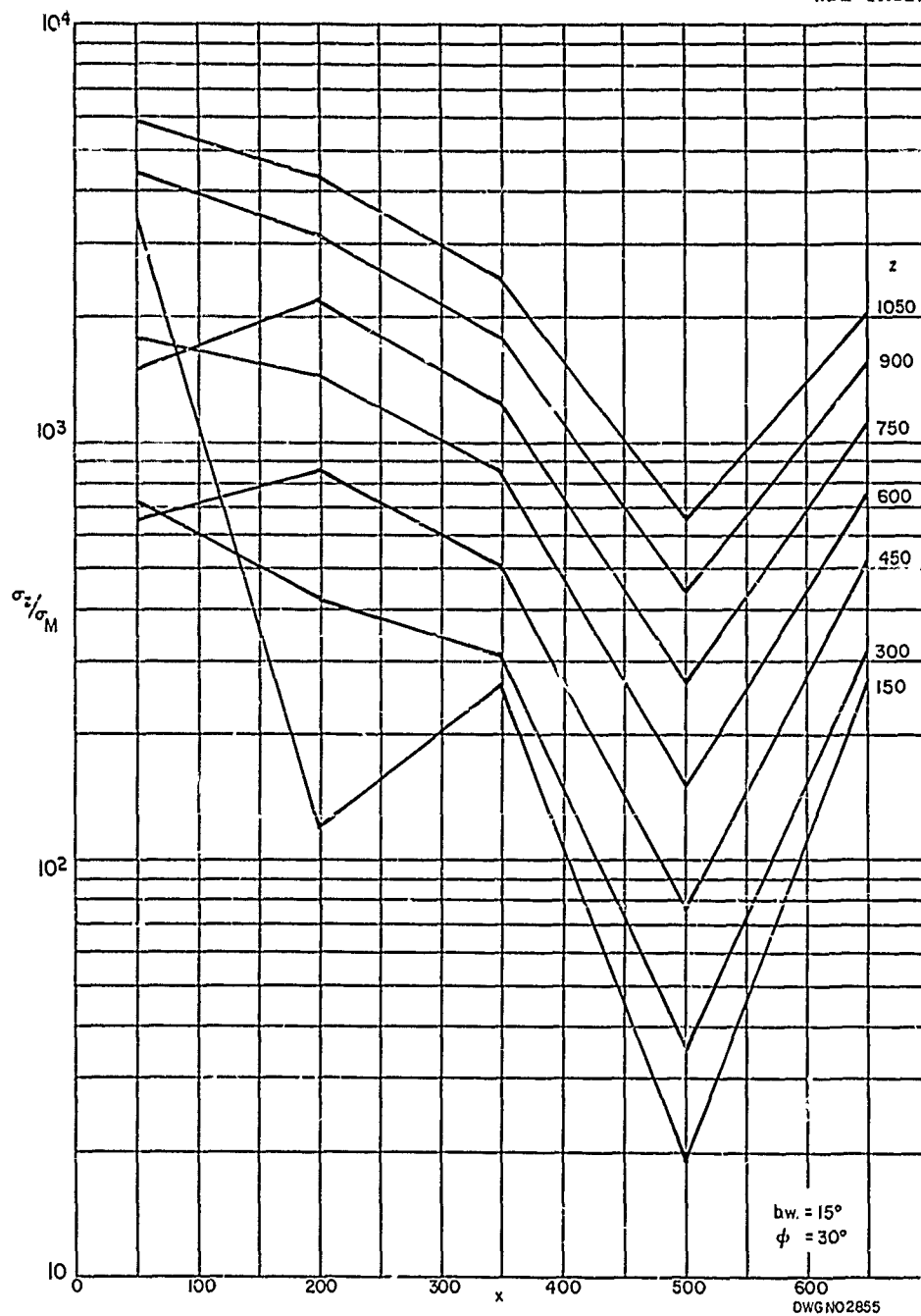


Figure 24b

C-63

PHILCO

GOVERNMENT & INDUSTRIAL GROUP
WESTERN DEVELOPMENT LABORATORIES

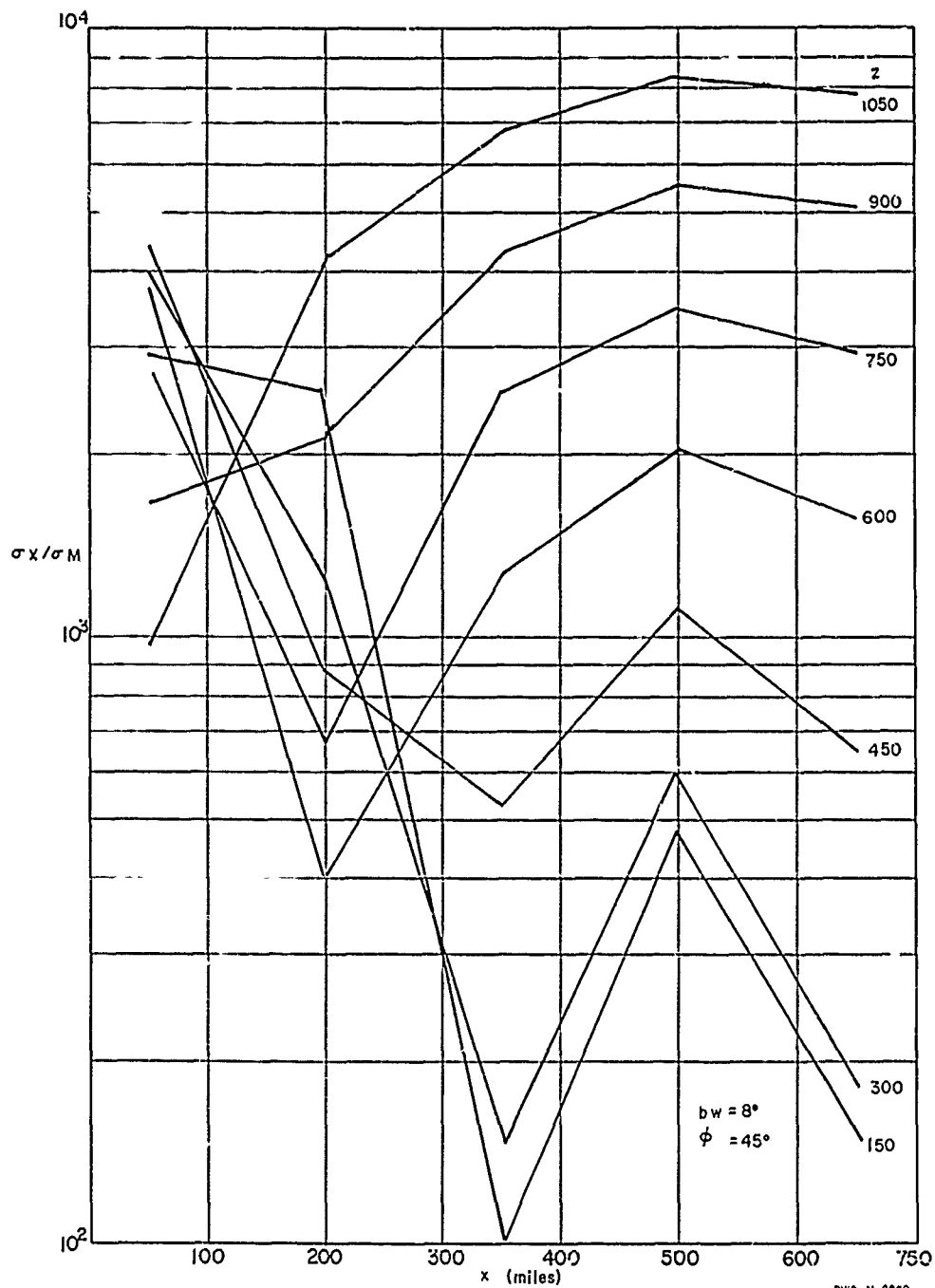


Figure 25a

C-64

PHILCO

GOVERNMENT & INDUSTRIAL GROUP
WESTERN DEVELOPMENT LABORATORIES

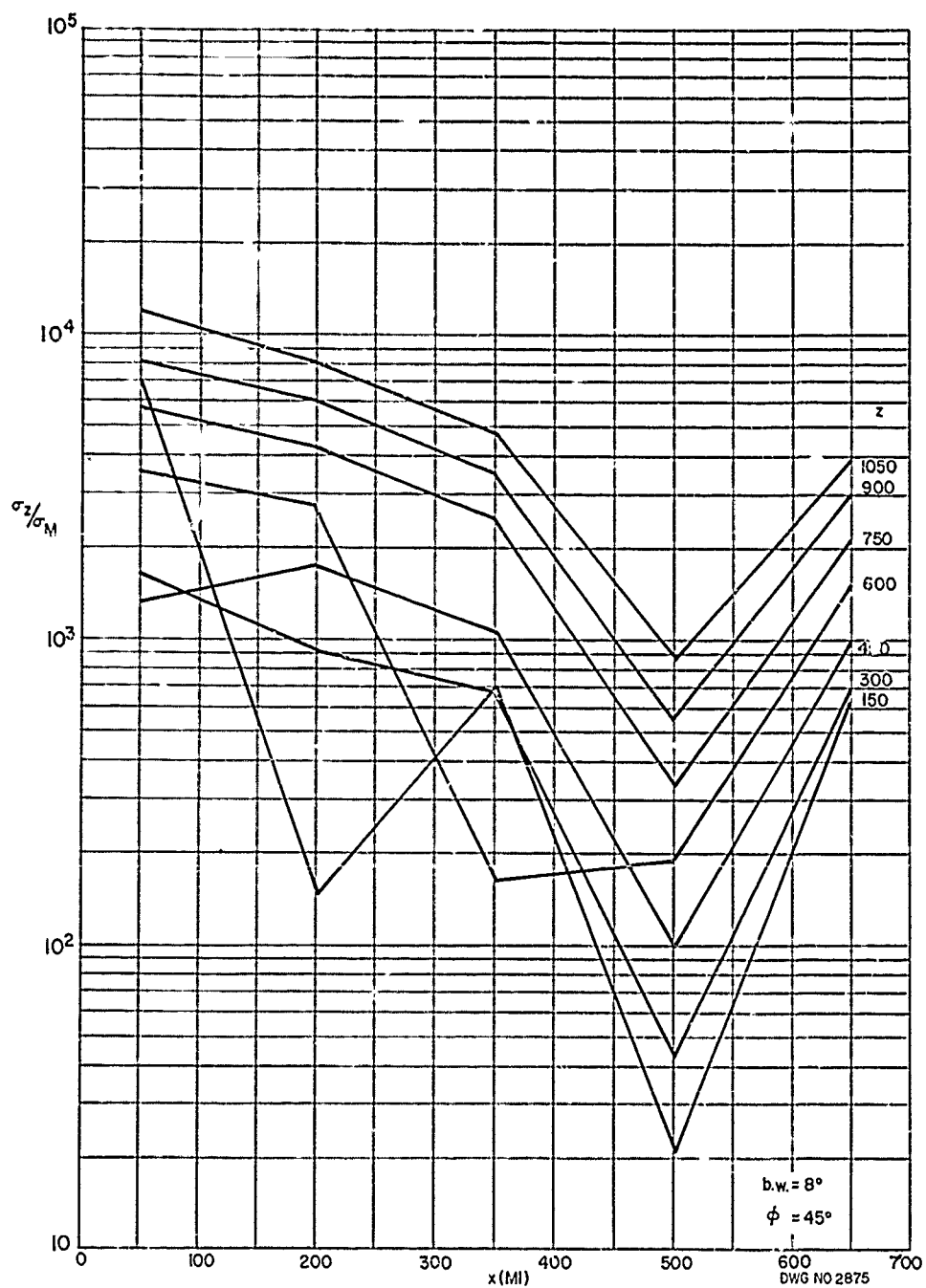


Figure 25b
C-65

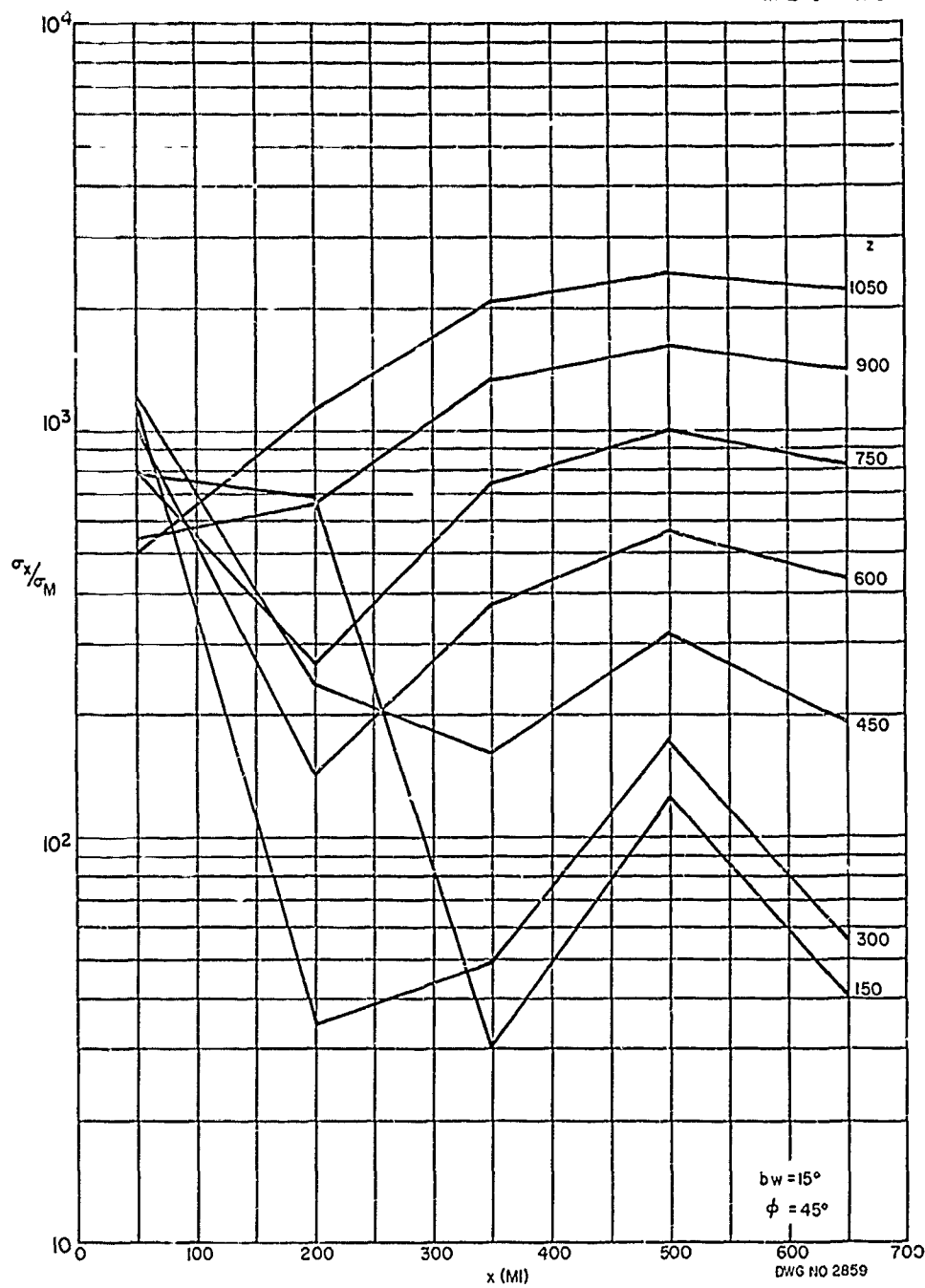


Figure 26a
C 66

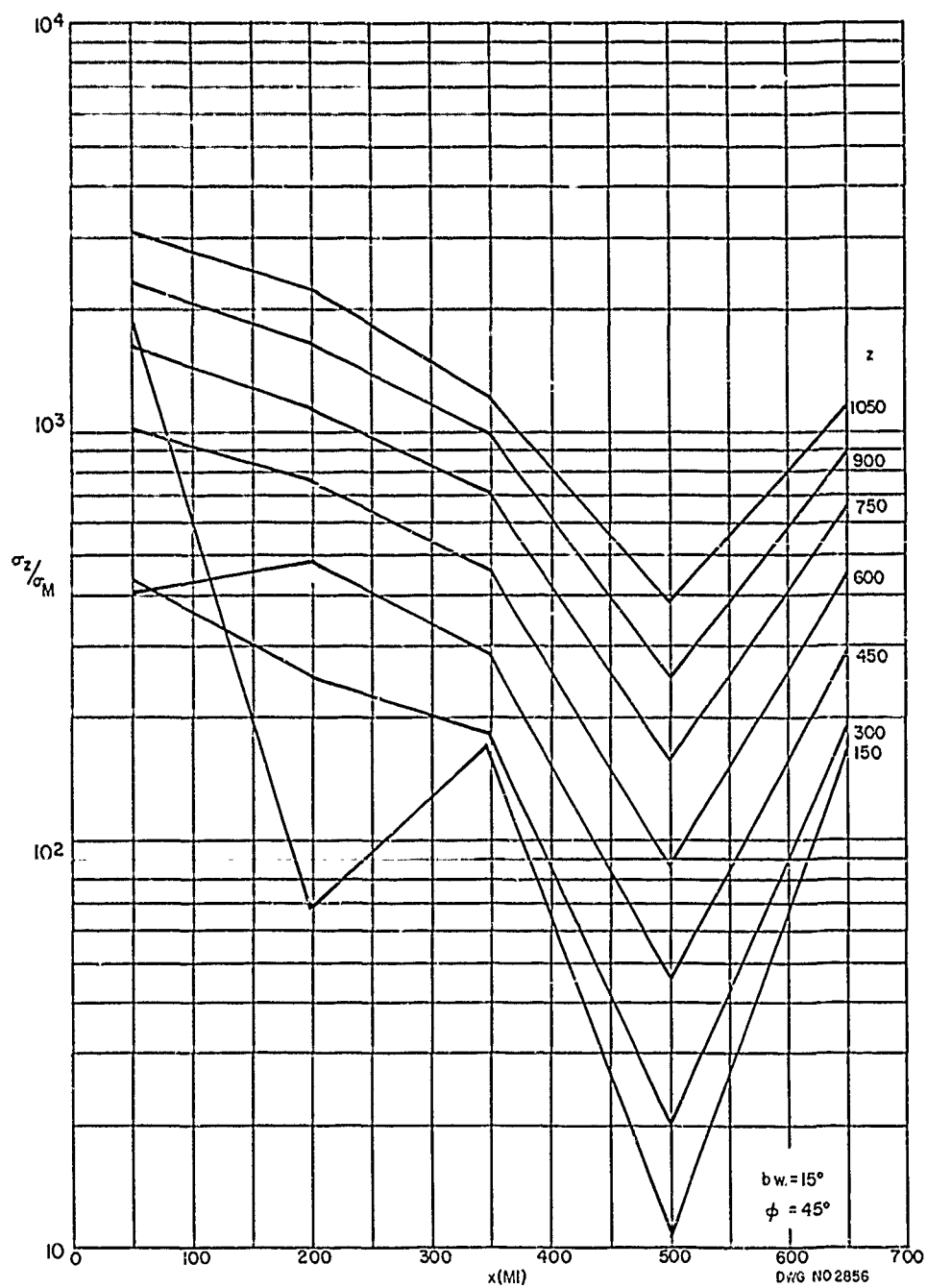


Figure 26b

(6)

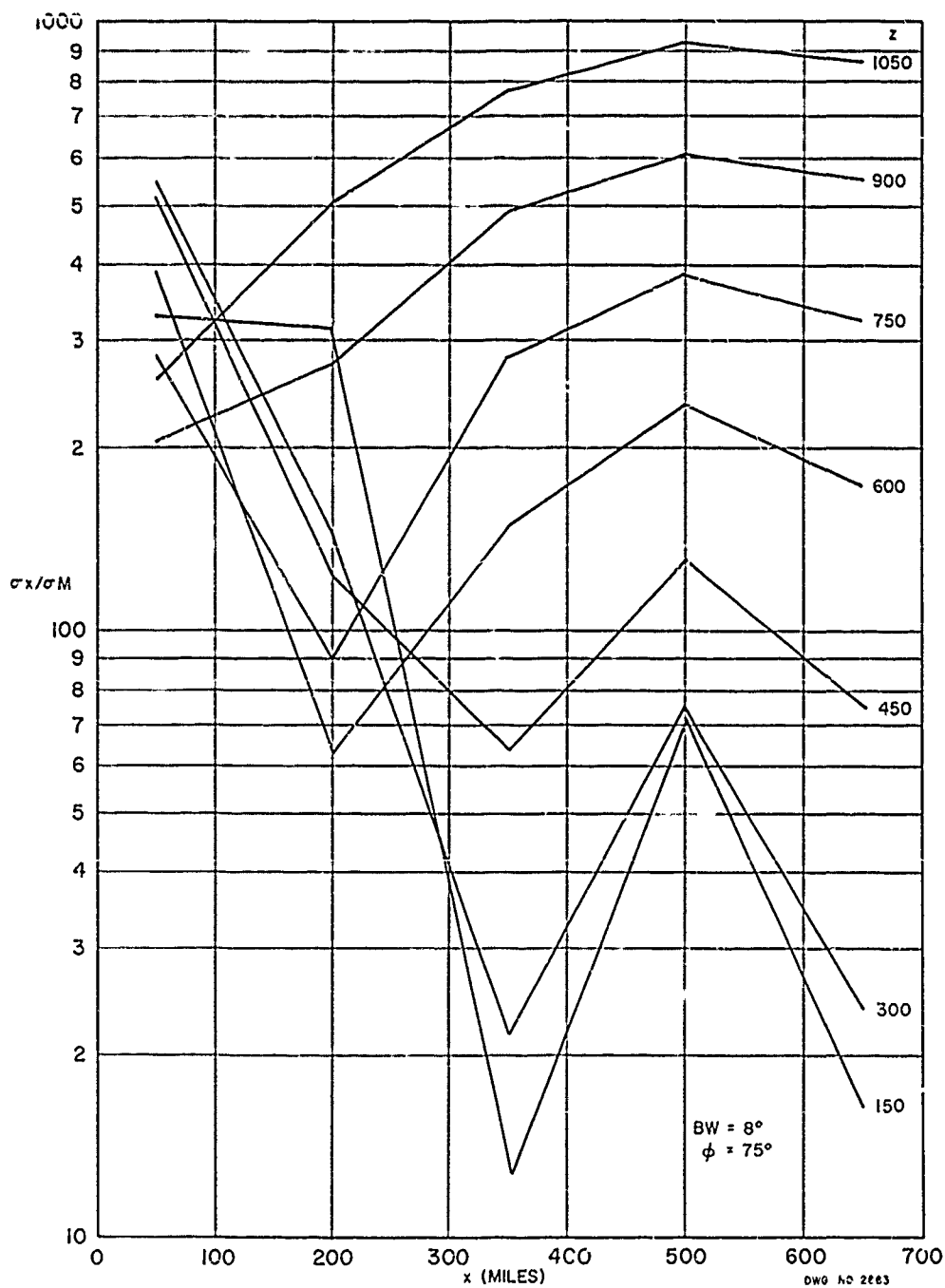


Figure 27a

Q-68

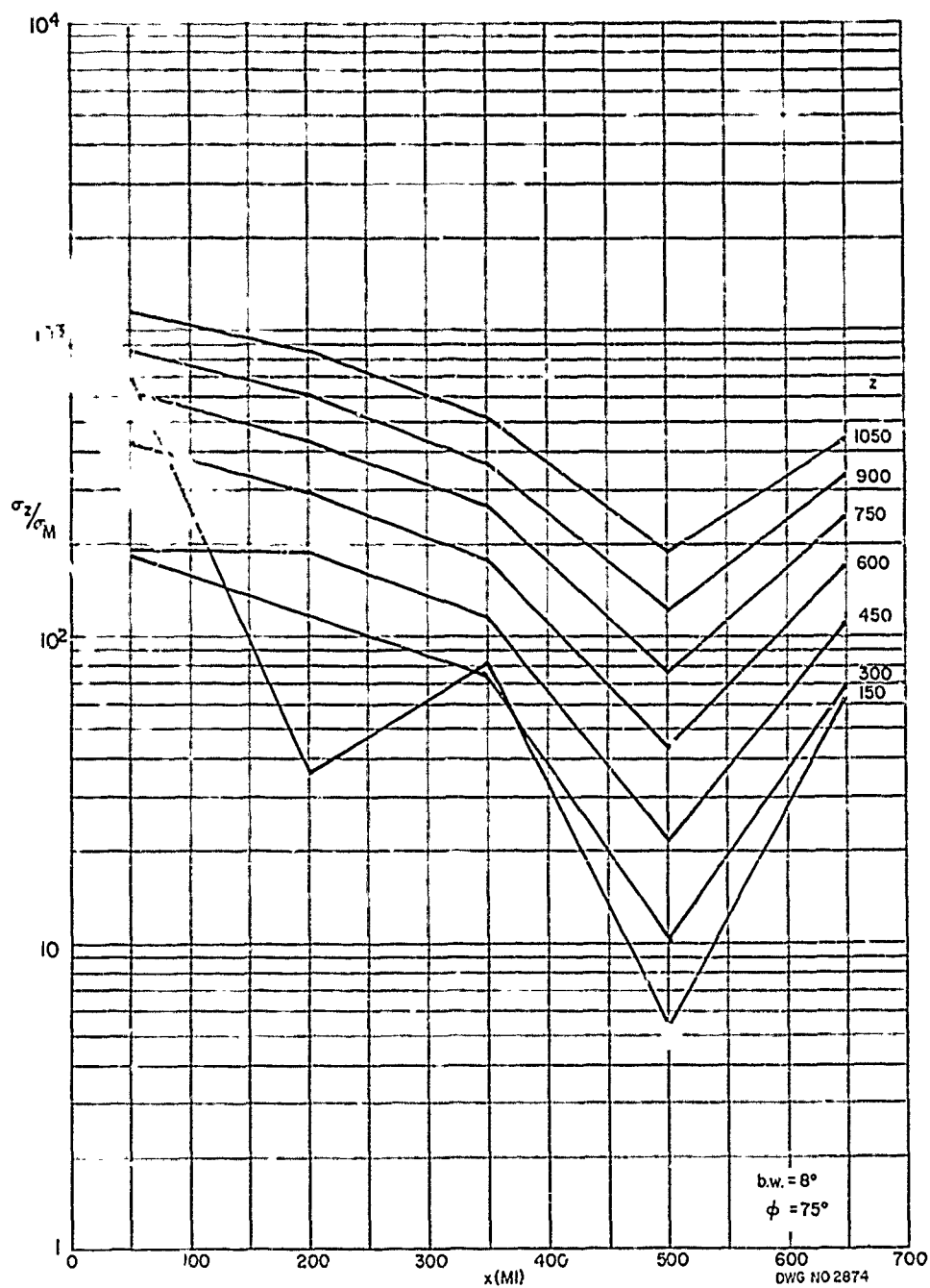
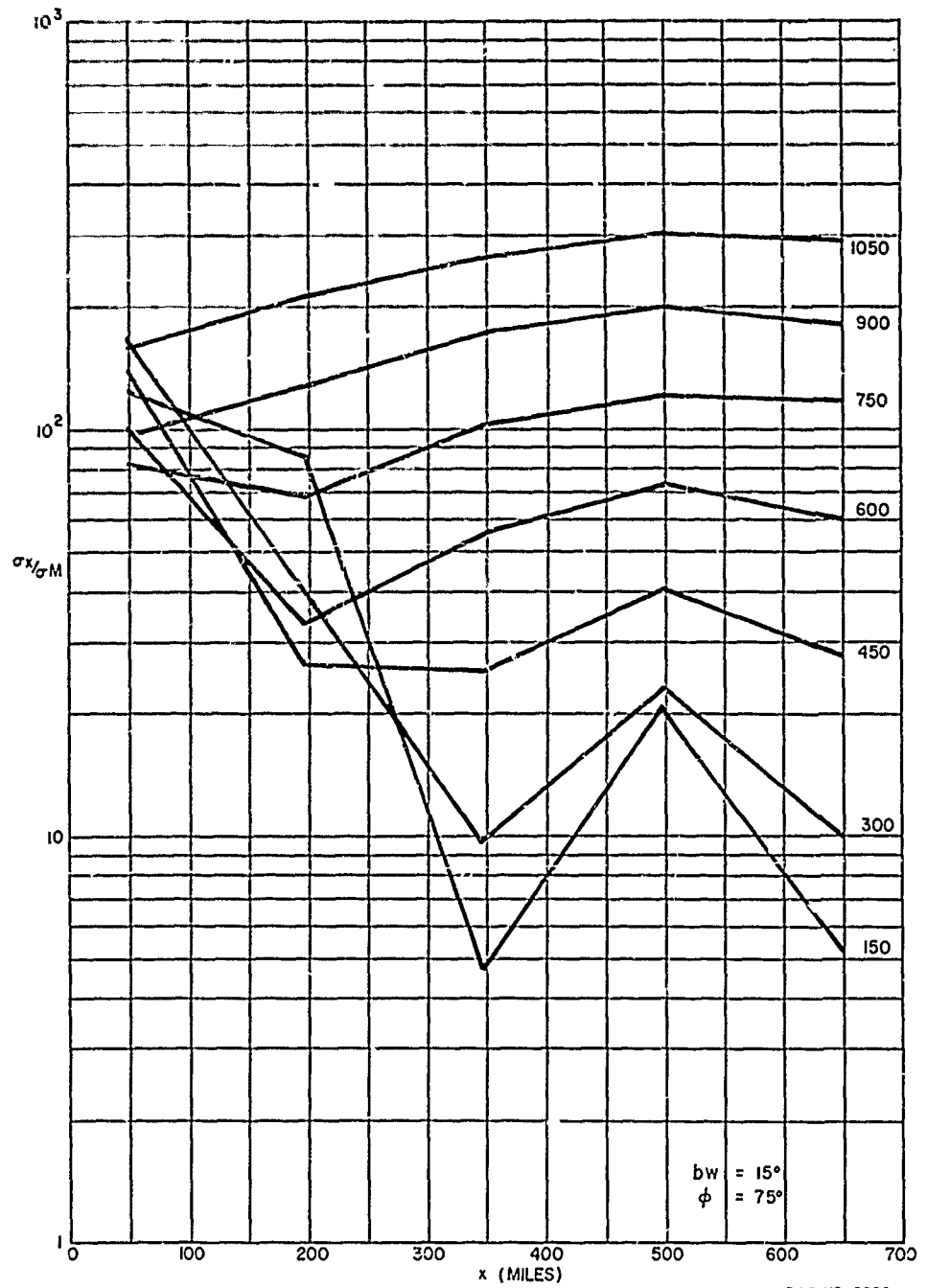


Figure 27b
C-69

Figure 28a
C-70

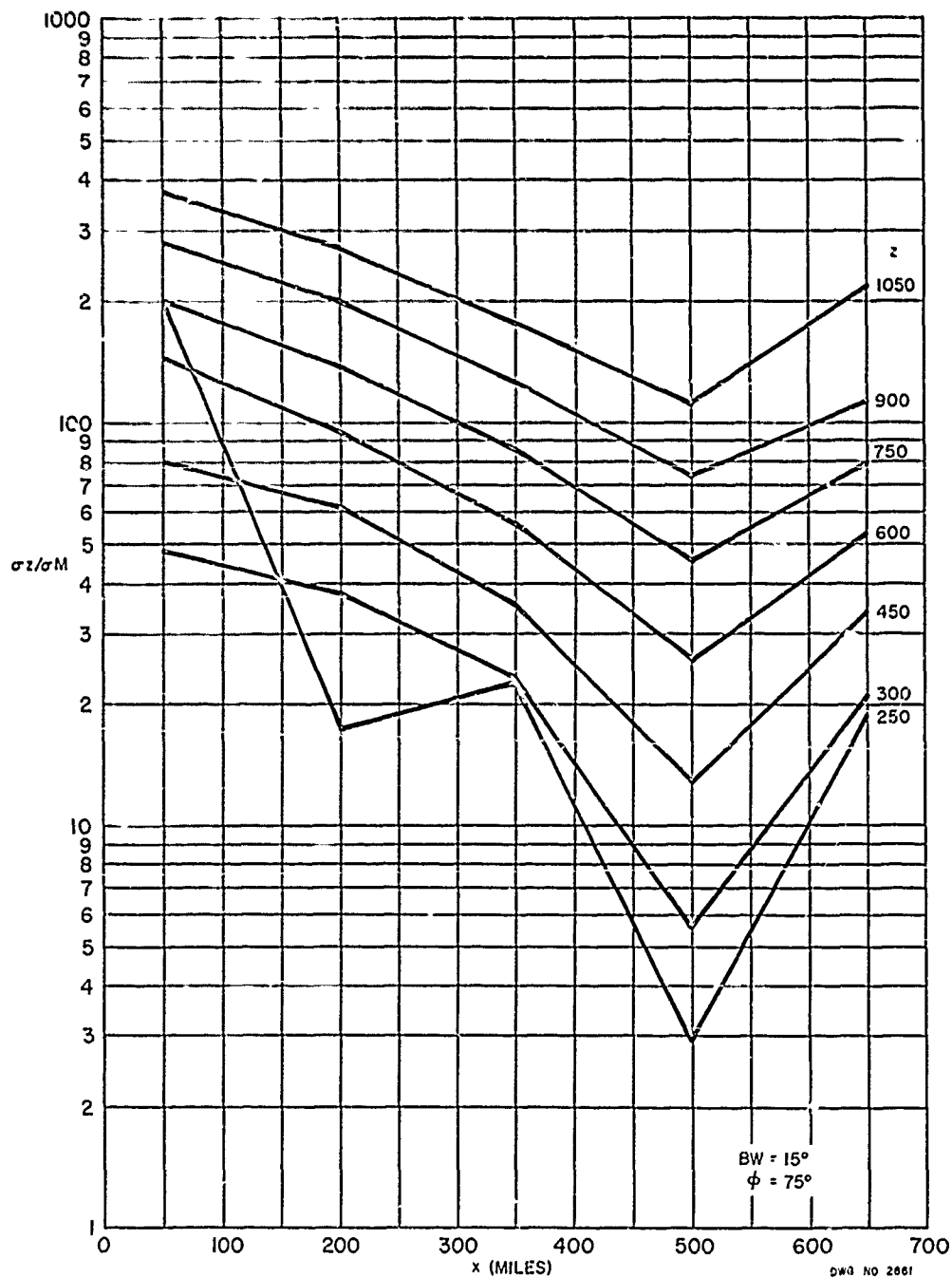


Figure 28b
C-71

PHILCO

GOVERNMENT & INDUSTRIAL GROUP
WESTERN DEVELOPMENT LABORATORIES

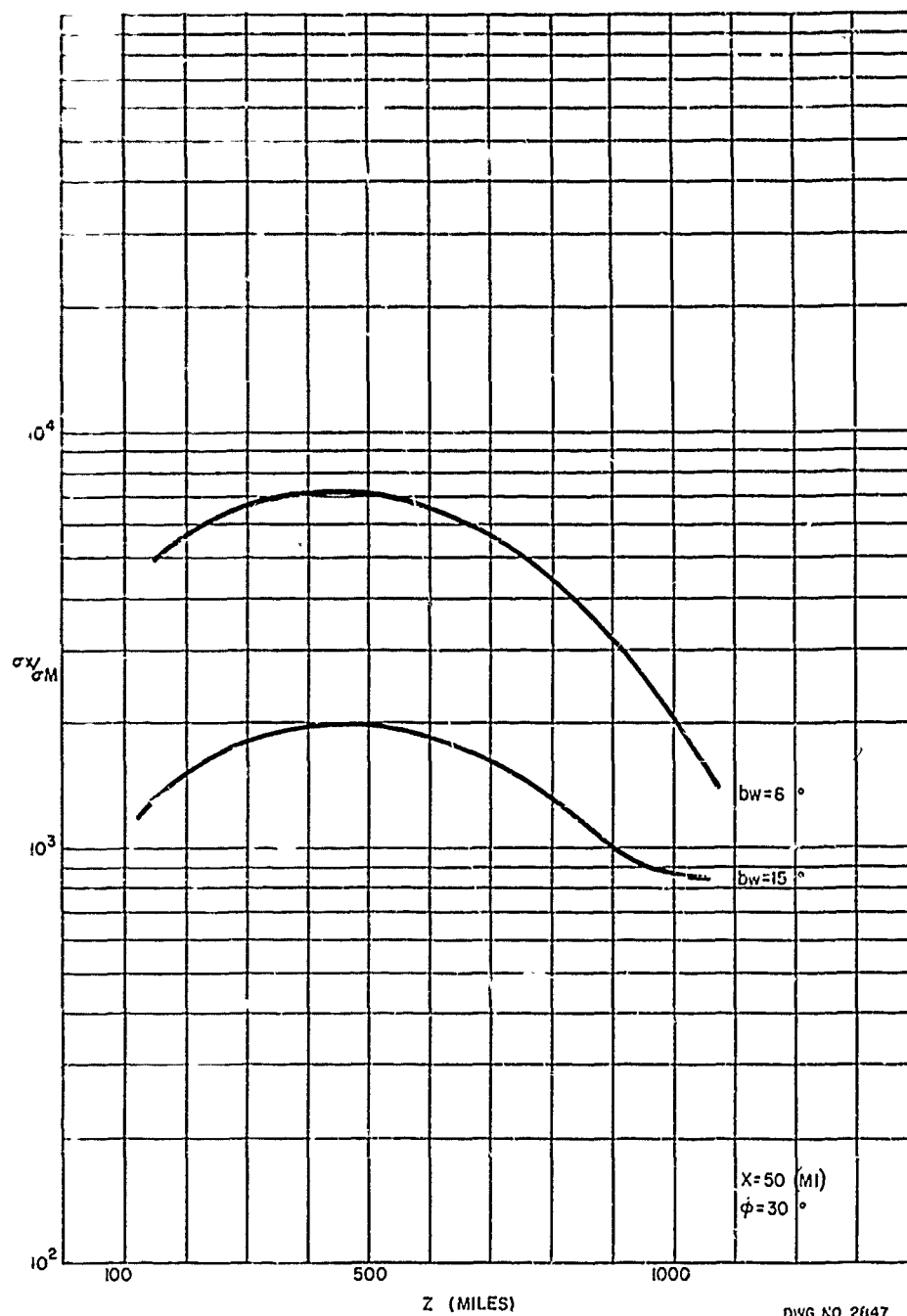


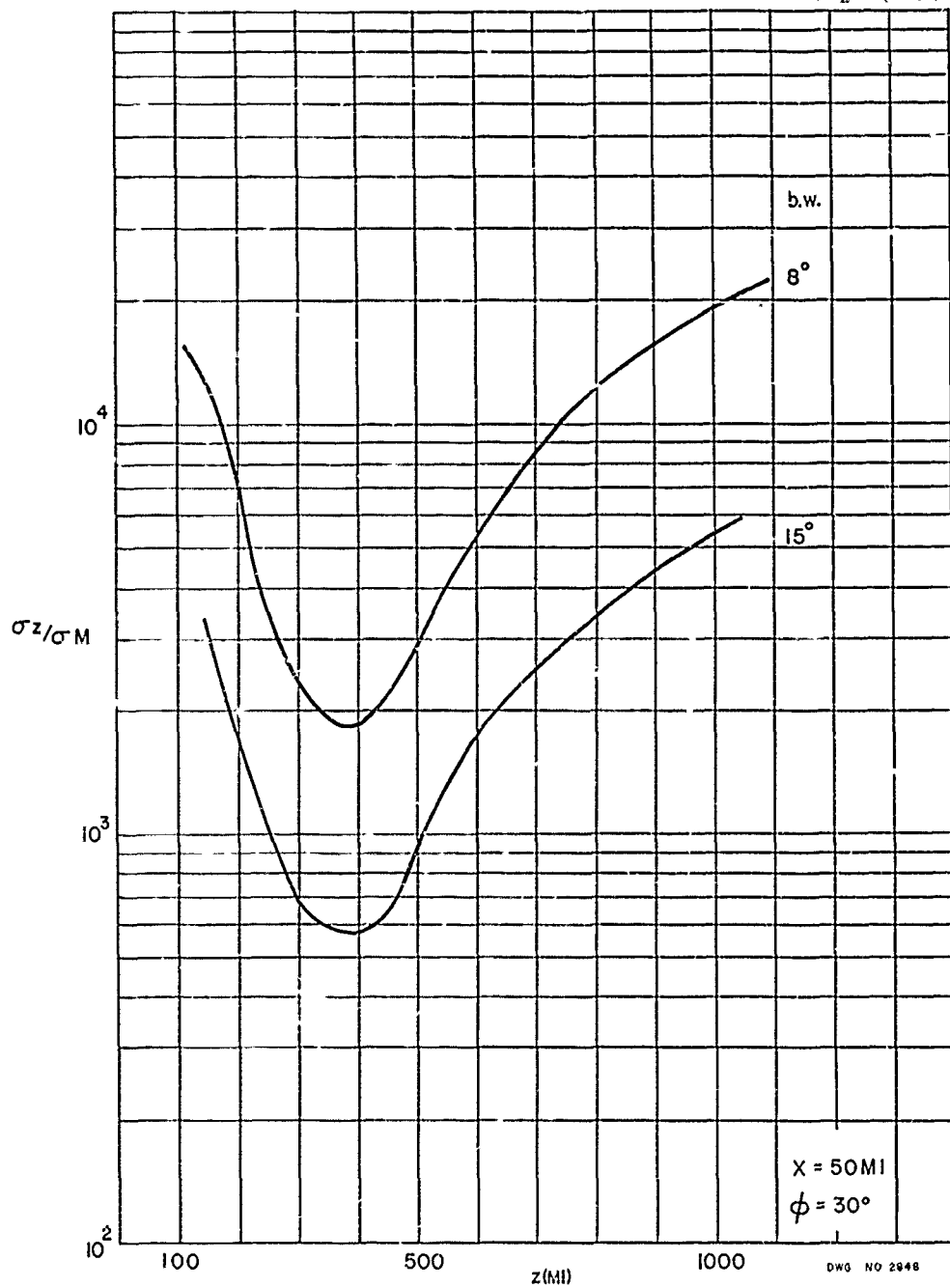
Figure 29a

(-72

PHILCO

GOVERNMENT & INDUSTRIAL GROUP
WESTERN DEVELOPMENT LABORATORIES

ML-13-125



3. 4. 5. 6. 7. 8. 9. 10.

PHILCO

GOVERNMENT & INDUSTRIAL GROUP
WESTERN DEVELOPMENT LABORATORIES

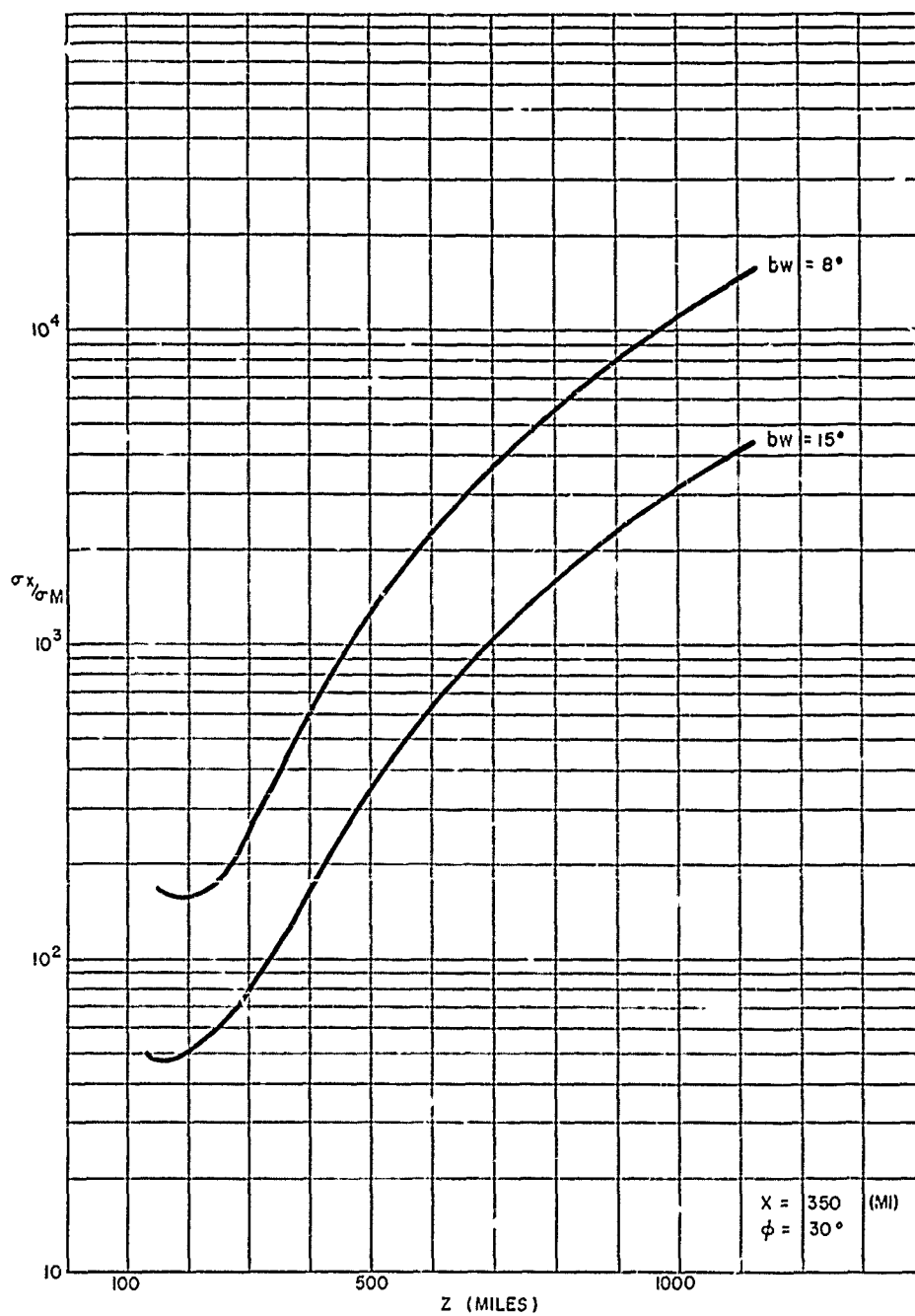


Figure 30a

C-74

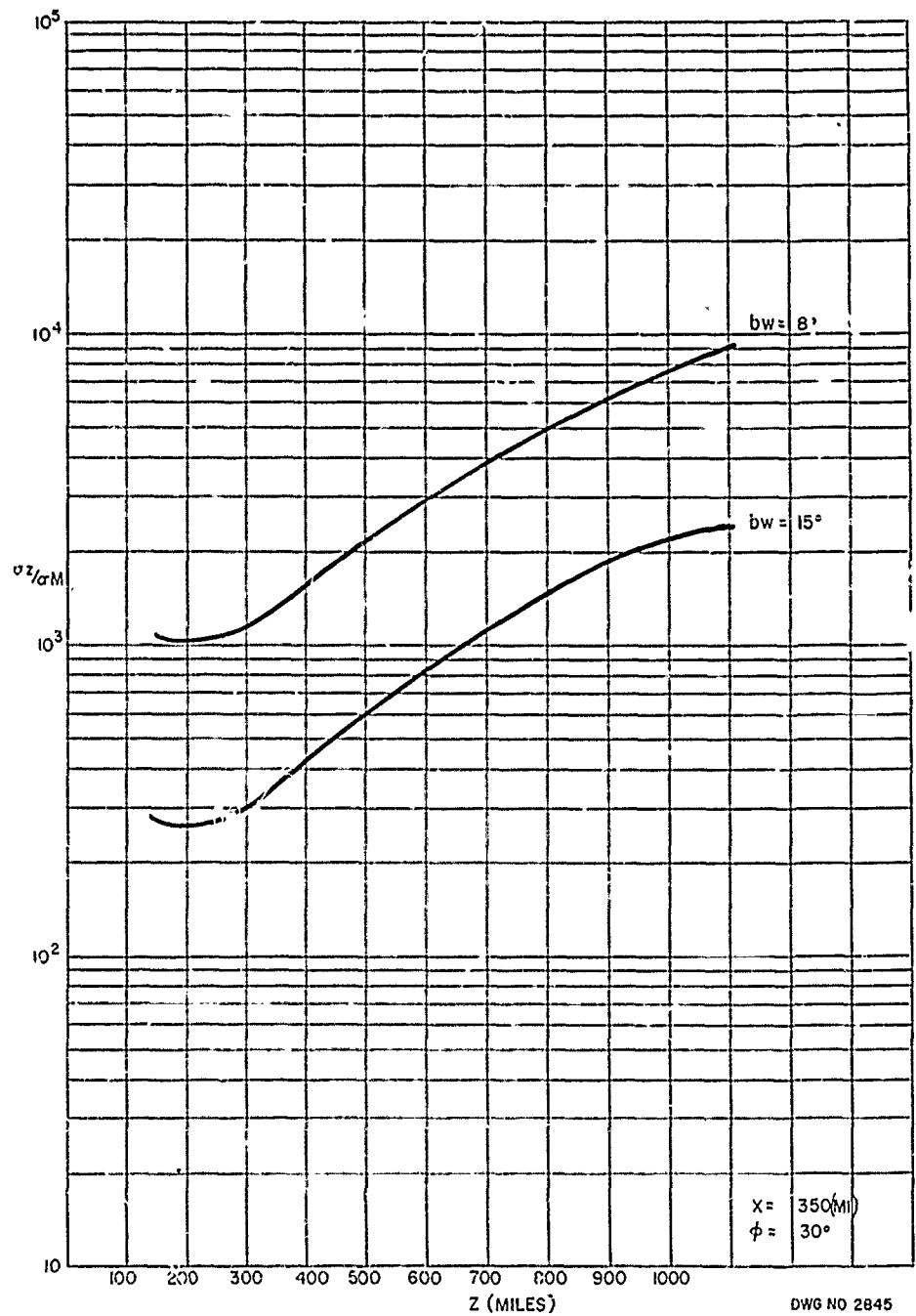


Figure 30b

C-75

PHILCO

GOVERNMENT & INDUSTRIAL GROUP
WESTERN DEVELOPMENT LABORATORIES

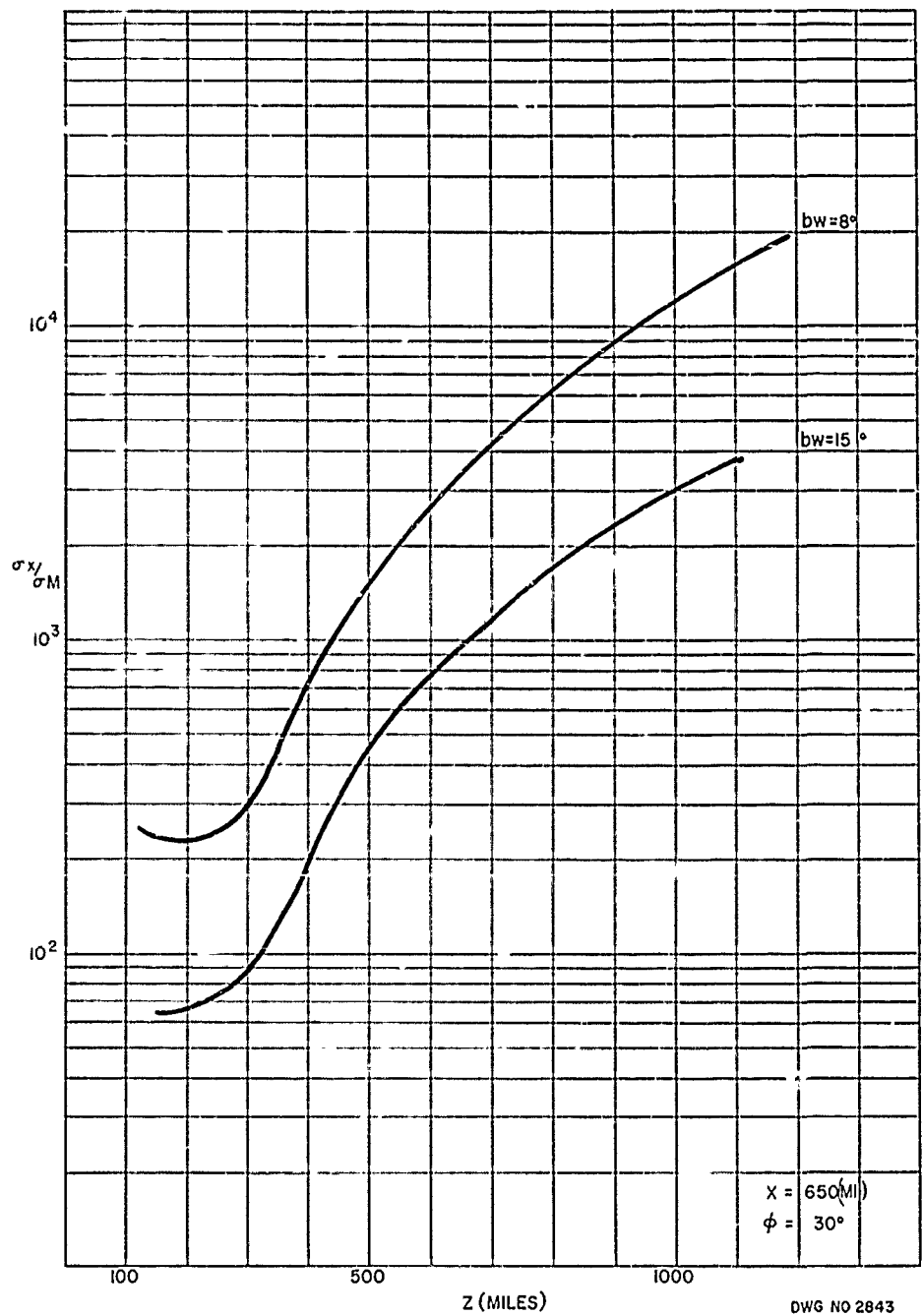


Figure 31a

C-76

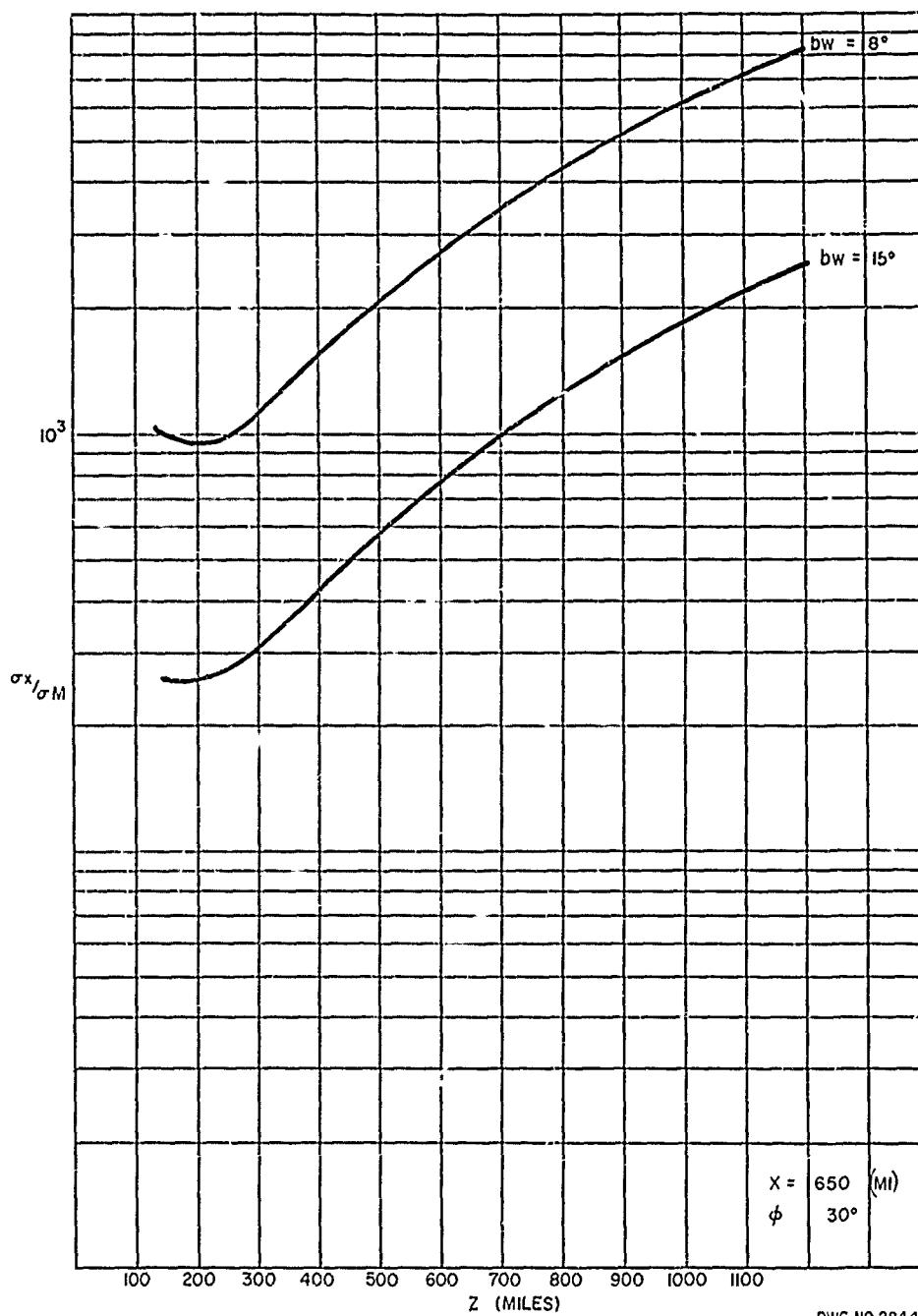
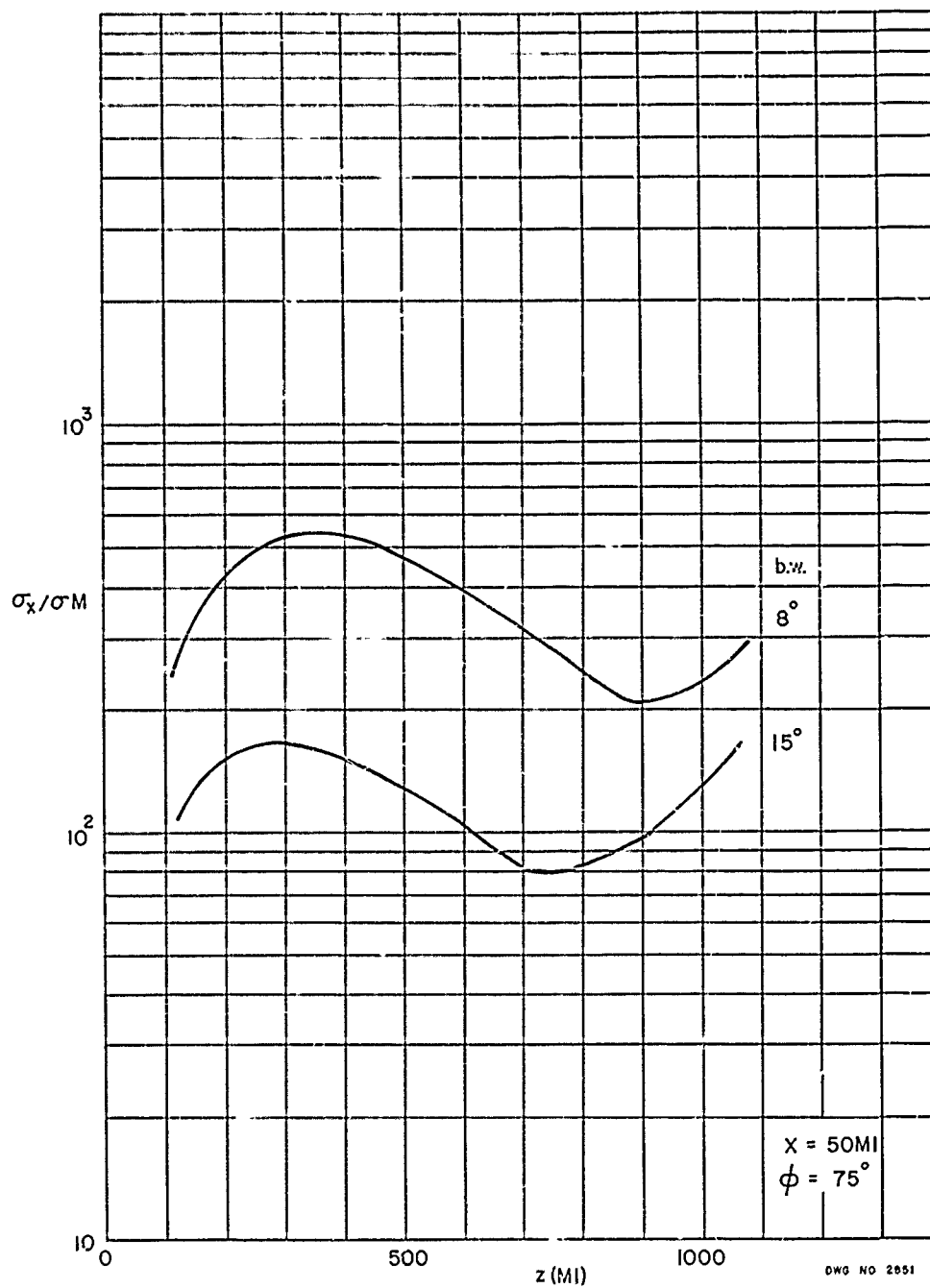


Figure 31b

DWG NO 2844

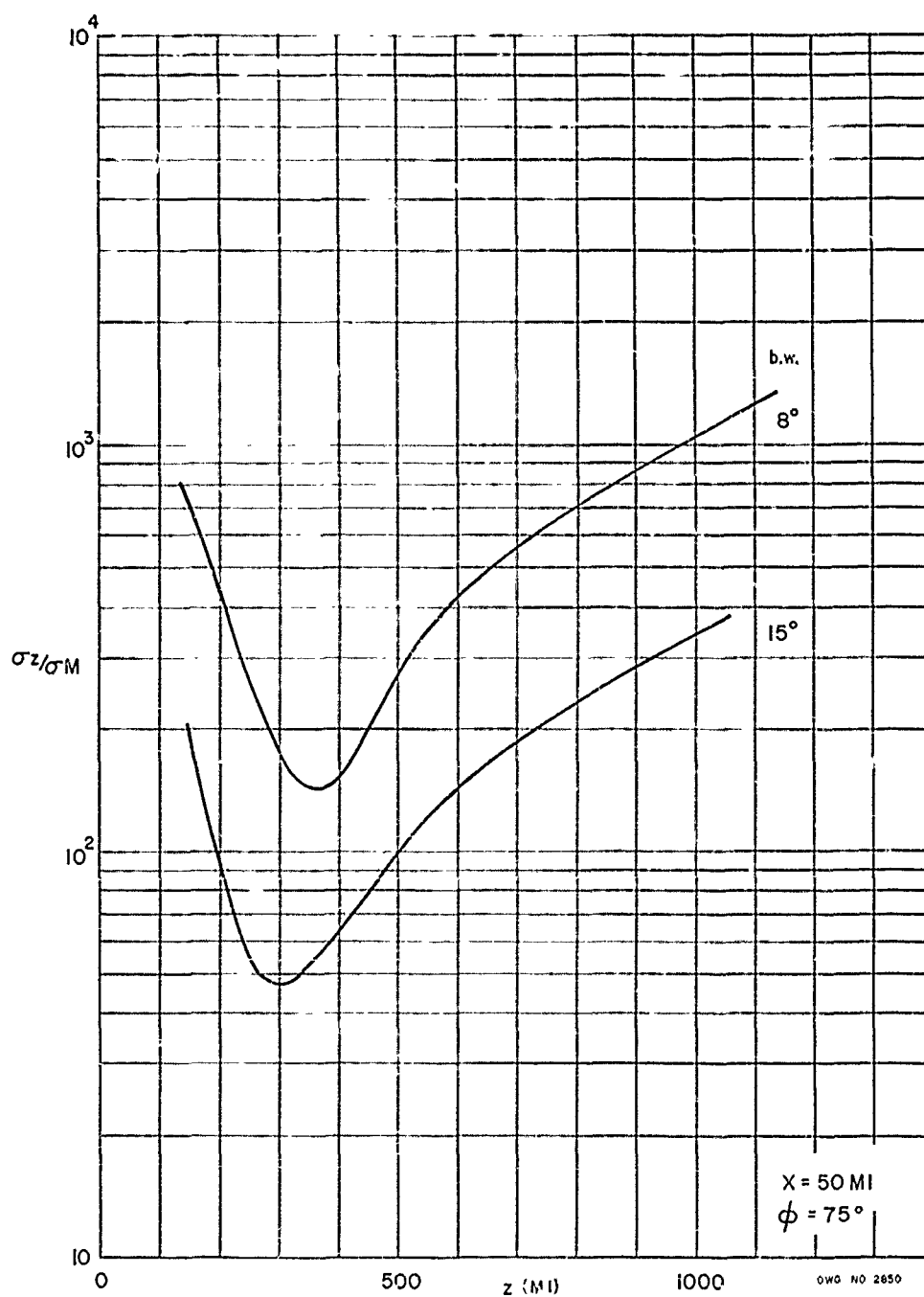
PHILCO

GOVERNMENT & INDUSTRIAL GROUP
WESTERN DEVELOPMENT LABORATORIES



DWG NO 2851

Figure 1278
 (15)



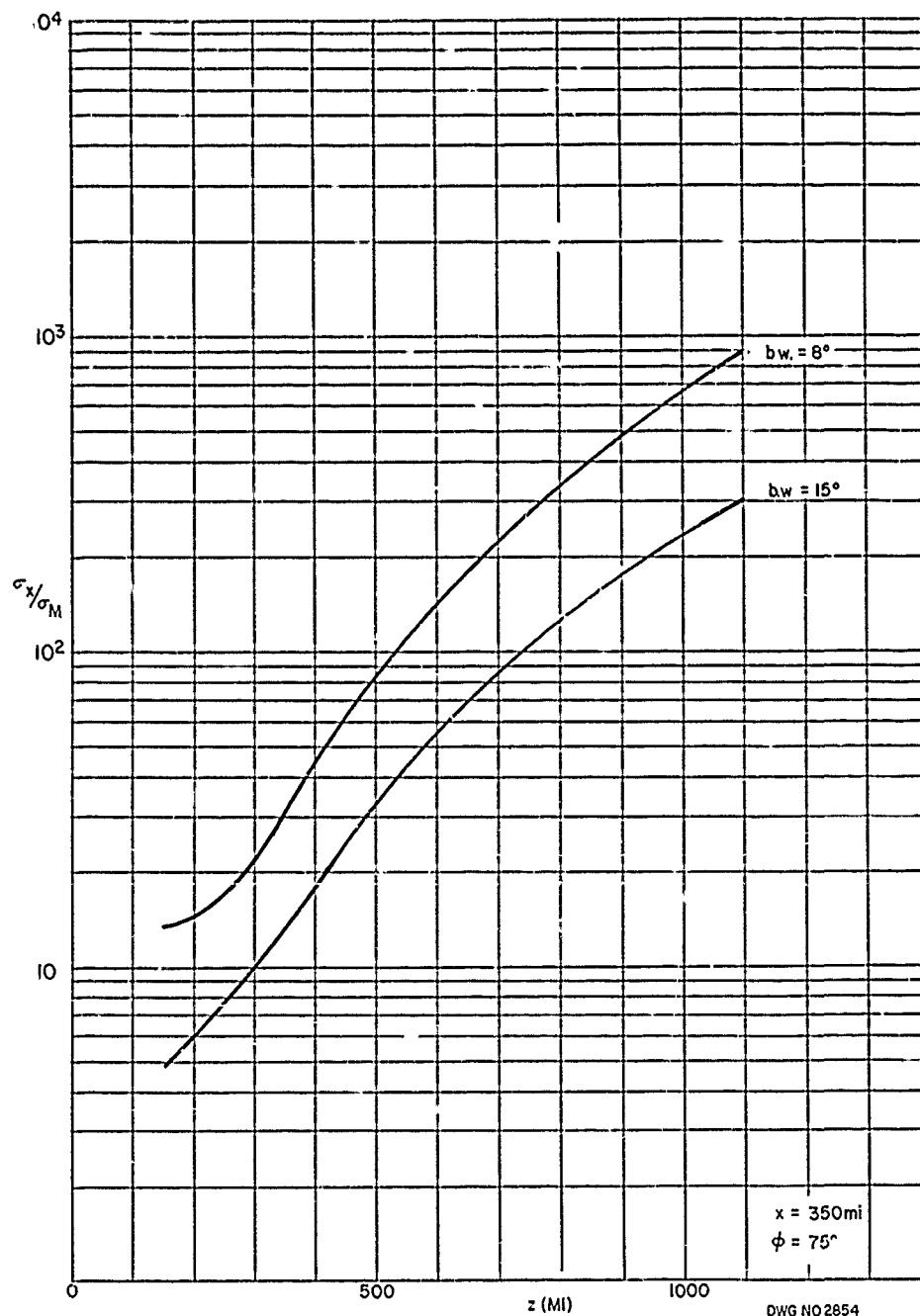


Figure 33a

C-80

PHILCO

GOVERNMENT & INDUSTRIAL GROUP
WESTERN DEVELOPMENT LABORATORIES

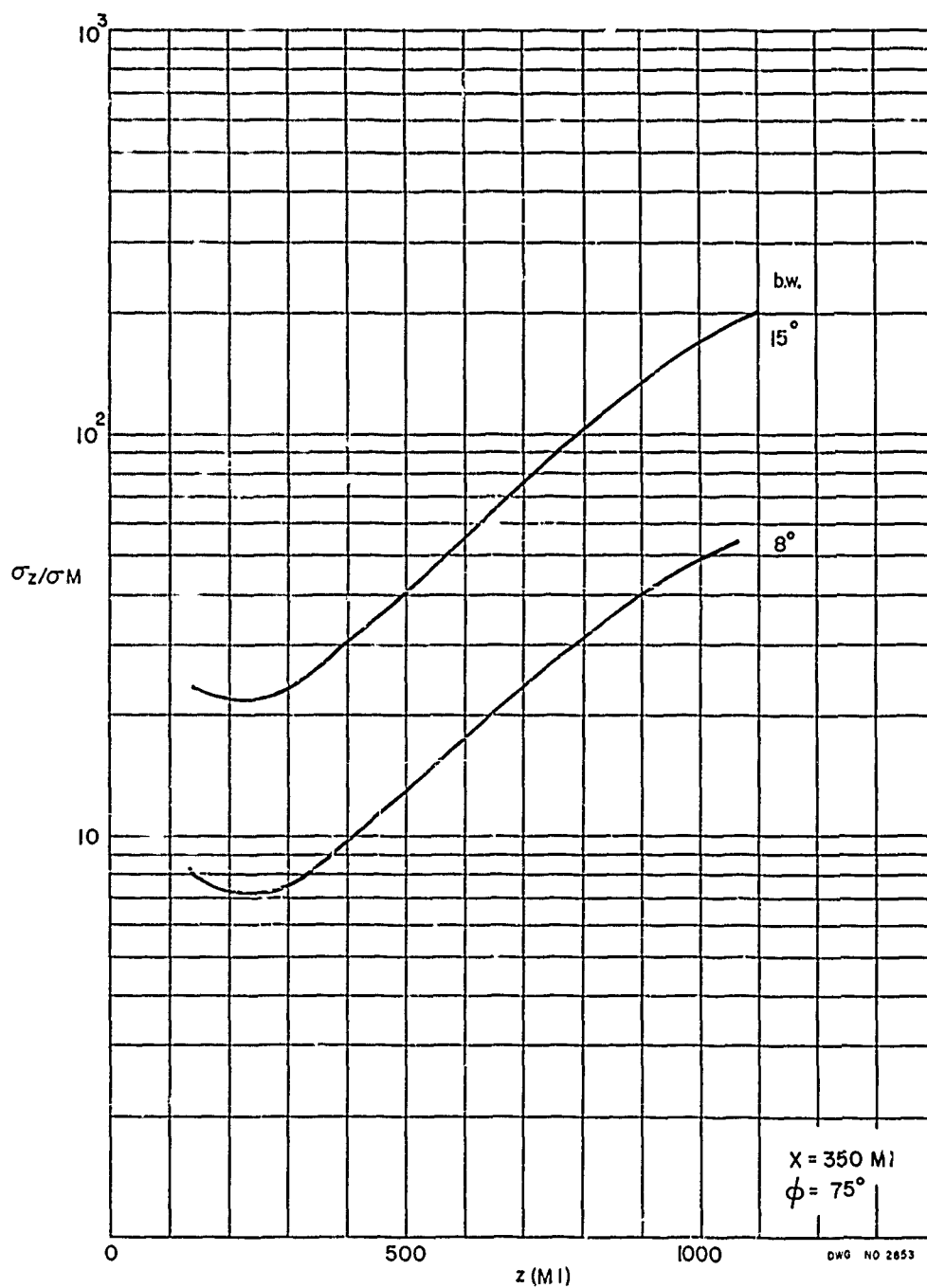


Figure 33b

C-81

PHILCO

GOVERNMENT & INDUSTRIAL GROUP
WESTERN DEVELOPMENT LABORATORIES

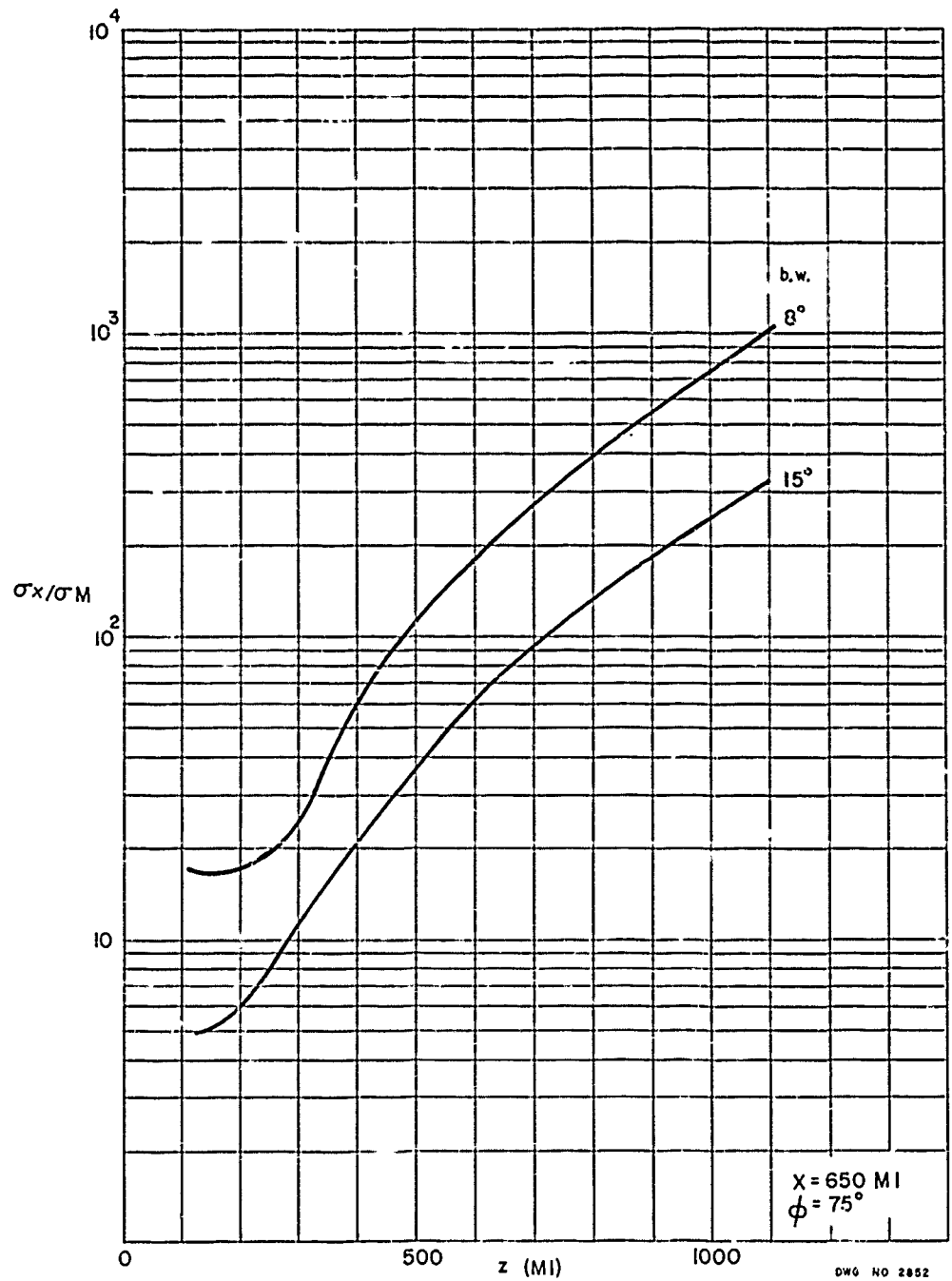


Figure 34a
C-82

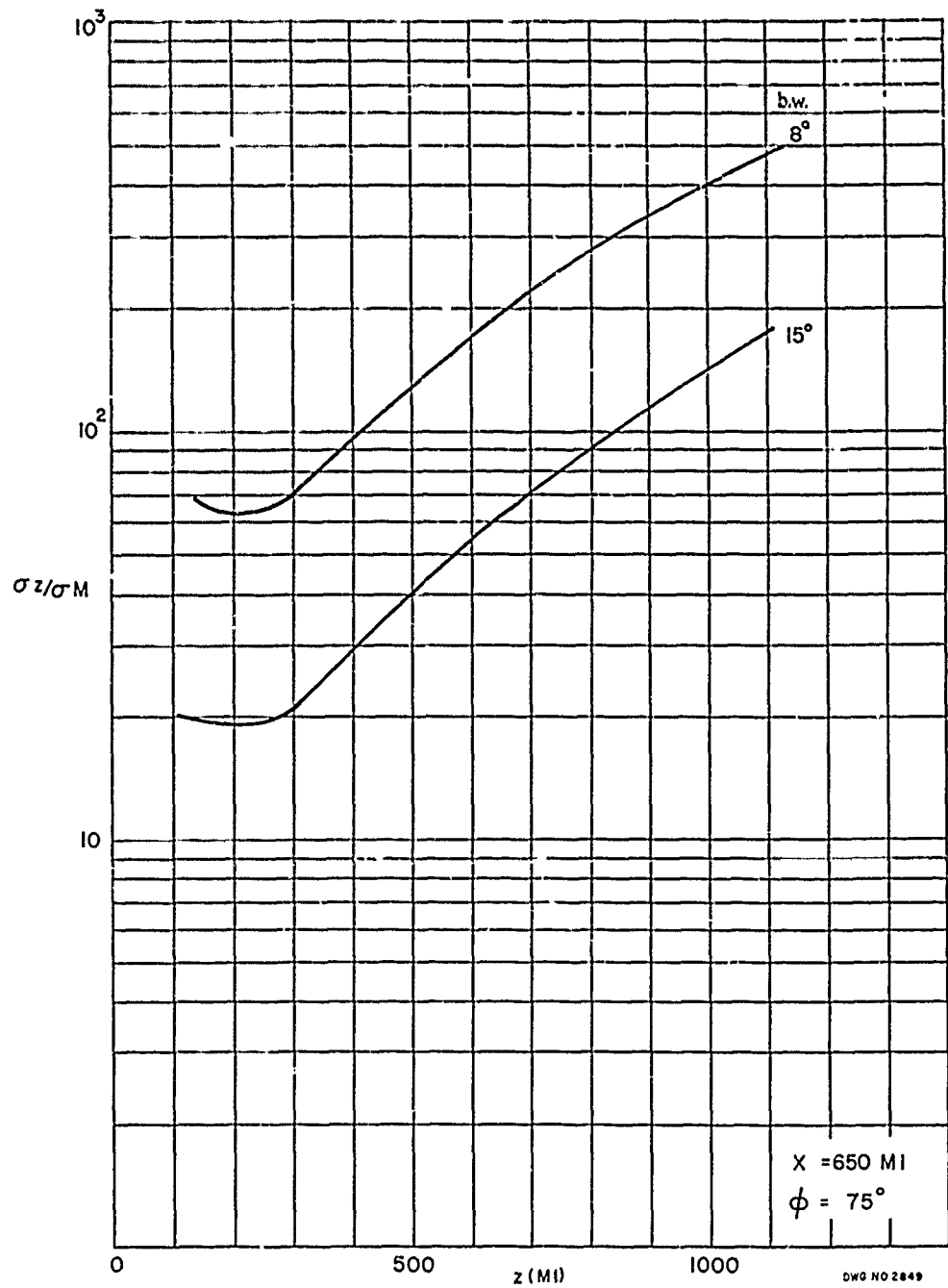


Figure 34b

C-23

PHILCO

GOVERNMENT & INDUSTRIAL GROUP
WESTERN DEVELOPMENT LABORATORIES

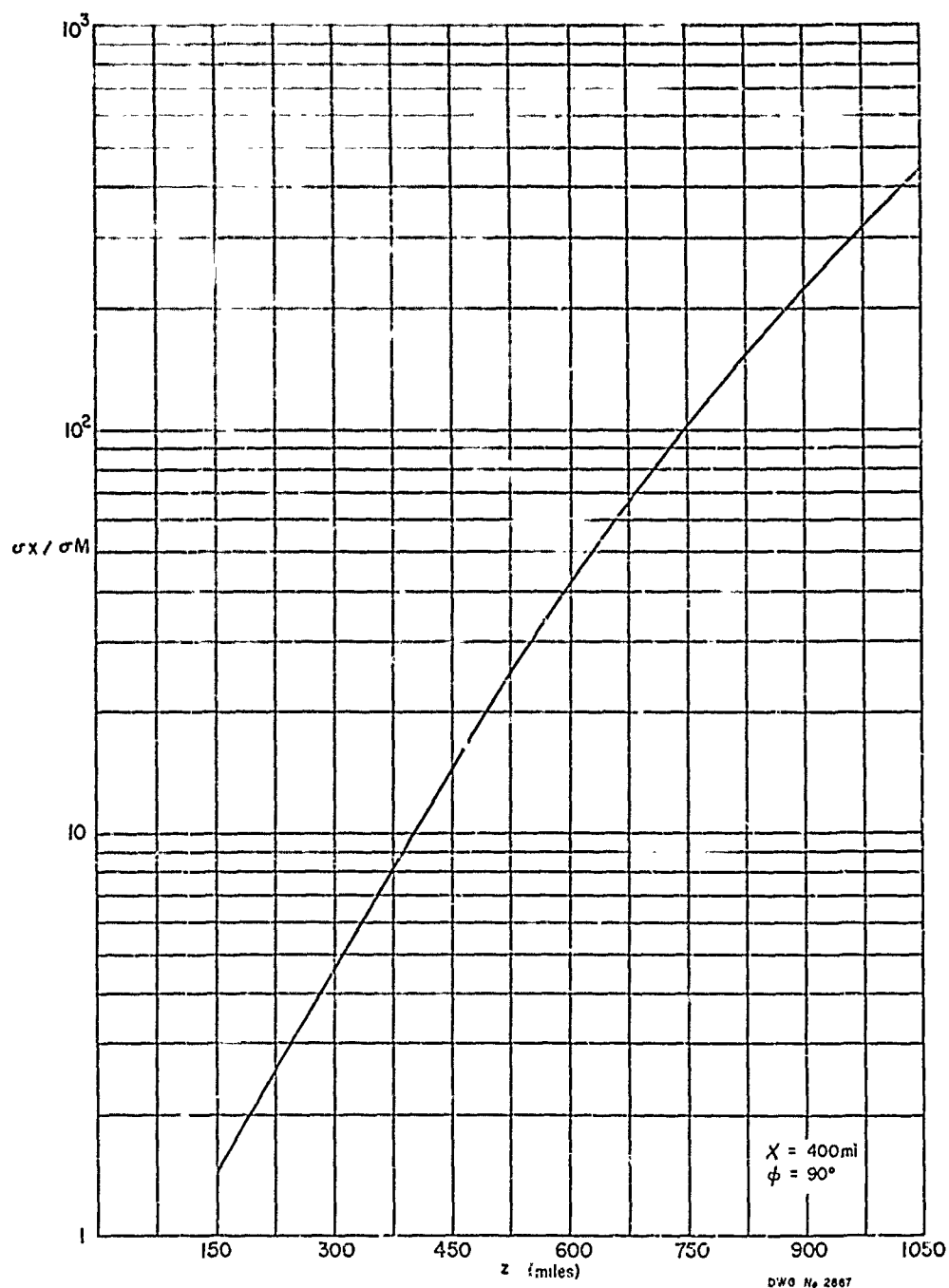
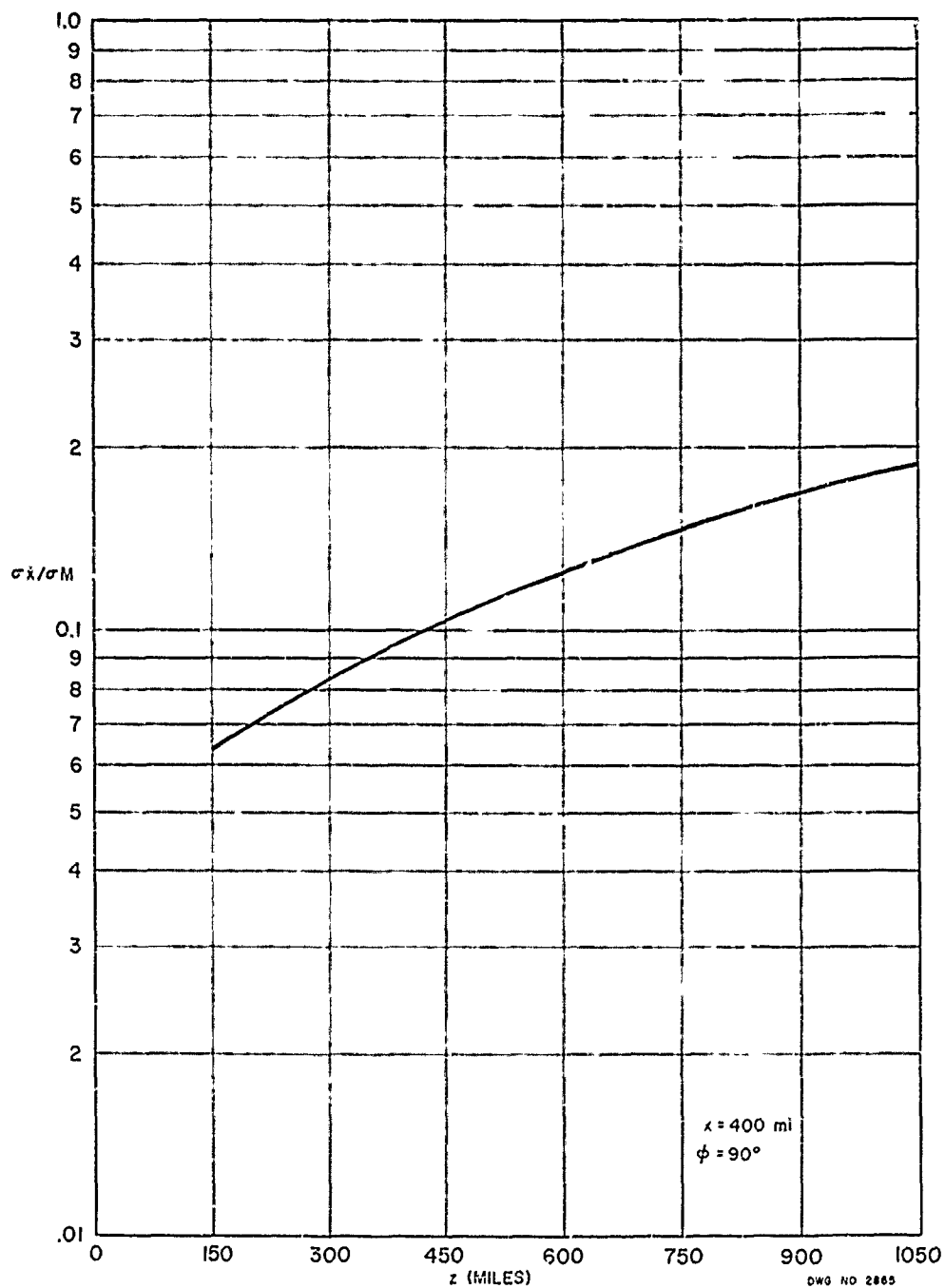


Figure 35a
C-8c



PHILCO

GOVERNMENT & INDUSTRIAL GROUP
WESTERN DEVELOPMENT LABORATORIES

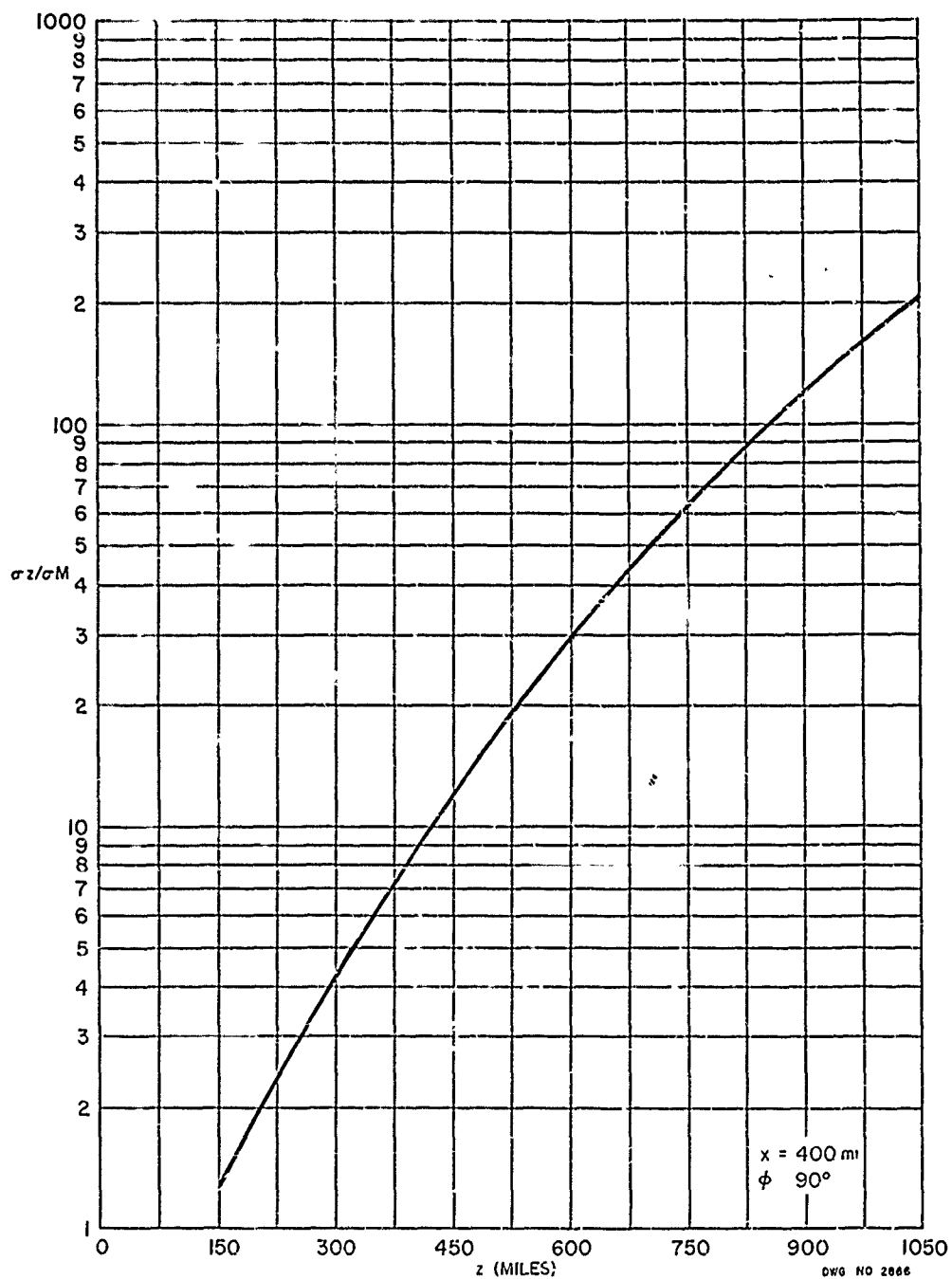


Figure 33c

C-86

PHILCO

GOVERNMENT & INDUSTRIAL GROUP
WESTERN DEVELOPMENT LABORATORIES

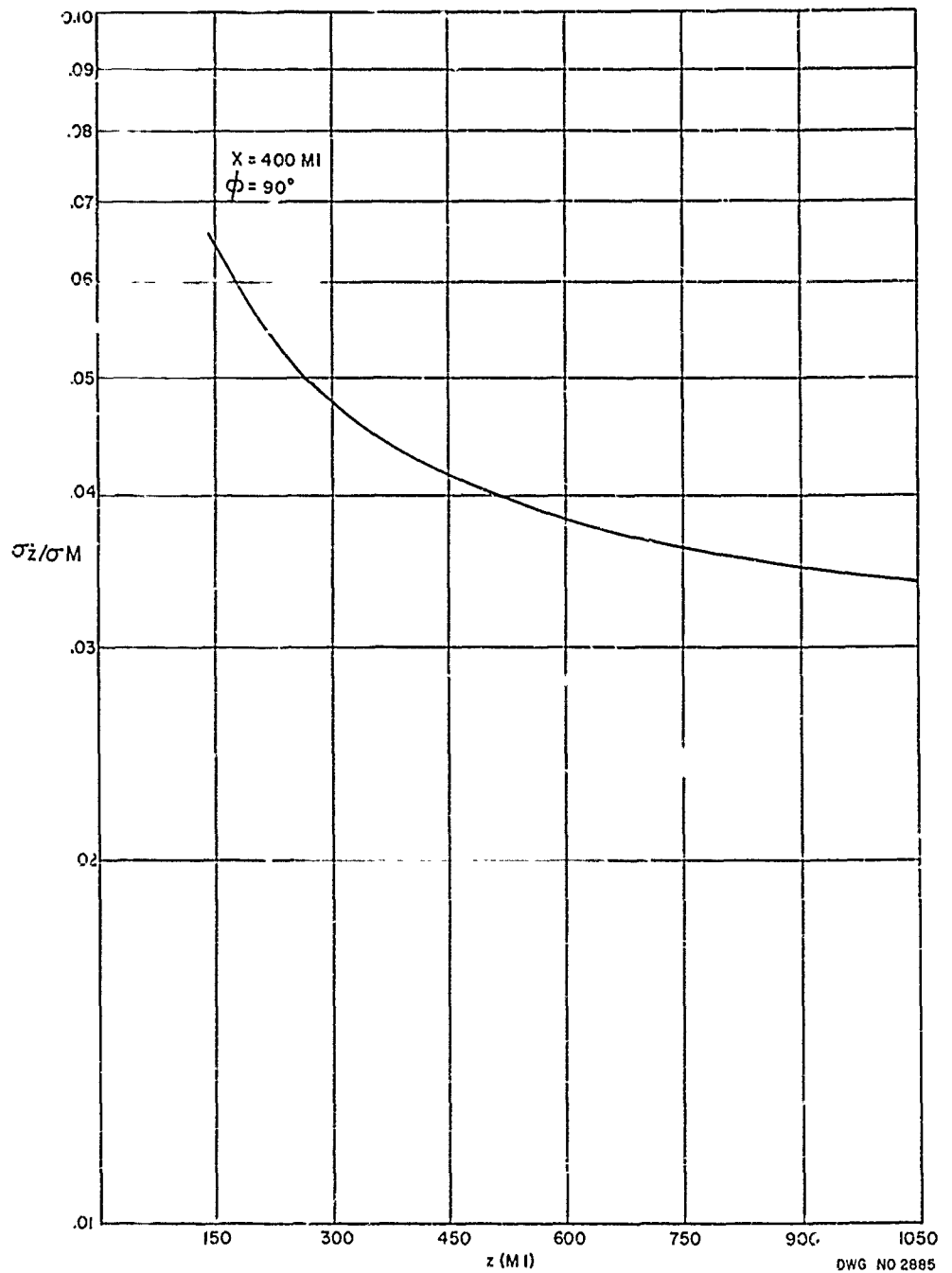


Figure 35d
C-87

BIBLIOGRAPHY

1. Brown, Duane C., RCA Data Reduction Technical Report No. 39. A Treatment of Analytical Photogrammetry, ASTIA Document No. 124144.
2. Monthly Progress Reports, Philco Western Development Laboratories, submitted to Ballistics Research Laboratories, Contract DA-04-200-21X4992. 509-ORD-1002.
3. McCormick, P.T., Continuous Wave Transmitter Carrying Vehicle ~~and~~ a Four-Station System by Utilizing the Doppler Effect, 12 August 1959 Philco Internal Memo.
4. Dawson, C.H., Inactive Doppler Acquisition Systems, Philco Internal Memo, 4 April 1960.